A STUDY OF PHOSPHOPROTEIN AND PHOSPHOPEPTIDE INTERACTIONS WITH CALCIUM IONS AND DICALCIUM PHOSPHATE DIHYDRATE CRYSTALS

by

Frederick W. Muskett

Ph.D.

UNIVERSITY OF EDINBURGH

1992

DECLARATION

I declare that this thesis was composed by me, that the work of which it is a record was done by me, except where stated in the text. This work has not been submitted elsewhere in any previous application for a degree. All sources of information have been acknowledged.

I have always known that at last I would take this road.

But yesterday I did not know

it would be today

-Narihara.

To my wife, Anne

ACKNOWLEDGEMENTS

ABSTRACT

Phosphoproteins interact with calcium minerals in numerous biological systems but despite the importance of this phenomenon it is little understood. The interaction of phosphoproteins with calcium minerals is observed in milk where caseins interact with calcium phosphate to form micelles. Further understanding of this interaction was sought through two approaches. First, the adsorption isotherms for binding of the casein ß-CN A and its N-terminal phosphopeptide (ß-CN (f1-25)) to crystalline dicalcium phosphate dihydrate (DCPD) were measured. Secondly, attempts were made to grow co-crystals of calcium ions with phosphopeptides or with phosphoserine.

A method of measuring phosphoprotein and phosphopeptide adsorption to DCPD was developed. From the adsorption isotherms the affinity and capacity of adsorption could be determined using a model of the adsorption process. Adsorption isotherms for ß-CN A were all described using a simple Langmuir model of adsorption, adsorption occurring to identical and independent sites on the DCPD crystals. ß-CN (f1-25) appears to adsorb to the same adsorption sites as ß-CN A and also to a second family of adsorption sites which have a lower intrinsic affinity but which are more abundant. Adsorption isotherms for ß-CN (f1-25) were described using a modified version of the Langmuir model in which there are two sets of adsorption sites. A term was included to allow for cooperative adsorption to the second set of adsorption sites.

The effects of methylation of lysyl residues, buffer pH, incubation temperature, the presence of 6.0 M urea in the buffer and of crystal size were all examined. The adsorption of ß-CN (f1-25) to DCPD crystals appears to be athermal since the measured isotherm does not change significantly with temperature (over the measured range), requiring that adsorption is due to an entropy gain. Comparison of the results of the ß-CN A and ß-CN (f1-25) adsorption experiments suggests that adsorption probably occurs *via* the N-terminal region of ß-CN A, consistent with the hypothesis that the binding of phosphoproteins to calcium minerals occurs primarily through their phosphoseryl residues.

The phosphopeptide Ser(P)-Ser(P) was prepared by chemical synthesis for use in crystallisation and binding studies, so that a model of phosphoprotein/calcium mineral adsorption might be developed. Several methods of phosphorylation were investigated. However, the synthesis was not completed in time to allow adsorption or crystallographic studies to be performed.

Co-crystals of calcium ions and phosphoserine were produced but, because of their small size and instability, these crystals were not suitable for structure determination by conventional X-ray diffraction techniques. However, conventional X-ray diffraction techniques were used to solve the crystal structures of two small molecules of pharmacological importance.

List of Figures

List of Tables

<u>List of Abbreviations and Symbols</u>

The abbreviations used here are those described as 'accepted' in the instructions to authors of the Biochemical Journal (Biochem. J. (1988), **249**, 1-20) and of the Journal of Biological Chemistry (IUPAC-IUB Commission on Biochemical Nomenclature Symbols for Amino-Acid Derivatives and Peptides Recommendations (1971); J. Biol. Chem. (1972), **247**, 977-983), with the following additions.

A	area occupied by an adsorbed molecule
acidic PRP's	acidic proline-rich-phosphoproteins
BET	Brunauer, Emmett and Teller
c	equilibrium, free concentration of adsorbate
c^o	solubility of adsorbate
CCP	colloidal calcium phosphate
cf.	*confer*
DBPC	dibenzylphosphoryl chloride
DCCI	N.N-dicyclohexylcarbodiimide
DCPD	dicalcium phosphate dihydrate
DMF	dimethyl formamide
DPPC	diphenylphosphoryl chloride
Γ	adsorbed amount per unit area
k, l	affinity constants
m, n	number of adsorption sites per unit area
MCP	micellar calcium phosphate
Rg	radius of gyration
TCPC	Bis-(2,2,2-trichloroethyl)phosphoryl chloride
THF	tetrahydrofuran

viz.   *videlicet*

<u>Crystallography</u>

a, b, c   unit cell axial lengths

$\overset{\circ}{A}$ angstrom unit $(1 \overset{\circ}{A} = 0.1$ nm)

1-ATN   1-aza-5-oxa-6-(1',3'-dithianyl)-7,8-benzo-9-oxobicyclo[4.3.0]nonane

d   distance between adjacent planes in the crystal

D_{calc} calculated density

$F_{(hkl)}$, F, $F_{(000)}$ The structure factor for the unit cell, for the reflection *hkl*. It is the

ratio of the amplitude of the wave scattered by the entire contents of

the unit cell to that scattered by a single electron. A phase angle for

the scattered wave is also involved. $F_{(000)}$ is thus equal to the total

number of electrons in the unit cell.

h, k, l   Miller indices of a reflection

5-HT$_{1A}$ 5-hydroxytryptophan receptor 1A

I   intensity (on an arbitrary scale) for each reflection

1-MPP   1-(2-methoxlphenyl)-4-[4-(2-phthalimido)but-2Eynyl]piperazine

NAN-190   1-(2-methoxlphenyl)-4-[4-(2-phthalimido)butyl]piperazine

R   discrepancy index, $R = \{\Sigma |F_{observed} - F_{calculated}|\}/\{\Sigma F_{observed}\}$

R_w weighted discrepancy index,

$R_w = (\{\Sigma Weight*[F_{observed} - F_{calculated}]^2\}/\{\Sigma Weight*[F_{observed}]^2\})^{1/2}$

S $S = |\Sigma_w (|F_{observed}| - |F_{calculated}|)^2 / (m - n)|^{1/2}$

x, y, z   atomic coordinates as fractions of a, b, and c

Z   number of molecules in a unit cell

α, β, γ Interaxial angles between b and c, a and c and a and b respectively

λ wavelength

σ standard deviation

θ the Bragg angle

ω angle between diffraction vector and plane of χ circle on

diffractometer

List of Contents

CHAPTER ONE

GENERAL INTRODUCTION

Biomineralisation is a complex process. The products and processes of biomineralisation have been partly elucidated over the past few decades and the range of organisms and the diversity of minerals known to be involved in this process is still expanding. The majority (two thirds) of known biomineralisation products are calcium minerals, almost two thirds are hydrated and one quarter consist of colloidal material (Lowenstam, 1981; see Table 1.1).

Two fundamentally different processes of biomineralisation have been identified. Firstly, in some bacteria and in various green and brown algae, bulk extracellular and/or intracellular mineral formation is observed. This process results in polycrystalline aggregates of the mineral constituents, of random orientation (Borowtzka *et al.*, 1974; Bohn *et al.*, 1978). The second system of biomineralisation, the "organic matrix-induced" process, is more elaborate and specific than the first and is observed in numerous animal species. The organism "builds" an organic frame (the extracellular matrix) into which appropriate ions are introduced and then induced to form crystals which then grow. The mineral type, orientation of crystallographic axis and microarchitecture all appear to be under close control. Examples of this system of biomineralisation include bone (Spector and Glimcher, 1973; Hauschka *et al.*, 1975; Cohen-Solal *et al.*, 1978; Glimcher, 1984; Romberg *et al.*, 1986), teeth (Butler *et al.*, 1972; Lee *et al.*, 1977; Glimcher *et al.*, 1979; Termine *et al.*, 1979; Zanetti *et al.*, 1981), the shells of molluscs (Borbas *et al.*, 1991) and the avian egg shell (Silyn-Roberts and Sharp, 1986). Examination of the protein constituents of the extracellular matrix (the "organic matrix") of the mineralised tissues (*e.g.* teeth and bone) of mammals has shown that the non-collagenous, organic fraction contains various phosphoproteins. These phosphoproteins are a heterogeneous group which includes: the phosphophoryns of teeth, the bone phosphoproteins, the caseins of milk, statherin and the acidic proline-rich-phosphoproteins (PRP's) of saliva, osteonectin, the phosphoproteins of egg and mollusc shells, the phosphoproteins of urine and the egg phosvitins.

Mineral Type	Formula	Organism (function)
Calcium Phosphate: Hydroxyapatite	$Ca_{10}(PO_4)_6(OH)_2$	Vertebrates (endoskeletons, teeth, calcium store)
Octa-calcium phosphate	$Ca_8H_2(PO_4)_6$	Vertebrates (precursor phase in bone?)
Amorphous	?	Mussels (calcium store) Vertebrates (precursor phase in bone?)
Calcium Carbonate:		
Calcite	$CaCO_3{}^*$	Algae (exoskeletons) Trilobites (eye lens)
Aragonite	$CaCO_3$	Fish (gravity device) Molluscs (exoskeleton)
Vaterite	$CaCO_3$	Ascidans (spicules)
Amorphous	$CaCO_3.nH_2O$	Plants (calcium store)
Calcium Oxalate:		
Whewellite	$CaC_2O_4.H_2O$	Plants (calcium store)
Weddellite	$CaC_2O_4.H_2O$	Plants (calcium store)
Group IIA metal sulphates:		
Gypsum	$CaSO_4$	Jelly fish larvae (gravity device)

*Includes a range of magnesium-substituted calcites

Table 1.1   The Types and Functions of the main Calcium Minerals found in Biological Systems (Mann *et al.*, 1989)

Phosphoproteins play a very important role in the biomineralisation process; helping to determine mineral type, crystallinity and growth. Phosphoproteins are also important in several, calcium-saturated, exocrine secretions, such as milk and saliva, where part of their function is maintaining the integrity of the secretion.

In spite of the widespread interaction of phosphoproteins with calcium minerals the mechanism and process is little understood and little is known at a fundamental level of the stereochemistry, kinetics or thermodynamics of the interaction. This is undoubtedly due to the inherent problems associated with their study. Such problems include: difficulty in obtaining the phosphoproteins in a pure form, lack of precise secondary and tertiary structural information and the fact that biological calcium phosphates themselves are not easy to define (chemical composition, the levels of impurities and the degree of crystallinity are all variable).

The two most extensively characterised phosphoprotein/calcium mineral systems in biology are, arguably, the acidic proline-rich-phosphoproteins of saliva and the caseins of milk. This thesis is mostly concerned with the adsorption of bovine β-casein A (β-CN A) and its tryptic peptide derivative (β-CN (f1-25)) to the calcium phosphate mineral dicalcium phosphate dihydrate (DCPD; Chapter 3). In addition, investigations into the general features of phosphopeptide/calcium phosphate mineral interaction were undertaken. An attempt was made to grow co-crystals of phosphoserine with calcium ions (Chapter 4) and a phosphorylated dipeptide was synthesised (Chapter 2) which could be used in adsorption experiments and for co-crystallisation with calcium ions. The background to these three separate approaches is contained in the relevant chapter introductions. Thus by combining the results of these studies it was hoped to gain an understanding of the phosphoprotein/calcium mineral interactions which would give information about the formation and structure of casein micelles.

CHAPTER TWO

THE SYNTHESIS OF THE PHOSPHORYLATED
DIPEPTIDE Ser(P)-Ser(P)

2.1 Introduction

The preparation of peptides by chemical synthesis enables the production of large quantities (milligrams or even grams) of highly-pure, highly-specific peptides. The more conventional methods, such as enzyme digestion or acid hydrolysis of a purified, parent protein, are often inferior to chemical synthesis in both quantity and purity. Furthermore, tailor-made (chemically synthesised) peptides are useful for the production of chemical analogues (*e.g.* peptides that contain non-naturally occurring amino acids) which may be used to investigate the relationship between chemical structure and biological function. Synthetic peptides are also useful for the unambiguous assignment of structures to their naturally-occurring counterparts and as simplified, experimental models of proteins.

In the present study, a phosphorylated dipeptide was synthesised in order to examine both its binding to a calcium phosphate phase and its crystal structures (in the presence and absence of calcium ions). Fundamental information (such as the stereochemistry and thermodynamics of its binding) obtained would give some insight into the more complex binding of phosphoproteins to calcium phosphate phases.

2.2. General Conditions for Reactions of Peptide Synthesis

Peptide synthesis is the joining together of chiral amino acids to form chains of pre-determined length and sequence. Formation of a peptide bond consists simply of condensing the carboxyl group of one amino acid to the amino group of another with the elimination of water. However, the dipolar nature of amino acids renders this elimination reaction thermodynamically unfavourable and the excessively high temperatures required would undoubtedly lead to a mixture of peptides together with cyclised, racemised and polymerised reaction products. In order to synthesise a specific peptide in the laboratory, three conditions must be

6

fulfilled. Firstly, the dipolar nature of the reacting amino acids must be destroyed. Secondly, as amino acids are di- or poly- functional, the amino or carboxyl group must be differentiated from the other functional groups. The specific coupling of the carboxyl group of one amino acid to the amino group of another can only be achieved by protecting the functional groups we do not wish to react. Thirdly, the carboxyl group must be activated to allow formation of a peptide bond. The first two requirements are met by the use of suitable protecting agents (R and P in Fig. 2.1; considered in section 2.3), many of which have been developed both for amino groups and carboxyl groups (as well as for the functional groups occurring on the side chains of amino acids). For a protecting group to be suitable it must a) be easy to introduce into the amino acid or peptide, b) protect the functional group under the conditions of amide bond formation and c) be easily removed to leave the peptide bonds intact. The third requirement is met by the introduction of an electronegative substituent (X; see Fig. 2.1) and/or a coupling agent (considered in section 2.4) to enable peptide bond formation to occur with a high efficiency and under mild conditions. In the present case, protecting groups must also be stable under the conditions used for phosphorylation of the peptide, and their removal (deprotection) must leave the phosphate ester bond intact. Lastly, it is necessary to consider the methods available for phosphorylation of synthetic peptides (at serine, threonine or tyrosine residues; section 2.5). Overleaf is a schematic diagram showing the essential features of peptide synthesis (Fig. 2.1).

2.2.1 Assembly of the Peptide - Strategy of Synthesis

After careful consideration of the protecting groups to be used and the method of coupling it is essential to consider the method of assembling the peptide. There are three basic strategies available (reviewed by Bodanszky, 1984), each with its own advantages and disadvantages:
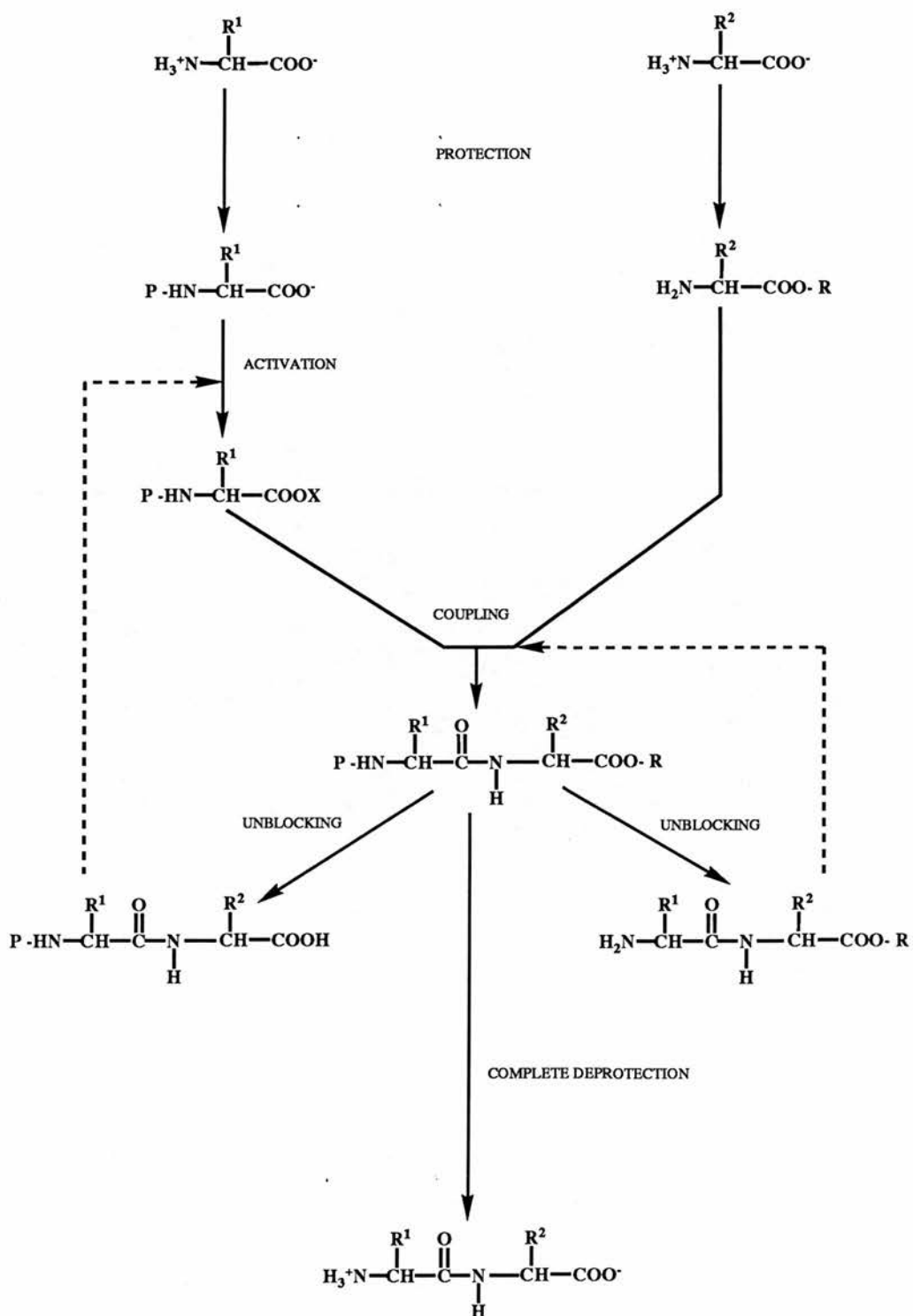
Figure 2.1   Schematic Diagram of Peptide Synthesis

1) Stepwise elongation starting from the C-terminal amino acid.

2) Stepwise elongation starting from the N-terminal amino acid.

3) Fragment condensation - the joining together of smaller peptides.

1) Stepwise Elongation from the C-terminus

This strategy, beginning with the C-terminal residue of the peptide (first amino acid protected at the carboxyl group) is probably the most commonly applied strategy of peptide synthesis. It has the great advantage of producing racemate-free peptide, especially if the protecting groups Z- (benzyloxycarbonyl; see section 2.3.1.1) or Boc- (*tert*-butoxycarbonyl; see section 2.3.1.2) are used. The procedure is shown overleaf (Fig. 2.2).

In addition, this strategy is the one employed for solid phase synthesis of peptides (Merrifield, 1963, 1969). The solid phase method has proved to be extremely important for the synthesis of longer peptides (of more than about 15 amino acids) when solution phase becomes impractical due to low yields, increased risk of racemisation and poor solubility of the peptide.

2) Stepwise Elongation from the N-terminus

This strategy is comparable to that which occurs during protein synthesis *in vivo*. The N-terminal, protected amino acid is activated at the carboxyl group and then coupled to the second amino acid. Elongation proceeds in this manner until the peptide is completed (see Fig. 2.3). Deprotection of the amino group and any side chain protecting groups completes the synthesis.

This strategy assumes that the carboxyl group of the amino component is protected by the addition of a base, by converting the zwitterion form of the amino acid to a salt and thus leaving the amino group free to act as a nucleophile in the acylation reaction. The number of steps, in protection and deprotection, is therefore

9
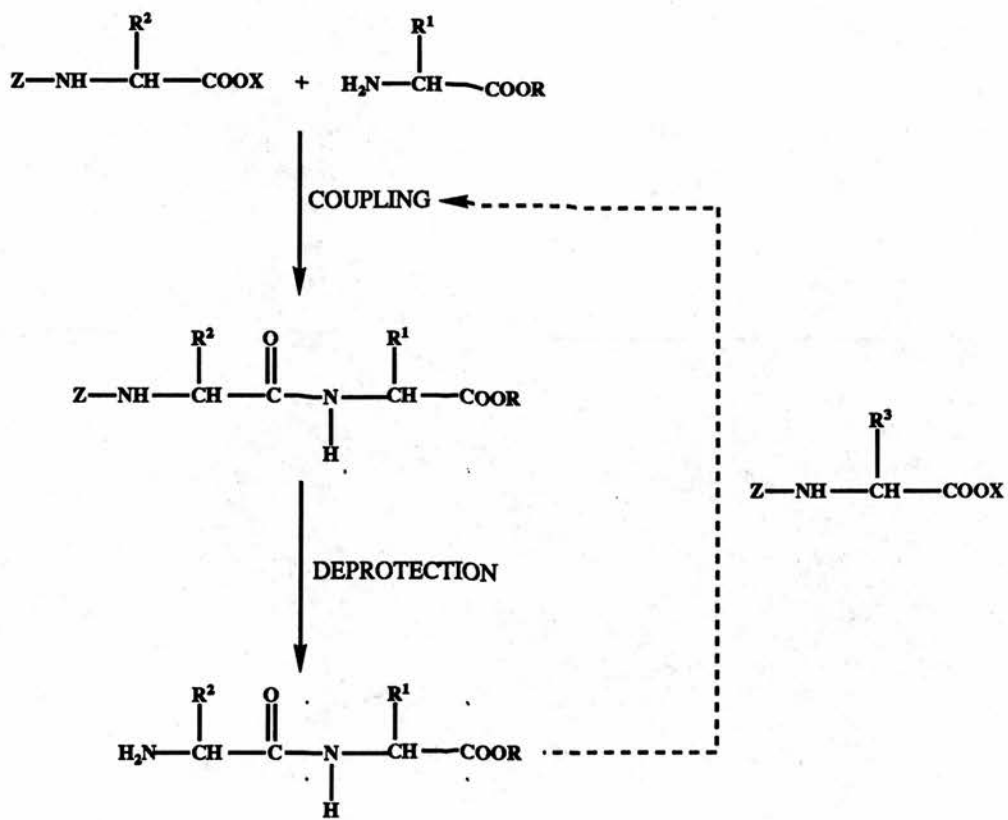
Figure 2.2   Peptide Synthesis - Stepwise Elongation from the C-terminus
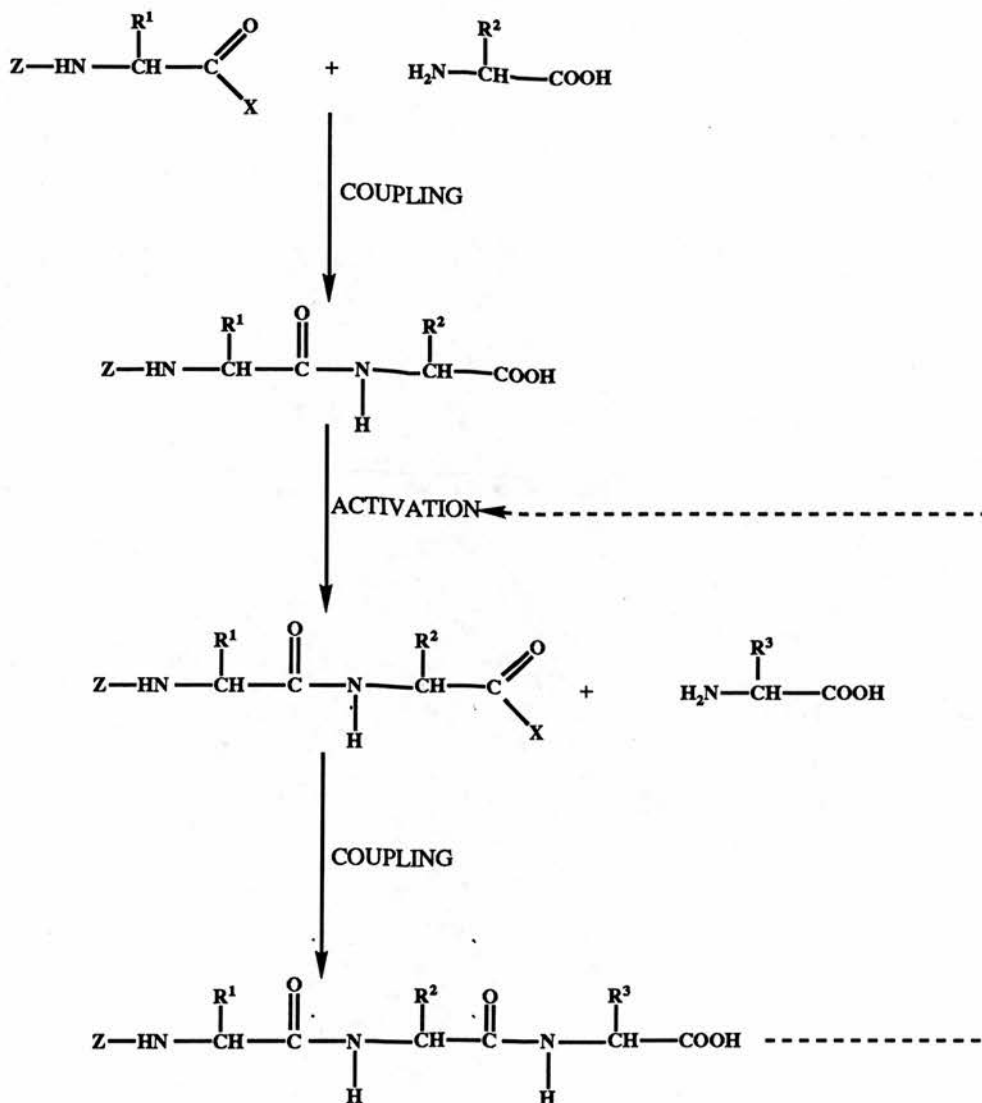
Figure 2.3   <u>Peptide Synthesis - Stepwise Elongation from the N-terminus</u>

11

reduced to a minimum. However, racemisation can occur at the C-terminal residue of the intermediate peptide during activation and coupling. This strategy is of limited value in practical peptide synthesis.

3) Fragment Condensation

As its name implies, this strategy involves taking pre-formed fragments of the peptide and coupling them together. However, care must be taken, as the risk of racemisation is high because it is the carboxyl group of the peptide which has to be activated rather than the protected amino acid (see section 2.6). Racemisation can be minimised by adding of N-hydroxysuccinimide (Zimmerman and Anderson, 1967) or 1-hydroxybenzotriazole (Konig and Geiger, 1970; see section 2.4.1). Due to the inherent problems of racemisation this method is rarely used.

As the peptide to be synthesised in this study was a dipeptide there will be no further consideration of the above strategies.

2.3 Protecting Agents for the Functional Groups of Amino Acids

At present, the choice of protecting agents for amino, carboxyl and side chain functional groups is vast. Final selection depends upon consideration of several factors: the ease of introduction, the extent of protection provided, stability during peptide bond formation and any amino acid side chain modification, protection of the adjacent chiral centre from racemisation and, lastly, ease of removal upon completion of synthesis. For a more complete discussion of protecting agents the reader is referred to the reviews of Schroder and Lubke (1965), Gross and Meienhoffer (1979a) and Bodanszky (1984).

2.3.1 Amino- protecting Groups

The amino group can undergo several reactions unless it is protected. It can be acylated or alkylated and is able to form Schiffs bases and salts. The following sections describe three popular amino-protecting groups.

2.3.1.1 Benzyloxycarbonyl group (Z-)

The introduction of the benzyloxycarbonyl (Z-) group by Bergmann and Zervas (1932) marked the beginning of modern peptide synthesis. N-Benzyloxycarbonyl derivatives have several virtues: they are stable compounds which are readily obtainable in high yields, they protect the amino acid from acylation (Folsch, 1967) and, perhaps most importantly, they protect the amino acid from racemisation.

Another advantage of Z- derivatives is that there are several alternative methods for deprotection: hydrogenolysis (Bergmann and Zervas, 1932; Bergmann *et al.*, 1935), reduction with liquid ammonia (Sifferd and du Vigneaud, 1935), treatment with hydrochloric acid solutions (White, 1934), or solvolysis with hydrogen chloride (Albertson and McKay, 1953) hydrogen bromide (Ben-Ishai and Berger, 1952) or hydrogen iodide (Waldschmidt-Leitz and Kuhn, 1951) in acetic acid. Solvolysis in hydrogen bromide or hydrogenolysis are the most commonly used of these methods.

There are some limitations in using N-benzyloxycarbonyl protection, namely sensitivity to alkali, where formation of hydantoin derivatives may result if the protected amino group is adjacent to a glycine residue (MacLaren, 1958). Also, hydrogenolysis fails if sulphur-containing amino acids are present in the peptide (due to catalytic poisoning). However, these problems can be overcome, to some extent, by the use of dry liquid ammonia as solvent (Kuromizu and Meienhofer, 1974). Other side reactions are possible, such as the formation of N-carboxyanhydrides if

13

acid chloride derivatives of Z-amino acids are heated (Bergmann *et al.*, 1935). In addition, de-methylation and subsequent benzylation of methionine residues occur if hydrogen bromide in acetic acid is used for Z-group removal (Albertson and McKay, 1953; McKay and Albertson, 1957; Guttmann and Boissonnas, 1958). Nevertheless, the success of the N-benzyloxycarbonyl group and a number of modified versions (halo- and nitro- substituted forms) make it the first choice of amino-protecting group for peptide synthesis.

2.3.1.2 *tert*-Butoxycarbonyl group (Boc-)

The t-butoxycarbonyl group was first reported by Carpino (1957) as a general amino protecting group and its application to peptide synthesis followed soon after (Anderson and McGregor, 1957; McKay and Albertson, 1957). Formation of Boc- amino acid derivatives is not as simple as that of Z- derivatives because of the temperature sensitivity (at temperatures above -10°C) of the protecting agent t-butylchloroformate (described by Woodward *et al.*, 1966). However, several alternative methods do exist for the synthesis of Boc- amino acids, in which a more temperature stable protecting agent is employed (Schwyzer *et al.*, 1959; Schwyzer and Rittel, 1961). For example the azide method, which utilises t-butyloxycarbonyl azide as protecting agent, is the most commonly used. Unfortunately this method is not simple and careful temperature control is still required (reaction kept below 5°C) or explosion is likely (Schnabel, 1967).

The Boc-group, unlike the Z-group, is stable to hydrogenolysis and resistant to hydrolysis by alkali but it is easily cleaved by mild acid. Thus Z- and Boc- groups can be used in conjunction on the same molecule allowing selective protection and deprotection. This adds versatility to the synthesis scheme for a complex peptide. Since Boc- groups can be removed with hydrogen bromide in acetic acid, the simultaneous removal of both Z- and Boc- groups is also possible.

2.3.1.3 Trifluoroacetyl group (TFA-)

The TFA- group was first used in peptide synthesis by Weygand and Csendes (1952); protection of the amino acid being achieved by the action of trifluoroacetic acid anhydride on the amino acid. However, there is a great danger of racemisation which can be overcome by performing the reaction in ethyl thiotrifluoroacetic acid in aqueous solution at pH 8-9 (Schallenberg and Calvin, 1955). Sodium, barium or ammonium hydroxide or pyridine solutions are commonly used to deprotect the amino group (Schallenberg and Calvin, 1955).

Summary

The three amino protecting groups discussed above are those most commonly used by peptide chemists, although many others have been reported (Schroder and Lubke, 1965; Gross and Meienhoffer, 1979a; Bodanszky, 1984). Each protecting group has its own individual qualities and selection depends ultimately upon the sequence of the peptide to be synthesised.

2.3.2 Carboxyl- protecting Groups

The prime objective of the substitution of the carboxyl group is not protection but rather release of the amino acid from its zwitterion state. Carboxyl groups can be protected in three general ways: 1) by esterification 2) by hydrazide or amide formation or 3) by salt formation. The most important type of substitution is esterification, three of which are discussed below.

2.3.2.1 Benzyl ester (OBzl-)

Bergmann *et al.* (1935) introduced not only the benzyloxycarbonyl group but also the benzyl ester group. Esterification of the amino acid with benzyl alcohol has the advantage of being a relatively simple procedure resulting in good yields (Brenner and Huber, 1953). The esterification reaction is acid-catalysed; commonly used catalysts being thionyl chloride, p-toluenesulphonic acid and benzenesulphonic acid (Schroder and Lubke, 1965). The reaction is greatly enhanced if the water which forms during the reaction is removed by azeotropic distillation (Lutz *et al.*, 1959). The OBzl- group can be removed by catalytic hydrogenolysis (Haussler, 1960), by treatment with hydrogen bromide in acetic acid (Ben-Ishai, 1954) or by treatment with sodium in liquid ammonia (Roberts, 1954). However, it is not possible to cleave benzyl esters selectively in the presence of N-benzyloxycarbonyl- groups (Z- groups; see section 2.3.1.1). Two modified benzyl ester groups are available; the p-nitrobenzyl (Schwyzer *et al.*, 1959) and p-methoxybenzyl group (Weygand and Hunger, 1962). These groups have the advantage of being stable to hydrogen bromide in acetic acid, which allows selective cleavage of the ester. In addition, the p-nitrobenzyl esters tend to be readily crystallisable which can aid their purification (Schroder and Lubke, 1965).

2.3.2.2 Methyl and Ethyl esters

Along with the benzyl ester group, methyl and ethyl esters are probably most widely used to protect the carboxyl group of amino acids or amino acid derivatives. Moreover, methyl and ethyl esterification is arguably the most convenient method for carboxyl group protection. Esterification is achieved simply by mixing methanol or ethanol with thionyl chloride (which acts as a catalyst) and then adding the amino acid (Brenner and Huber, 1953). Alternative catalysts include phosphorus pentachloride, p-toluenesulphonic acid and sulphuric acid. Carboxyl

groups are usually deprotected by hydrolysis of the alkyl ester with mild alkali in an organic solvent such as methanol, dioxane or acetone. The main disadvantage of these protecting groups is that the use of excess alkali during deprotection may result in cyclisation, racemisation or the formation of urea or hydantoin derivatives (MacLaren, 1958). These esters also form intermediates in the synthesis of peptide bonds *via* the azide method (see section 2.4.2).

2.3.2.3 Tertiary-Butyl Esters (O^{t}Bu)

The introduction of t-butyl esters for use in peptide synthesis (Anderson and Callahan, 1960) was a very important development in protecting group methodology. The t-Butyl esters of amino acids have several advantages over the methyl, ethyl and benzyl esters including their greater stability which allows storage and distillation of the protected amino acid. The O^{t}Bu- amino acid derivatives can be easily hydrolysed in acidic conditions whereas the other esters described above (see section 2.3.2.2) require more vigorous treatment to achieve hydrolysis. t-Butyl esters are prepared by an acid-catalysed, addition reaction of isobutane either to the free amino acid in dioxane (Roeske, 1959) or to N-protected amino acids in dichloromethane (Anderson and Callahan, 1960). The t-butyl ester can be cleaved in several ways: with hydrogen bromide in acetic acid, p-toluenesulphonic acid in benzene or with trifluoroacetic acid.

2.3.3 Protection of Amino Acid Side Chains

If an amino acid side chain contains an active functional group then consideration must be given to its protection. The peptide to be synthesised in this study contained only serine residues, which have free β-hydroxyl groups. The β-hydroxyl group of serine can undergo several undesirable side reactions: elimination reactions, condensation reactions, O-acylation reactions, acid-catalysed

17

N - O acyl shifts and reactions with other amino acids (Schroder and Lubke, 1965; Folsch, 1967). The β-hydroxyl group is usually protected, if the completed peptide is intended to have a free hydroxyl group, by the formation of a benzyl ether (Schroder and Lubke, 1965). Protection of serine derivatives, that are to be O-phosphorylated, would require additional reactions for the selective removal of the β-hydroxyl-protecting groups to allow subsequent phosphorylation. In the reaction scheme which I chose (Fig. 2.9 in section 2.7), the β-hydroxyl group was not protected for the above reason and because side reactions (during peptide bond formation) involving the free hydroxyl group can be avoided if care is taken. As the β-hydroxyl group of serine was not protected during this study no further comment will be made on protection of amino acid side chains. The reader is referred to the reviews of Schroder and Lubke, (1965) and Gross and Meienhoffer, (1979a).

2.4 Formation of the Peptide Bond

The principal reaction of peptide bond formation is acylation of the amino group of an amino acid by the carboxyl group of a second amino acid. A multitude of methods has been developed for peptide synthesis under mild conditions (reviewed by Gross and Meienhoffer, 1979a). Without exception, these methods activate the carboxyl group of an amino protected amino acid or peptide. Activation is the enhancement of the electrophilicity of the carboxyl carbon by introduction of an electronegative substituent (X), which allows peptide bond formation under mild conditions. Three of the most commonly used methods for peptide bond formation are discussed below.

2.4.1 N,N-Dicyclohexylcarbodiimide (DCCI)

This coupling agent was first used to form a peptide bond by Sheehan and Hess (1955). DCCI gives good yields in a relatively short time and has the great

advantage of very little tendency to cause racemisation. The by-product of peptide bond formation is N,N-dicyclohexylurea which is insoluble in most of the solvents used in coupling reactions and therefore is easily removed by filtration. DCCI is usually used to produce N-protected, amino acid, active esters (Elliot and Russell, 1957; Bodansky and du Vigneaud, 1959). The mechanism of coupling was first investigated by Khorana (1955) and was re-investigated by DeTar and Silverstein (1966). These workers proposed that the addition of the N-protected amino acid to the reagent (DCCI) forms an O-acylisourea intermediate (see Fig. 2.4) which can then undergo several reactions.

Firstly, the peptide bond can form as a result of reaction of the amino component of the C-protected amino acid with the intermediate. Secondly, in the presence of acid, addition of a second proton may occur resulting in the formation of a symetrical anhydride together with disubstituted urea which then may acylate the amine. Finally, O - N acyl migration can occur, with the formation of N-acylurea. However, the latter, undesirable by-product can be avoided if the reaction is performed in dichloromethane or acetonitrile (Sheehan *et al.*, 1956).

Use of DCCI as coupling agent may, in some instances, cause racemisation, especially if acyl peptides are being activated. To help avoid this N-hydrosuccinimide (Weygand *et al.*, 1966; Wunsch and Drees, 1966), 1-hydroxybenzotriazole (Konig and Geiger, 1970) or ethyl-2-hydroximino-2-cyanoacetate (Itoh, 1973) can be added to the reaction and the commonly used solvent dimethylformamide (DMF) should be avoided (Bodanszky and Birkhimer, 1960; Schroder and Lubke, 1965).

2.4.2 The Azide Method

This is probably the most highly regarded method for peptide bond formation (Hofmann *et al.*, 1960). The reaction has several steps. The acylamino acid ester is converted to the hydrazide which is then treated with nitrous acid to form the azide.
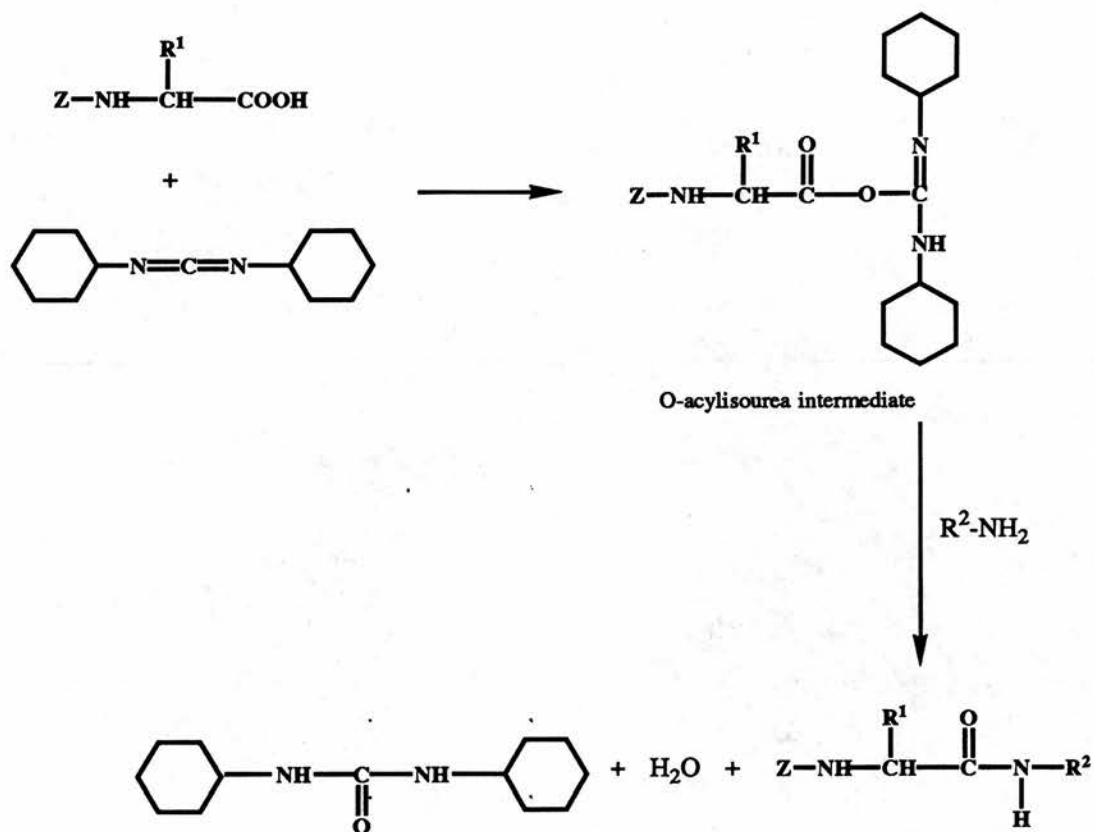
Figure 2.4   N.N-Dicyclohexylcarbodiimide as Coupling Agent

20

The azide is then reacted with the amino acid that is to form the peptide bond under Schotten-Baumann conditions to form the acyldipeptide (see Fig. 2.5). However, problems do exist with this reaction, as the acylazide formed is unstable and can undergo Curtius re-arrangement to form the isocyanate (Curtius, 1904). Nevertheless, this method remains very popular for coupling both peptides and amino acids.

There are a number of methods available for preparing the hydrazide intermediate (*e.g.* Hofmann *et al.*, 1950; Sheehan and Hess, 1955) but care must always be taken to avoid formation of by-products. Favourable conditions for this reaction are a low temperature, a homogenous solution, high acidity and the presence of organic nitrite such as t-butyl nitrite or nitrosyl chloride.

2.4.3 The Mixed Anhydride Method

The mixed anhydride method (Wieland *et al.*, 1950), being compatible with many protecting groups, is used when a rapid coupling reaction is necessary. The mixed anhydride method has several attractive features: high reaction rates at low temperature, ease of manipulation, comparatively high purity of product and readily available and inexpensive reagents (Vaughan and Osato, 1951, 1952). However, unless care is taken, there is a risk of racemisation, but this can be minimised by use of a tertiary base (Anderson *et al.*, 1967).

Formation of the peptide bond, by the mixed anhydride procedure, involves two separate stages: 1) activation of the carboxyl group, *i.e.* generation of a mixed anhydride, and 2) coupling with the amino group (peptide bond formation). Stage 1 is carried out by addition of carbonic acid monoalkyl ester chloride (Wieland and Bernhard, 1951) to a cold solution of the amino protected amino acid in the presence of tertiary base (*e.g.* triethylamine or N-ethylmorpholine; Fig. 2.6A). Anhydrous conditions are required; commonly used solvents include toluene, chloroform, dioxane or tetrahydrofuran (THF). The mixed anhydride formed can then be used
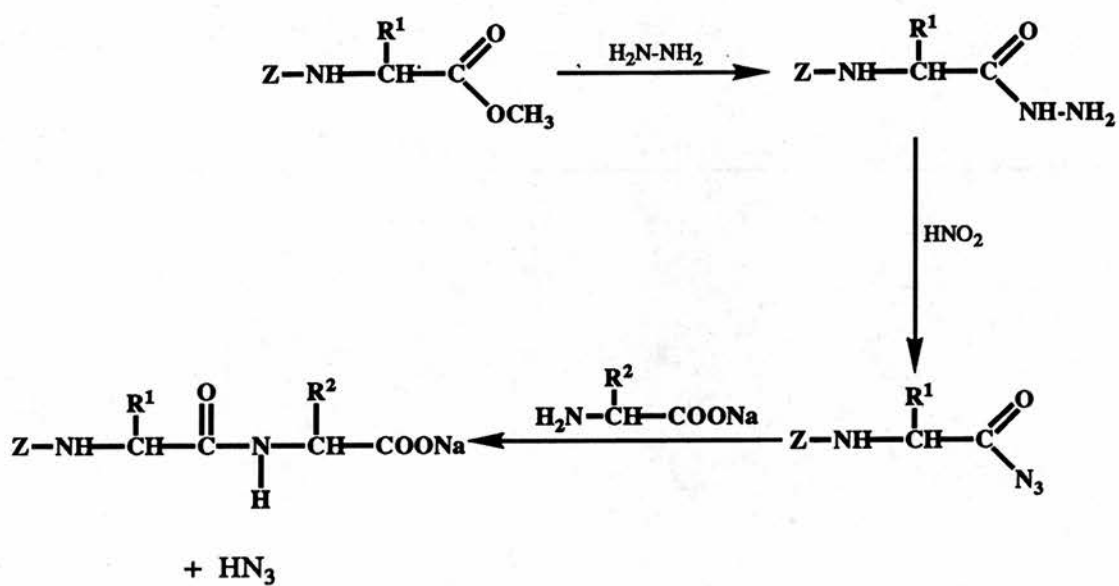
Figure 2.5   The Azide Method

22

$$Z-NH-\overset{\overset{\displaystyle R^1}{|}}{CH}-COO^- \; + \; \left[NH(C_2H_5)_3\right]^+ \; + \; R^2-O-\overset{\overset{\displaystyle O}{\|}}{\underset{Cl}{C}} \longrightarrow Z-NH-\overset{\overset{\displaystyle R^1}{|}}{CH}-\overset{\overset{\displaystyle O}{\|}}{C}-O-\overset{\overset{\displaystyle O}{\|}}{C}-O-R^2$$

$$+$$

$$\left[NH(C_2H_5)_3\right]^+ Cl^-$$
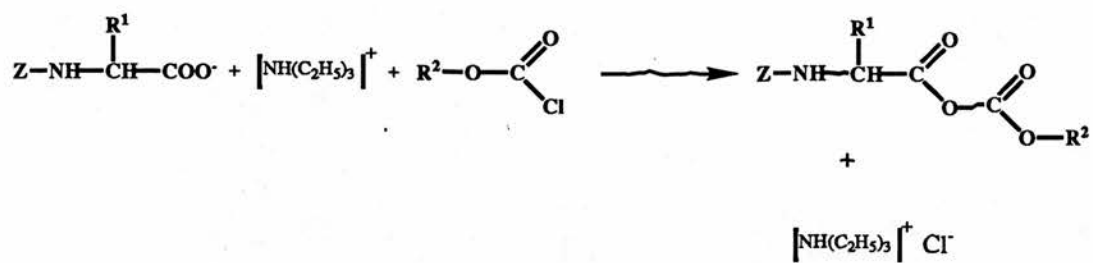
Figure 2.6A   <u>The Mixed Anhydride Method - Stage 1) Activation of the Carboxyl Group</u>

$$Z-NH-\overset{\overset{\displaystyle R^1}{|}}{CH}-\overset{\overset{\displaystyle O}{\|}}{\underset{\underset{\underset{R^2-O}{|}}{\overset{|}{\underset{\|}{C=O}}}}{C-O}} \; + \; H_2N-R^3 \longrightarrow Z-NH-\overset{\overset{\displaystyle R^1}{|}}{CH}-\overset{\overset{\displaystyle O}{\|}}{C}-\underset{\underset{\displaystyle H}{|}}{N}-R^3$$

$$R^2\text{-OH} \; + \; CO_2$$
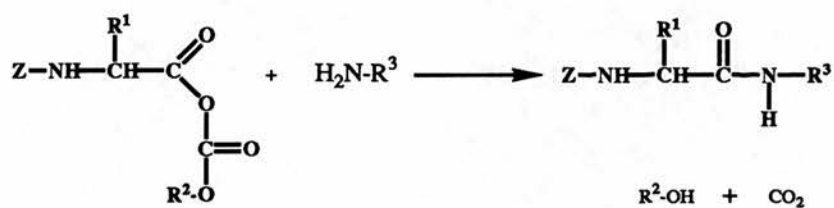
Figure 2.6B   <u>The Mixed Anhydride Method - Stage 2) Peptide Bond Formation</u>

directly in the acylation reaction (stage 2) simply by adding the second amino acid. Peptide bond formation is usually rapid with the liberation of both carbon dioxide gas and the corresponding alcohol as by-products (Fig. 2.6B).

2.5 Phosphorylation of the β-hydroxyl Group of L-serine

Phosphoproteins are widespread in biological systems. Characteristically, they yield their phosphate groups as O-phospho-L-serine (Ser(P)) and, to a lesser extent, O-phospho-L-threonine (Thr(P)), after acid hydrolysis (Donella *et al.*, 1976). Due to the difficulties encountered in the purification and structural determination of the natural phosphopeptides subsequent workers have attempted to obtain peptides containing Ser(P) (and Thr(P)) residues by chemical synthesis (Folsch *et al.*, 1959, 1965, 1966; Theodoropoulos *et al.*, 1960; Alewood *et al.*, 1981; Perich *et al*, 1986a,b; 1987a,b; Schlesinger *et al.*, 1987; Perich and Johns, 1988a,b,c).

Riley *et al.* (1957) were the first to phosphorylate successfully N-carbobenzyloxy-L-serine ethyl ester with diphenylphosphoryl chloride (DPPC), and the synthesis of Ser(P)-containing peptides soon followed (Folsch, 1959). The original phosphorylation methods used aryl- or alkyl- phosphoryl chlorides as phosphorylating agents. However, due to inherent problems associated with these phosphorylating agents, new methods and agents were developed. These include aryl- or alkyl- phosphochloridites and aryl- or alkyl- phosphoramidites (see section 2.5.4). All of these phosphorylation reactions must be carried out under strictly anhydrous conditions.

Synthesis of phosphopeptides is theoretically possible by use of at least two different approaches:

1) Unprotected or suitably protected O-phosphoserine is coupled with amino acid or peptide derivatives.

2) The protected peptide whose sequence includes serine with a free β-hydroxyl group is first synthesised. The hydroxyl group is then phosphorylated and the protecting groups are finally removed.

2.5.1 Coupling of O-phosphoserine to an Amino Acid or Peptide Derivative

Approach 1) has been little used, mainly due to problems incurred with the special solubility and reactivity properties of Ser(P) and its derivatives. L-serine was first phosphorylated by Levene and Schormuller (1934) using phosphorus oxychloride and phosphorus pentoxide. This method has since been refined (Plimmer, 1941; Posternak and Grafl, 1945; Neuhaus and Korkes, 1958). Direct amide bond formation, with the readily available Ser(P), would be of great value since it would eliminate many of the laborious protection steps and also possibly allow phosphopeptides to be synthesised by solid phase methods (Merrifield, 1963, 1969; Atherton and Sheppard, 1989).

However, addition of amide- or carboxyl- protecting groups to Ser(P) has proved to be very difficult (Folsch, 1967). Esterification of the carboxyl group of Ser(P) can be achieved (Brenner and Huber, 1953; Folsch, 1967) but attempts to prepare the benzyl ester have failed (Folsch, 1967). In addition, side reactions involving the unprotected phosphate group, such as elimination reactions and the formation of some types of amide, are suspected (Riley *et al.*, 1957; Folsch, 1967). This route, therefore, was not considered practical for the synthesis of phosphopeptides, and indeed almost all synthetic peptides of Ser(P) reported have been synthesised by approach 2) (namely the phosphorylation of the peptide after synthesis) of which the chemistry has been investigated extensively (reviewed by Folsch, 1967). Even though synthetic phosphopeptides have been produced for some 32 years, their successful synthesis, in good yields, still requires a great deal of care and experience and a certain degree of luck.

25

2.5.2 Phosphorylation of L-serine-containing Peptide Derivatives

Methods for the phosphorylation of serine (see section 2.5.1) use the advantage of the acid stability of Ser(P) and so cannot be used for compounds containing acid labile bonds such as the peptide bond. The first successful synthesis of a peptide derivative of phosphoserine (the second approach outlined in section 2.5) was by Folsch in 1959 who used dibenzylphosphoryl chloride as the phosphorylating agent. There are now a number of phosphorylating agents available which are suitable for peptides, but for many years the two most commonly used were dibenzylphosphoryl and diphenylphosphoryl chloride.

2.5.2.1 Diphenylphosphoryl chloride (DPPC)

Diphenylphosphoryl chloride (DPPC) appears to be a more powerful phosphorylating agent than its benzyl analogues as triester yields of about 90% are obtainable (as opposed to yields of 40-60%; see section 2.5.2.2). The great advantage of DPPC is its stability, allowing phosphorylation to be carried out at room temperature in pyridine solution. However, its major drawback is the slowness of the hydrogenolytic removal of the phenyl groups. Typical reaction conditions are a pure hydrogen atmosphere (at 138 kPa and at room temperature) 80% acetic acid solution as solvent with 1.1 mmol platinum IV oxide per mmol of phenyl group as catalyst (Perich et al., 1986a; Perich and Johns, 1988a). Therefore, the major drawbacks to using DPPC are the expense of the reaction and the need for specialist equipment.

2.5.2.2 Dibenzylphosphoryl chloride (DBPC)

DBPC suffers from several disadvantages compared to its diphenyl analog (DPPC). DBPC is an unstable compound and must be prepared fresh for each

reaction as it decomposes during storage (Atherton *et al.*, 1945, 1948). Triester yields are generally lower than with DPPC, being about 40-60%, and to achieve even these yields the reaction needs to be maintained at -20° to -40°C. The low yields are due to DBPC decomposing during the reaction (Alewood *et al.*, 1984) and to the formation of pyrophosphate analogs of the peptides (Folsch, 1959; Alewood *et al.*, 1984).

However, DBPC has the great advantage that its protecting groups are easily removed. Removal requires palladium on carbon (10%) catalyst, 85% ethanol as solvent (with a few drops of acetic acid) and a pure hydrogen atmosphere for approximately four hours (Folsch, 1959, 1967; Koehn and Kind, 1965). These conditions are relatively mild compared to those required for DPPC.

Summary

Both DPPC and DBPC have several drawbacks as phosphorylating agents for peptides and work is continuing to find more efficient methods and agents. The major disadvantage with both DPPC and DBPC is the low yields after catalytic hydrogenolysis; typically 50 - 60%. Also with large and multi-phosphorylated peptides, incomplete phosphorylation is frequently observed (Johnson and Coward, 1987) which is thought to result from steric hindrance by the bulky protecting groups on the phosphate group (Folsch, 1967; Perich and Johns, 1988a). After catalytic hydrogenolysis a mixture of products results (unphosphorylated, partly phosphorylated and partly deprotected peptide). In addition, the low yields of phosphopeptide(with DPPC is used as phosphorylating agent) are thought to result from pyridine mediated dephosphorylative rearrangement during the product isolation procedure (Perich and Johns, 1990a), resulting in the formation of diphenyl hydrogen phosphate. The rate of dephosphorylation by this route is influenced by the nature of the N- and C- terminal protecting groups (Perich and Johns, 1990a).

2.5.2.3 Bis-(2,2,2-trichloroethyl)phosphoryl chloride (TCPC)

TCPC is a phosphorylating agent that was first used to phosphorylate nucleosides by Eckstein and Scheit (1967). Since then it has been used to phosphorylate nucleosides (Franke *et al.*, 1968; Owen *et al.*, 1976), phosphonamides and phosphoramides (Thorsett *et al.*, 1982) and inositols (Cooke *et al.*, 1989). TCPC has not been used to phosphorylate serine-containing peptides but has been successfully used to phosphorylate Boc-Ser-OBzl (Paquet and Johns, 1990). Removal of the phosphate-protecting (2,2,2-trichloroethyl) groups can be achieved in three ways: by using zinc dust in 80% acetic aacid, by using zinc/copper dust in dimethylformamide (Eckstein and Scheit, 1967) or by using sodium in liquid ammonia (Cooke *et al.*, 1989).

As the phosphate protecting groups can be removed by the relatively simple and inexpensive method of zinc dust in 80% acetic acid (*cf.* DPPC derivatives which require platinum IV oxide catalyst and high pressure hydrogen atmosphere, see section 2.5.2.1) which has been used (Paquet and Johns, 1990) to phosphorylate Boc-Ser-OBzl, TCPC was chosen as a novel, alternative phosphorylating agent for the dipeptide Z-Ser-Ser-OBzl.

2.5.3 New Methods for Phosphorylation of Peptide Derivatives

In 1979, Okawa *et al.* proposed an alternative method for synthesis of phosphopeptides: the aziridine ring opening reaction. This method requires the aziridine peptide to be prepared (Okawa *et al.*, 1975) which is then phosphorylated with either dibenzylphosphoric acid or with 85% phosphoric acid. This method gives good yields of about 70%, but because of the added complication of having to prepare the aziridine peptide before proceeding, this method has proved to be unpopular. Therefore, until 1986, dibenzyl- and diphenyl- phosphoryl chloride featured prominently in the synthesis of phosphopeptides on account of the ready

28

availability or preparation of these phosphorylating agents and of the relatively simple phosphorylation procedure.

In 1982, Alewood *et al.* introduced a novel method for phosphorylation of peptides using diethylphosphochloridite as phosphitylating agent. This method also allowed the rapid synthesis of a protected phospho-amino acid, suitable for incorporation in solution or solid phase peptide synthesis (previous methods required phosphorylation to be performed at the end of peptide synthesis, see section 2.3.3). However, the drastic reaction conditions required to remove the diethyl- protecting groups (Kitas *et al.*, 1988) make this phosphitylating agent unsuitable for phosphopeptide synthesis. More recent investigations have given rise to two new methods of phosphopeptide preparation, using either phosphite triesters or phosphoramidites as phosphitylating agents.

Perich and Johns (1987b) reported the extremely efficient reactions (yields > 90%) of primary, secondary and tertiary alcohols with N,N-diethyl dibenzyl phosphoramidite as phosphitylating agent. Soon after, de Bont *et al.* (1987) used this same method to phosphorylate protected serine and threonine derivatives which were then successfully coupled to Boc-Ala with final yields of approximately 80%. Several similar phosphitylating agents have also been reported, these include: bis[2,2,2-trifluoroethyl] phosphite (Gibbs and Larsen, 1984) dimethyl-, diphenyl- and diethyl- phosphochloridite (Perich *et al.*, 1986b), S,S-diphenyl phosphorodithioate (Kuyl-Yeheskiely *et al.*, 1987, 1988), N,N-diethylphosphoramidite (Perich and Johns, 1988b), diisopropyl phosphite (Ji *et al.*, 1988), N,N-diethylamino-dibenzylphosphoramidite (de Bont *et al.*, 1988) di-t-butyl N,N-diethylphosphoramidite (Bannworth and Tzeciak, 1987; Perich and Johns, 1988c, 1990b; Staerkaer *et al.*, 1991) and dibenzyl N,N-diethylphosphoramidite (Perich and Johns, 1990c)

These new developments in phosphorylation techniques have allowed previously impractical methods to be exploited. For example, the synthesis of a phosphopeptide entirely by solid phase methods (Lacombe *et al.*, 1990) and the

coupling of protected phosphorylated amino acids to pre-existing peptides (Perich and Johns, 1988b,c; Meggio *et al.*, 1991). However, most of these phosphitylating agents have to be synthesised prior to each reaction as they decompose upon storage. These new methods also appear to overcome one of the major problems of peptide phosphorylation (using DPPC or DBPC): obtaining the phosphopeptide in a pure form.

2.6 The Problem of Racemisation

To produce a biologically active peptide it is essential to maintain a high degree of optical purity throughout synthesis as, unfortunately, racemisation can occur at every stage of synthesis. To prevent racemisation, careful selection of protecting groups and coupling agents is essential. Loss of optical purity during synthesis has lead to extensive investigations into possible mechanisms and hence to knowledge of how racemisation may be overcome (reviewed by Bodanszky and Ondetti, 1966; Gross and Meienhofer, 1979a,b; Bodanszky, 1984). Such investigations have lead to the proposal of two possible mechanisms: a) base-catalysed racemisation and b) the formation of a 5-oxazolone intermediate which can undergo internal nucleophilic attack and so racemise.

Withdrawal of a proton from the chiral α-carbon tends to occur in amino acids or Z-amino acids that have an electronegative group in the β- position (*i.e.* phenylalanine, cysteine, serine or threonine). These amino acids can undergo base-catalysed racemisation (Bohak and Katchalski, 1963; Liberek, 1963). The functional group at the β-carbon facilitates proton abstraction from the α-carbon atom and so removes the chiral centre (MacLaren *et al.*, 1958; see Fig. 2.7).

The second mechanism proposed involves the formation of a 5-oxazolone intermediate. This can occur if an N-acyl-α-amino acid derivative is sufficiently electronegative to undergo internal nucleophilic attack. The presence of base tends
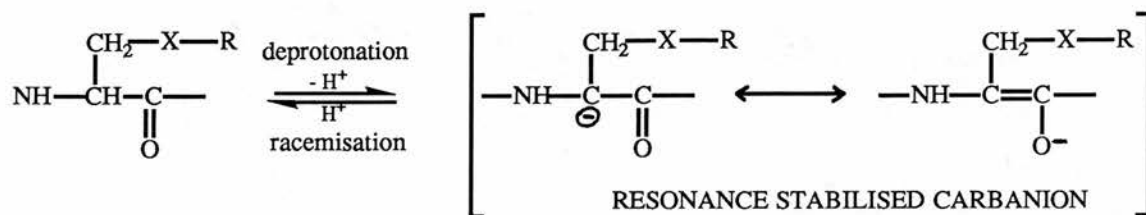
Figure 2.7   Base Catalysed Racemisation

31

RESONANCE STABILISED OXAZOLONE INTERMEDIATE
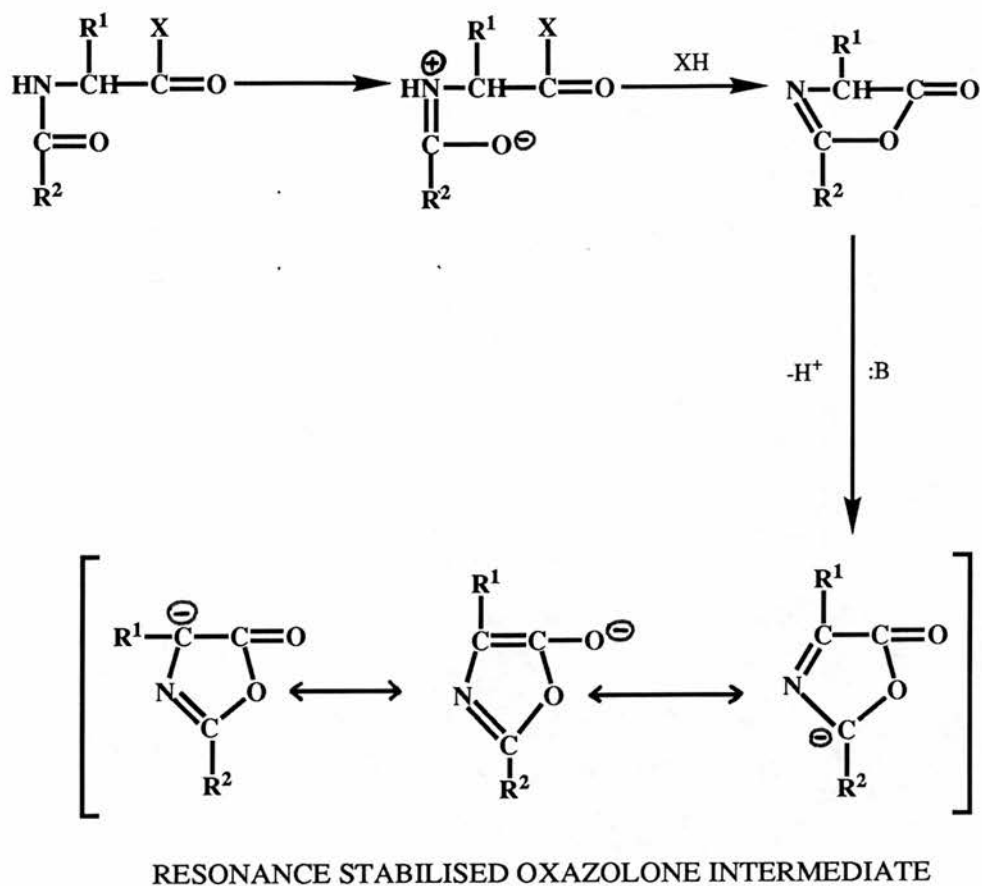
Figure 2.8   Formation of the 5-Oxazolone Intermediate

to cause the loss of a proton and the resonance-stabilised, oxazolone intermediate anions form (Barrass and Elmore, 1957; see Fig. 2.8).

There are several strategies that can be adopted in order to reduce the problem of racemisation: using the step-wise strategy for peptide synthesis (see section 2.2.1) or the azide method for coupling (see section 2.4.2), or glycine or proline as the carboxyl component (which is not always possible) and, finally, certain additives can be used when N,N-dicyclohexylcarbodiimide is the coupling agent (see section 2.4.1).

2.7 Methods Adopted for Peptide Synthesis

To synthesise the dipeptide Ser(P)-Ser(P), the method of Folsch (1959) was followed with a few modifications to improve overall yields and final purity. Essentially, the amino group of one sample of serine was protected with the Z- group and the carboxyl group of another, with the OBzl- group. The resulting Z-Ser and Ser-OBzl were then coupled using N,N-dicyclohexylcarbodiimide (DCCI) as coupling agent. This protected dipeptide was then phosphorylated with either diphenylphosphoryl chloride (DPPC) or bis-(2,2,2-trichloroethyl)phosphoryl chloride (TCPC). Deprotection was then effected by catalytic hydrogenolysis, or in the case of the TCPC derivative, by treatment with zinc dust in 80% acetic acid. The method used is illustrated in the schematic diagram overleaf (see Fig. 2.9)

2.7.1 General Materials and Methods

All chemicals were purchased from Aldrich Ltd. unless otherwise stated. Melting points were determined in open capillaries in a Gallenkamp melting point apparatus and are uncorrected.

[1]H-n.m.r. spectra were recorded on a Bruker WP-200 (80 MHz) spectrometer and a Bruker WP-200 (200 MHz) spectrometer by Mr. J Millar and Dr. D. Reed,

(3)   Z-Ser-Ser-OBzl with OH groups above and below

$(Cl_3CCH_2)-O$ $O-(CH_2CCl_3)$
        $P=O$
         Cl

+

→ Pyridine →

$(Cl_3CCH_2)-O$ $O-(CH_2CCl_3)$
        $P=O$
         O
    Z-Ser-Ser-OBzl   (5)
         O
        $P=O$
$(Cl_3CCH_2)-O$ $O-(CH_2CCl_3)$

↓ Pd/C
  H_2

$(Cl_3CCH_2)-O$ $O-(CH_2CCl_3)$
        $P=O$
         O
      Ser-Ser   (7)
         O
        $P=O$
$(Cl_3CCH_2)-O$ $O-(CH_2CCl_3)$

Ser(P)-Ser(P) ← Zn / 80% acetic acid ←

(8)

Figure 2.9

35
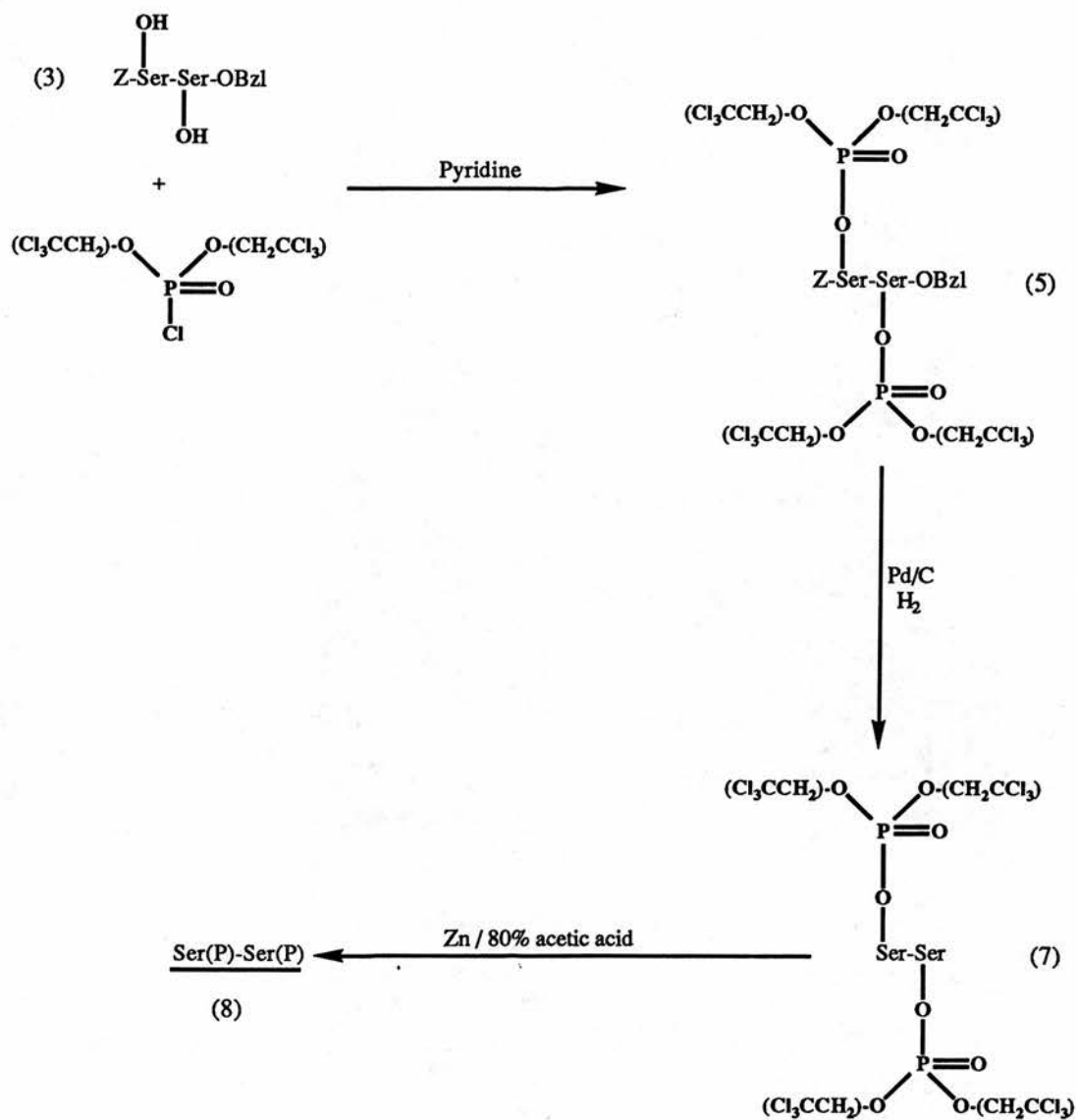
Department of Chemistry, University of Edinburgh and interpreted with the help of Mr. D. Will, Department of Chemistry, University of Edinburgh. ^{31}P-n.m.r. spectra were recorded on a Jeol FX-90Q spectrometer by Mr. D. Will, Department of Chemistry, University of Edinburgh.

Fast atom bombardment (FAB) mass spectra were recorded on a Kratos MS 50 TC mass spectrometer by Mr. A. Thomas, Department of Chemistry, University of Edinburgh.

C,H,N analysis was performed by Butterworth Laboratories Ltd., Middlesex.

Thin layer chromatography (t.l.c.) of the protected peptide was performed on pre-coated silica plates of silica 60 (220-440 mesh ASTM) and 0.2 mm thickness (by Merck), purchased from Fluka, eluting with the following solvent systems:

a) Dichloromethane/Methanol   (9:1 v/v)

b) Dichoromethane/Ethyl acetate   (1:1 v/v)

c) Dichoromethane/Ethyl acetate   (3:1 v/v)

d) Hexane/Ethyl acetate   (1:1 v/v)

e) Dichloromethane/Methanol/Acetic acid   (10:2:1 v/v)

f) n-Butanol/Acetic acid/Water   (3:1:1 v/v/v)

Thin layer chromatography (t.l.c.) of the deprotected peptide was performed on pre-coated cellulose plates (Art. 5577 DC-Plastikfolien Cellulose) of 0.1 mm thickness, purchased from Merck, eluting with:

g) Pyridine/Water   (8:2 v/v)

h) n-Butanol/Acetic acid/Water   (4:1:5 v/v/v)

i) Ethanol/Water   (7:3 v/v)

The protected peptide was visualised by u.v. absorption, or with 0.5 mM potassium permanganate or with 1% (w/v) ninhydrin in ethanol. The de-protected

peptide was visualised with 1% (w/v) ninhydrin in ethanol. Protected phosphorylated peptide was purified by column chromatography using silica gel 60 (230-400 mesh ASTM), of particle size 0.04-0.063 mm, purchased from Fluka.

2.7.2 Synthesis of L-Seryl-O-benzyl ester-p-toluenesulphonate (1)

Synthesis of (1) was by the technique of azeotropic distillation as described (Miller and Waelsch, 1952; Folsch, 1959). Briefly, 4.2 g (40 mmol) of serine (Sigma Chemical Co.) and 8.0 g (42 mmol) of p-toluenesulphonic acid were dissolved in 20 ml of hot benzyl alcohol (Cipera and Nicholls, 1955). Hot carbon tetrachloride was added and the solution distilled until no more water was formed (approximately 3-5 hr). The ester salt (1) was then precipitated with dry diethyl ether, and after about 18 hr at 4°C was collected by filtration.

Crude (1) was then purified by re-crystallisation from methanol/diethyl ether, after which analysis by t.l.c. in solvent systems a (R_f 0.31) and b (R_f 0.2) showed one spot indicating a single compound. Yields were approximately 72% and the melting point range was 115-117°C. The following analytical results were obtained for (1):

^{1}H-n.m.r. 'δ_H (p.p.m.) [200.130 MHz, D$_6$-DMSO] 7.78-7.04 [9H, m, (ArH)] 5.19 [2H, s, (bzl CH_2)] 4.05-4.13 [1H, t, (αCH)] 4.04-3.93 [2H, d, (βCH_2)] 2.32 [3H, s, (CH_3)]

2.7.3 Synthesis of N-Benzyloxycarbonyl-L-serine (2)

Synthesis of (2) was by the method of Baer and Maurukas (1955). Briefly, 12.5 g (0.31 mol) of magnesium oxide and 10.5 g (0.1 mol) of serine were mixed with 175 ml of water and 80 ml of diethyl ether in a flask (on ice). To the flask, 26.4 g of benzyl chloroformate was added, dropwise. After 2 hours the flask was

removed from the ice bath and the reaction allowed to continue for a further 30 min. The magnesium oxide was then removed by filtration, and the aqueous phase washed with diethyl ether. The aqueous phase was then chilled to 4°C, acidified to pH 3.44 with 5 M hydrochloric acid and, after 12 hr, a precipitate of crude (2) was isolated by filtration. Crude (2) was purified by re-crystallisation from ethyl acetate/light petroleum spirit (40-60°C), and t.l.c. in solvent systems a (R_f 0.76) and b (R_f 0.42) showed one spot indicating a single compound. Yields were approximately 70% and the melting point range was 119-120°C. The following analytical results were obtained for (2)

^{1}H-n.m.r. 'δ_H (p.p.m.) [200.130 MHz, D_6-DMSO] 7.36-7.2 [5H, m, (ArH)] 5.1 (2H, s, (bzl CH_2)] 4.38-4.19 [1H, m, (αCH)] 3.94-3.81 [2H, t, (βCH_2)]

2.7.4 Synthesis of N-Benzyloxycarbonyl-L-seryl-L-serine-O-benzyl ester (3)

Synthesis of (3) was by two methods, that of Schlesinger *et al.* (1987) and that of Folsch, (1959) both of which use N,N-dicyclohexylcarbodiimide as coupling agent.

2.7.4.1 Method of Schlesinger *et al.* (1987) for Preparing (3)

A total of 20 mmol of (1) was dissolved in 30 ml of dimethylformamide containing 20 mmol of triethylamine. 20 mmol of (2) was dissolved in 50 ml of dimethylformamide containing 20 mmol of N,N-dicyclohexylcarbodiimide. The two solutions were mixed at 0°C and the reaction was allowed to continue overnight at room temperature. The dicyclohexylurea formed was removed by filtration, the solvent was evaporated and the oily residue dissolved in ethyl acetate. The residue was then washed successively with 1) 10% (w/v) potassium hydrogen sulphate (three times), 2) water, 3) 10% (w/v) sodium bicarbonate (three times) and 4) water. The

38

ethyl acetate solution was then dried over anhydrous magnesium sulphate. The crude product was re-crystallised from ethyl acetate/light petroleum spirit (40-60°C), and analysis by t.l.c in solvent systems a (R_f 0.56) and c (R_f 0.38) showed one spot indicating a single compound. Yields were 61% and the melting range for (3) was 152-154°C. The following analytical results were obtained.

[1]H-n.m.r. 'δ_H (p.p.m.) [200.130 MHz, D_6-DMSO]

8.20 [1H, d, NH, $J_{NH-\beta CH}$ = 7.7 Hz] 7.35-7.27 [11H, m, (NH), (Ar-H)]

5.17-5.03 [5H, m, (bzl- CH_2), (OH)] 4.91 [1H, t, (OH), $J_{OH-\beta CH2}$ = 5.6 Hz]

4.43 [1H, d of t, (α-CH), $J_{\alpha CH-\beta CH2}$ = 4.3 Hz, $J_{\alpha CH-NH}$ = 7.7 Hz]

4.23-4.13 [1H, m, α-CH] 3.83-3.37 [obscured by H_2O signal, m, (β-CH_2)]

[13]C-n.m.r. 'δ_c (p.p.m.) [50.130 MHz, D_6-DMSO] 54.65 (CH), 56.98 (CH), 61.17 (CH_2), 61.71 (CH_2), 65.43 (CH_2), 65.86 (CH_2), 127.49 - 128.29 (Ar-CH, overlapping), 135.83 (Ar-C), 136.85 (Ar-C), 155.88 (CO), 170.22 (CO), 170.29 (CO)

FAB mass spectra for $C_{21}H_{24}N_2O_7$ calc.: 416.16616 found: 416.16614 (< 1 p.p.m.)

2.7.4.2 Method of Folsch (1959) for Preparing (3)

A total of 20 mmol of (1), 20 mmol of triethylamine and 20 mmol of (2) were dissolved in 150 ml of tetrahydofuran : acetonitrile (1:1 v/v) and then cooled to 0°C. To this solution was added 20 mmol of N,N-dicyclohexylcarbodiimide. The reaction was then allowed to continue overnight at room temperature. The following day the precipitated dicyclohexylurea was removed by filtration and the filtrate poured into 3.0 litres of ice-cold water. After 12 hr at 4°C the precipitated

(3) was removed by filtration and dried *in vaccuo*.   Crude (3) was further purified by re-crystallisation from ethyl acetate/light petroleum spirit (40-60°C), and analysis by t.l.c. in solvent systems a (R_f 0.56) and c (R_f 0.38) showed one spot indicating a single compound.   Yields were 71% and the melting point range was 152-154°C. The following analytical results were obtained.

^{1}H-n.m.r. 'δ_H (p.p.m.) [200.130 MHz, D_6-DMSO]

8.20 [1H, d, N*H*, $J_{NH-\beta CH}$ = 7.7 Hz] 7.35-7.27 [11H, m, (N*H*), (Ar-*H*)]

5.17-5.03 [5H, m, (bzl- C*H*$_2$), (O*H*)] 4.91 [1H, t, (O*H*), $J_{OH-\beta CH2}$ = 5.6 Hz]

4.43 [1H, d of t, (α-C*H*), $J_{\alpha CH-\beta CH2}$ = 4.3 Hz, $J_{\alpha CH-NH}$ = 7.7 Hz]

4.23-4.13 [1H, m, α-CH] 3.83-3.37 [obscured by H_2O signal, m, (β-C*H*$_2$)]

^{13}C-n.m.r. 'δ_c (p.p.m.) [50.130 MHz, D_6-DMSO] 54.65 (CH), 56.98 (CH), 61.17 (CH$_2$), 61.71 (CH$_2$), 65.43 (CH$_2$), 65.86 (CH$_2$), 127.49 - 128.29 (Ar-CH, overlapping), 135.83 (Ar-C), 136.85 (Ar-C), 155.88 (CO), 170.22 (CO), 170.29 (CO)

FAB mass spectra for $C_{21}H_{24}N_2O_7$ calc.: 416.16616 found: 416.16614 (< 1 p.p.m.)

Anal. calc. for $C_{21}H_{24}N_2O_7$ (Mr 416.17): C 60.6, H 5.81, N 6.73, found: C 60.31, H 5.69, N 6.65

2.7.5 Phosphorylation of N-benzyloxycarbonyl-L-seryl-L-serine-O-benzyl ester (3)

Two methods of phosphorylating (3) were compared.   The first used diphenylphosphoryl chloride following the method of Folsch (1959).   The second method used Bis-(2,2,2-trichloroethyl)phosphoryl chloride according to the method

of Eckstein and Scheit, (1967) for the phosphorylation of nucleosides (see section 2.5.2.3).

2.7.5.1 Phosphorylation of (3) with diphenylphosphoryl chloride (DPPC).

To a solution of 10 mmol of (3) in 10 ml of anhydrous pyridine (on ice) was added, dropwise, 22 mmol of diphenylphosphoryl chloride. The solution was kept at 0^oC for 2 hr and then at room temperature overnight. Excess acid chloride was destroyed with water, the solution was then mixed with ethyl acetate and the aqueous phase was discarded. The ethyl acetate phase was then washed successively with 1) 20% (w/v) citric acid (three times), 2) water, 3) saturated sodium bicarbonate solution (three times) and 4) water. The ethyl acetate solution was dried over anhydrous magnesium sulphate, the solvents were then evaporated leaving a pale yellow oil (4). Yields were 90%. Crude (4) was further purified by flash column chromatography (Still *et al.*, 1978) using silica gel 60. The solvent system that gave the best purification was found to be dichloromethane, eluting with a 2.5-20% (v/v) methanol gradient. Afterwards, analysis by t.l.c. using solvent systems a (R_f 0.77) and c (R_f 0.66) showed one spot indicating a single compound. The following analytical results were obtained for (4):

^{1}H-n.m.r. 'δ_H (p.p.m.) [200.130 MHz, CDCl$_3$] 7.47-7.04 [30H, m, (Ar-*H*)]
5.16-5.02 [4H, m, (bzl C*H*$_2$)] 4.79-4.75 [1H, m, (α C*H*)]
4.60-4.05 [5H, m, (α-C*H*, β–C*H*$_2$)]

^{31}P-n.m.r. 'δ_P (p.p.m.) [CDCl$_3$] -11.579

FAB mass spectra for C$_{45}$H$_{44}$N$_2$O$_{13}$P$_2$ calc.: 880.22402 found: 880.22407
(< 1 p.p.m.)

41

2.7.5.2 Phosphorylation of (3) with

Bis-(2,2,2-trichloroethyl)phosphoryl chloride (TCPC).

To a solution of 25 mmol of Bis-(2,2,2-trichloroethyl)phosphoryl chloride in 3.0 ml of anhydrous pyridine (on ice) was added dropwise 10 mmol of (3) in 4.0 ml of anhydrous pyridine.   After 2 hr at room temperature, water was added, and the solution mixed with ethyl acetate.   The aqueous phase was then discarded and the ethyl acetate phase washed with 1) 20% (w/v) citric acid (three times), 2) water, 3) saturated sodium bicarbonate solution (three times), and 4) water.   The ethyl acetate solution was dried over anhydrous magnesium suphate and the solvent evaporated to leave a pale red oil (5);   yields were 90%.   Crude (5) was further purified by flash column chromotography (Still *et al.*, 1978) using silica gel 60.   The solvent system that gave the best purification was found to be dichloromethane eluting with a 2.5-20% (v/v) ethyl acetate gradient.   After this, analysis by t.l.c. using solvent systems a (R_f 0.82), c (R_f 0.61) and d (R_f 0.41) showed one spot indicating a single compound.   The following analytical results were obtained for (5):

[1]H-n.m.r. 'δ_H (p.p.m.) [CDCl$_3$] 7.52-7.25 [10H, m, (Ar-*H*)]

5.25-5.07 [4H, m, (bzl-C*H*$_2$)] 4.87-4.82 [1H, m, (α C*H*)]

4.71-4.41 [13H, m, (α-C*H*, β-C*H*$_2$, Cl$_3$C*H*$_2$)]

[31]P-n.m.r. 'δ_P (p.p.m.) [CDCl$_3$] -3.5, -4.038

FAB mass spectra for C$_{29}$H$_{30}$Cl$_{12}$N$_2$O$_{13}$P$_2$, calc.: 1101.74752

found: 1101.74751 (<1 p.p.m.)

2.7.6 Hydrogenolysis of Protected, Phosphorylated Dipeptide

The next step in the synthesis of O-phospho-L-seryl-O-phospho-L-serine was to remove the protecting groups from (4) and (5). This was achieved by catalytic hydrogenolysis.

2.7.6.1 Hydrogenolysis of Diphenylphosphoryl Chloride Derivative: (4)

3.7 mmol of (4) was dissolved in 10 ml of propan-2-ol:water:acetic acid (50:5:0.5 v/v/v) and 200 mg of palladium on carbon (10%) catalyst was added. These were then maintained in a pure hydrogen atmosphere for 3 hr or until hydrogen consumption ceased (Folsch, 1959). The catalyst was removed by filtration though celite, and the solvents evaporated. The residue was found to contain, by t.l.c. analysis (in solvent systems a (R_f 0.07), e (R_f 0.52) and f) and by ^{1}H-n.m.r., O-diphenylphosphorylated peptide (see section 2.5.2.2). The residue was therefore re-hydrogenolysed by dissolving in 80% acetic acid with 1.1 mmol of platinum (IV) oxide catalyst (Adams type) in a pure hydrogen atmosphere (138 kPa) for 16 hr (Perich and Johns, 1986a; see section 2.5.2.1). Then the catalyst was removed by filtration through celite and the solvents were evaporated, leaving a white solid (6). Analysis of (6) by t.l.c using solvent systems g, h and i indicated the presence of at least three componants. Therefore (6) was purified by ion-exchange chromatography (see section 2.7.7).

2.7.6.2 Deprotection of bis-(2,2,2-trichloroethyl) Derivative: (5)

The deprotection of derivative (5) required two independent steps in order to remove the protecting groups; first, catalytic hydrgenolysis to remove the Z- and OBzl-protecting groups followed by treatment with zinc in acetic acid two remove the (2,2,2-trichloroethyl)- protecting groups.

43

2.7.6.2.a Catalytic Hydrogenolysis

3.7 mmol of (5) was dissolved in 50 ml of propan-2-ol:water:acetic acid (50:5:0.5 v/v/v) and 200 mg of palladium on carbon (10%) catalyst was added, which was then maintained in a pure hydrogen atmosphere for 3 hr (or until hydrogen consumption ceased).   Then the catalyst was removed by filtration through celite, and the solvents evaporated to leave a white solid (7).   Analysis of (7) by t.l.c. in solvent system f showed one spot (R_f 0.64).

2.7.6.2.b Removal of (2,2,2-trichloroethyl)- groups from (7)

3.7 mmol of (7) was dissolved in 30 ml of 80% acetic acid with 44.4 mmol (12 equivalents) of zinc dust (Eckstein and Scheit, 1967).   This was then stirred at room temperature for 4 hours.   Analysis of the mixture by t.l.c. (in solvent system f) indicated the complete removal of 2,2,2-trichloroethyl- groups.   The remaining zinc dust was then removed by filtration through celite and the solvents evaporated to leave a white solid (8).

2.7.7 Purification of Ser(P)-Ser(P) by Ion-exchange Chromotography

The fully deprotected dipeptide Ser(P)-Ser(P) was purified from the crude samples (6) and (8) by ion-exchange chromatography using Dowex 1-X2 resin (Strid, 1959).   Dowex 1-X2 resin was first converted to the formate form by equilibration in 2.0 M sodium formate buffer pH 5.5 as described by Strid (1959). The resin was then re-suspended in 0.1 M formic acid and a column formed (26 x 230 mm) according to the manufacturer's instructions.

Crude dipeptide ((6) or (8)) was applied (100 mg samples) to the column, the flow rate being 3.4 mlh^{-1}cm^{-2}, and elution was effected by a linear gradient of

pyridine formate, from 0.0 to 1.25 M (pH 4.5), of 600 ml volume.   Fractions of 6.0 ml were collected which were analysed for the presence of amide bonds using the ninhydrin assay described by Moore and Stein (1954 a,b).

The elution profiles obtained from samples (6) and (8) are shown in Figs. 2.10, 2.11.   For crude dipeptide sample (6) two peaks were detected, and for crude dipeptide sample (8) three peaks were detected with the ninhydrin assay. Fractions were pooled as indicated, discarding any overlapping fractions, and the solvents evaporated.   A small amount of water was then added and the final traces of pyridine removed by use of Dowex 50(H^+) resin by the batch method (Folsch, 1959; Strid, 1959).   Each sample was then lyophilised and analysed by FAB mass spectrometry.   In each case, the peak eluting at 0.9 M pyridine formate, was found to be the dipeptide Ser(P)-Ser(P), and final yields were approximately 50%.   In every case the peak eluting at approximately 0.9 M pyridine formate was analysed by t.l.c. in solvent systems g, h and i (Folsch, 1959; 1966), and their R_f values standardised against phosphserine, *i.e.*

$$R_{Ser(P)} = \frac{R_f \text{ for the compound}}{R_f \text{ for phosphoserine}}$$

The $R_{Ser(P)}$ for Ser(P)-Ser(P) was found to be 0.5 (in solvent system g).

Analytical results for Ser(P)-Ser(P) are given below:

Ser(P)-Ser(P) phosphorylated with DPPC

^{1}H-n.m.r. 'δ_H (p.p.m.) [80.131 MHz, D_2O]

4.70 - 4.69 [obscured by H_2O signal, m, (αCH)]

4.61 - 4.28 [4H, m, (βCH_2)]
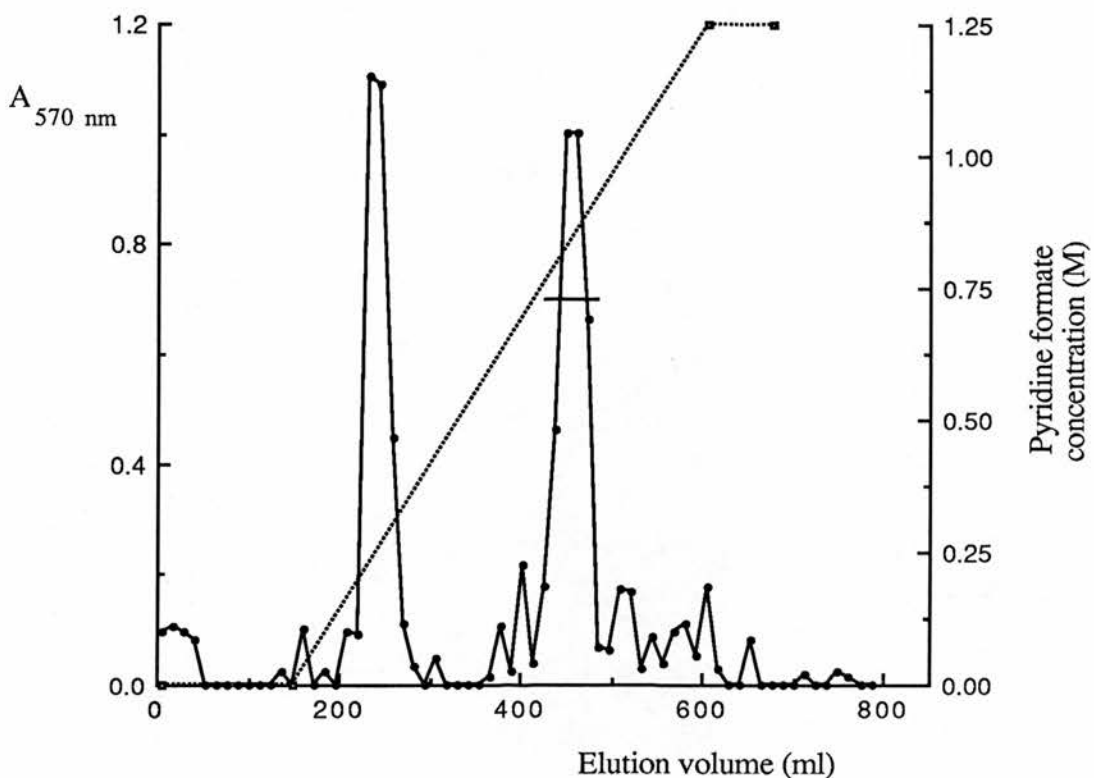
Figure 2.10   Dowex 1X-2 Ion-exchange Column Elution Profile for Sample (6)

Crude dipeptide sample (6) was applied to the Dowex 1X-2 ion-exchange column as described in section 2.8.6. Eluant was analysed for the presence of amine bonds using the ninhydrin assay (section 2.8.6) which gave the elution profile at $A_{570\,nm}$.

————•————   indicates absorbance at $A_{570\,nm}$

··········■··········   indicates pyridine formate concentration (M)

The horizontal bar indicates the fractions pooled

46
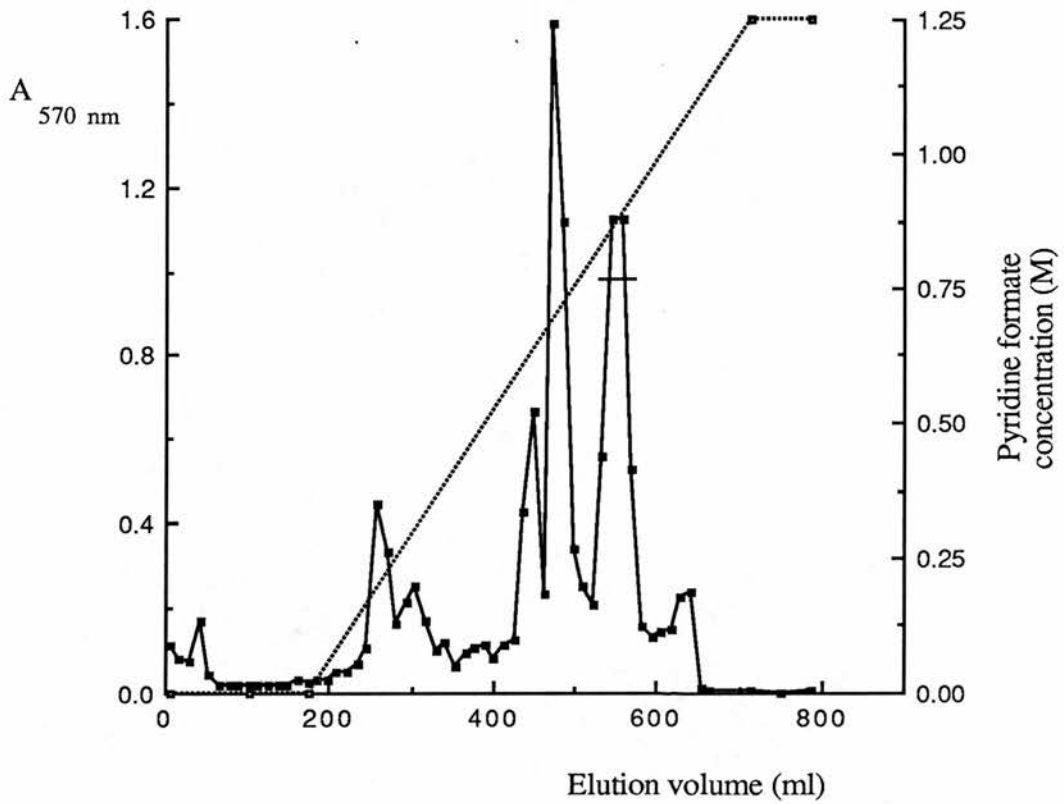
Figure 2.11   Dowex 1X-2 Ion-exchange Column Elution Profile for Sample (8)

Crude dipeptide sample (8) was applied to the Dowex 1X-2 ion-exchange column as described in section 2.8.6.   Eluant was analysed for the presence of amine bonds using the ninhydrin assay (section 2.8.6) which gave the elution profile at $A_{570\,nm}$.

    ————■————   indicates absorbance at $A_{570\,nm}$
    ········■·········   indicates pyridine formate concentration (M)
                    The horizontal bar indicates the fractions pooled

^{1}H-n.m.r. 'δ_H (p.p.m.) [360.132 MHz, H_2O:D_2O (9:1 v/v)]

9.041-9.021 [1H, d, (N*H*)] 4.955-4.864 [obscured by H_2O signal, m, (αC*H*)]

4.630-4.522 [1H, d of d, (αC*H*)]

4.399-4.156 [4H, m, (βC*H$_2$*)]

FAB mass spectra for $C_6H_{15}N_2O_{11}P_2$, calc.: 352.01510, found: 352.01509

(< 1 p.p.m)

Ser(P)-Ser(P) phosphorylated with TCPC

^{1}H-n.m.r. 'δ_H (p.p.m.) [360.132 MHz, H_2O:D_2O (9:1 v/v)]

9.032-9.010 [1H, d, (N*H*)] 4.933-4.812 [obscured by H_2O signal, m, (αC*H*)]

4.403-4.106 [4H, m, (βC*H$_2$*)]

^{1}H-n.m.r. 'δ_H (p.p.m.) [360.132 MHz, D_2O]

4.933-4.506 [4.893-4.871, d of d, (αC*H*)] 4.414-4.388 [1H, d of d, (αC*H*)]

4.358-4.158 [4H, m, (βC*H$_2$*)]

^{31}P-n.m.r. 'δ_P (p.p.m.) [360.132 MHz, D_2O] 0.8040, 0.4597

FAB mass spectra for $C_6H_{15}N_2O_{11}P_2$, calc.: 352.01510, found: 352.01508

(< 1 p.p.m.)

2.8 Discussion

The original incentives for the production of the dipeptide Ser(P)-Ser(P) were a) to provide a simple model for the binding of phosphoproteins to a calcium phosphate phase (see chapter 3) and b) to enable co-crystallisation with calcium ions and hence give stereochemical information about phosphoprotein/calcium ion

48

binding. These experiments require large quantities of peptide (approximately 2 g) in a highly pure form. Therefore Ser(P)-Ser(P) was prepared essentially by the method of Folsch, (1959) with a few modifications that would improve yields and purity.

The L-seryl-O-benzyl ester-p-toluenesulphonate (1) was synthesised as described (see section 2.7.2) utilising the method of azeotropic distillation first reported for the esterification of glycine by Cipera and Nicholls (1955). The benzyl ester was synthesised instead of the more popular methyl and ethyl esters for two reasons. Firstly, the OBzl- group can be removed under the same conditions as the Z- group and so the number of reaction steps can be reduced. Secondly, alkali treatment is required to remove methyl- and ethyl- protecting groups (see section 2.3.2.2) and this may cause dephosphorylation of the dipeptide by β-elimination (Longenecker and Snell, 1957; Riley et al., 1957), whereas OBzl groups can be removed by catalytic hydrogenolysis. Moreover, if the OBzl group is used the p-toluenesulphonate salt is formed during the reaction which renders serine soluble in benzyl alcohol and so improves the yield of the ester (Millar and Waelsch, 1952).

N-Benzyloxycarbonyl-L-serine (2) was synthesised as described following the method of Baer and Maurukas, (1955; see section 2.3.1.1). The Z- group is a useful protecting group for this synthesis as not only is it readily removed under the same conditions as the OBzl- group but it also confers stability against racemisation on the N-terminal residue.

Coupling of (1) and (2) to form N-Benzyloxycarbonyl-L-seryl-L-serine-O-benzyl ester (3) utilised N,N-dicyclohexylcarbodiimide (DCCI) as coupling agent (see section 2.4.1). This coupling agent has three advantages: it can be used to couple serine and threonine derivatives that have free β-hydroxyl groups (Sheehan et al., 1956), it has a low potential for causing racemisation and the coupled peptide is easily purified.

Of the two methods investigated that of Folsch (1959) was adopted primarily because of improved yields and ease of preparation (see section 2.7.4). The higher

yields obtained by the method of Folsch, (1959) are probably due to the reduced formation of the by-product, N-acylurea (see section 2.4.1). N-Acylurea can form as a result of O - N acyl migration (Folsch, 1967) but can be prevented if the reaction is carried out in acetonitrile (Sheehan *et al.*, 1956).

Z-Ser-Ser-OBzl (3) was then phosphorylated using either DPPC (see section 2.5.2.1) or TCPC (see section 2.5.2.3). The DPPC derivative, (4), was deprotected as described (see section 2.7.6.1) and then purified by ion-exchange chromatography (see section 2.7.7). The elution profile of the ion-exchange column (see Fig. 2.10) showed two major peaks. Each peak was analysed by t.l.c in solvent system g, h and i and showed one spot indicating a single compound. The $R_{Ser(P)}$ for the peak eluting at approximately 0.9 M pyridine formate was found to be 0.5 (in solvent system g), which is that determined for Ser(P)-Ser(P) by Folsch (1959). The peak eluting at approximately 0.9 M pyridine formate was confirmed to be Ser(P)-Ser(P) by [1]H-n.m.r and FAB mass spectral analysis. Further purification of the peptide was not considered necessary.

Several preparations of the DPPC derivative were found, by [1]H-n.m.r, to have a phenyl protecting group remaining on a phosphate residue after deprotection (results not shown; see section 2.5.2). Such samples eluted from the ion-exchange column at a similar pyridine formate concentration (0.9 M) as the dipeptide Ser(P)-Ser(P). This situation has been reported by several authors (Alewood *et al.*, 1981; Schlesinger *et al.*, 1987; Perich and Johns, 1988a). Before the peptide can be used in adsorption studies this phenyl group must be removed. The material would therefore have to be re-hydrogenated (see section 2.7.6.1) and the product re-purified by ion-exchange chromotography (see section 2.7.7).

The use of DPPC as a phosphorylating agent for peptides suffers from several disadvantages (see section 2.5.2). In brief these include: incomplete phosphorylation caused by steric hindrance, incomplete deprotection (as observed above), difficulty in purifying the deprotected phosphopeptide, low yields and the expense of large scale production of phosphopeptides. Therefore, alternative

phosphorylating agents were investigated in an attempt to circumvent some of the disadvantages associated with DPPC.

Diisopropyl-(2-cyanoethyl) chlorophosphine was investigated as a potential phosphitylating agent for Z-Ser-Ser-OBzl. This phosphitylating agent was developed for DNA synthesis (Sinha *et al.*, 1984) and has been used extensively as a phosphitylating agent for inositols (Cooke and Potter, 1987; Cooke *et al.*, 1987, 1988; Hamblin *et al.*, 1987a,b,c; Billington, 1989). However, due to the instability of the phosphitylated intermediate and the large number of reaction by-products (results not shown) the use of this agent was abandoned.

The phosphorylating agent TCPC (see section 2.5.2.3) was also investigated. Z-Ser-Ser-OBzl (3) was successfully phosphorylated using this agent (see section 2.7.5.2) in high yields (>90%). Deprotection of the phosphorylated derivative (5) was a two step procedure; first, catalytic hydrogenolysis (see section 2.7.6.2a) and secondly removal of (2,2,2-trichloroethyl)- groups with zinc dust (see section 2.7.6.2b).

The crude dipeptide sample (8) was then purified by ion-exchange chromotography (see section 2.7.7). Again, each peak was analysed by t.l.c in solvent system g, h and i, the $R_{Ser(P)}$ for the peak eluting at approximately 0.9 M pyridine formate was found to be 0.5 (in solvent system g), indicating Ser(P)-Ser(P). The peak eluting at approximately 0.9 M pyridine formate was confirmed to be Ser(P)-Ser(P) by ^{1}H-n.m.r and FAB mass spectral analysis.

The elution profile (see Fig. 2.11) obtained from the ion exchange column (see section 2.7.7) with the TCPC derivative showed an increase in the amount of reaction by-products compared to the DPPC derivative (see Fig. 2.10). This may be the result of partial dephosphorylation of the TCPC derivative during catalytic hydrogenolysis (see section 2.7.6.1). Similar observations have been reported by Yajima *et al.* (1971) and by Paquet and Johns (1990). This problem may be overcome by the use of hydrogen bromide in acetic acid (see section 2.3.1.1 and

2.3.1.2) to cleave the Z- and OBzl- groups or by using different protecting groups for the N- and C- terminal.

The use of TCPC as phosphorylating agent had no advantage over DPPC as regards final yield of the dipeptide Ser(P)-Ser(P) (approximately 50% in both cases). However, yields might be improved by using a different deprotection strategy (*e.i.* zinc/copper dust in DMF or sodium in liquid ammonia; see section 2.5.2.3). The main advantages of TCPC as a phosphorylating agent are that the specialised equipment employed for high pressure hydrogenolysis is no longer required and that the reagents are much cheaper.

CHAPTER THREE

THE ADSORPTION OF
β-CN A AND β-CN (f1-25) TO
DICALCIUM PHOSPHATE DIHYDRATE CRYSTALS

3.1 Adsorption of Proteins at the Solid/Liquid Interface

Since the 1930's, studies of protein adsorption (at the solid/liquid, liquid/liquid or liquid/gas interface) have been reported regularly in the literature (Lindau and Rhodius, 1935; Strain, 1949; Zittle, 1953; Cumper and Alexander, 1951; Silberberg, 1962; James and Augenstein, 1966; Hoeve, 1971; MacRitchie, 1972; 1978; 1978; Kamyshnyi, 1981; Lundstrom, 1984; Lyklema, 1984; Giaever and Keese, 1987). The original studies aimed to determine molecular weight (at the liquid/gas interface) as well as to investigate electrophoretic and chromatographic behaviour (reviewed by Zittle, 1953; James and Augenstein, 1966). Later, more emphasis was placed on the adsorption mechanism, with particular attention paid to the occurence of structural re-arrangements (Cumper and Alexander, 1951; Silberberg, 1962; Hoeve, 1971; MacRitchie, 1972, 1978).

3.1.1 Importance of Protein Adsorption at the Solid/Liquid Interface

The behaviour of proteins at interfaces is of relevance both in natural and technical processes. Many proteins are associated with the biological membrane (either intrinsically or extrinsically) where they interact with both an aqueous and non-aqueous environment. Such interactions are essential for their biological function. There are also many medical and technical instances, where the interaction between protein and interface may have significant consequences. For example, the relationship between protein adsorption and biocompatability of the sorbent material has been investigated (Kamyshnyi, 1981; Lundstrom, 1984; Lyklema, 1984; Giaever and Keese, 1987; Horbett 1987). Proteins are frequently used as emulsifiers and/or stabilisers in colloid dispersions for cosmetics, pharmaceuticals and food products. However, undesirable events occur, known as "bio-fouling", in food processing equipment, artificial kidney devices and on the

artificial materials used as prostheses (reviewed by Brash and Lyman, 1971; Morrissey and Stromberg, 1974; Giaever and Keese, 1987).

The adsorption process at the solid/liquid interface involves the transfer of a protein molecule from solution to the sorbent surface, with a concomitant displacement of solvent molecules and possibly other components from that surface. Adsorption of proteins at the solid/liquid interface depends upon the relative affinities of the solvent and the protein for the sorbent, which are determined by the properties of the protein and the nature of the interface. The interplay between the components of the system determines the environmental change upon adsorption and, therefore, the change in structure and biological functioning of the protein molecule. The following sections will review some of the general principles governing protein adsorption at the solid/liquid interface.

3.1.2 Protein Structure and Adsorption Behaviour

Proteins are co-polymers of some twenty different amino acids of varying hydrophobicity and, as a consequence, proteins are amphiphilic. The tertiary structure of a protein molecule is determined by the interactions of specific amino acid side chains, for example hydrogen bonds, van der Waals, ionic and hydrophobic interactions and disulphide bridges (reviewed with respect to adsorption behaviour by Norde, 1986). The protein molecule in solution is a complex structure with hydrophobic (mainly in the interior of the molecule and thus shielded from water), hydrophilic and charged regions (usually located on the periphery of the molecule). The three dimensional structure of the protein is the net result of intramolecular interactions and interactions between the protein molecule and its environment. Proteins can be divided into three main classes according to their tertiary structure:

1) molecules that are highly solvated and flexible, resulting in a "random coil" -like structure (*e.g.* the caseins).

55

2) molecules that have adopted a regular structure, like an α-helix or a
β-sheet (*e.g.* keratin, silk fibroin and collagen).

3) compact molecules that may contain helix, β-structures and unordered
segments: the globular proteins (*e.g.* enzymes and immunoglobins).

The adsorbed state of each class of protein is depicted in Fig 3.1, of which part A depicts a highly solvated molecule. Several small portions of the molecule, referred to as 'trains', attach to the sorbent with the remainder of the molecule forming loops and tails dangling free in the solution (Silberberg, 1962; 1971; Hoeve, 1971). As more protein adsorbs, the attached fractions (trains) reduce and hence a larger portion of the molecule protrudes into the solution. The fibrous proteins (Fig. 3.1B) can adsorb in a number of orientations with little change in conformation. As more protein adsorbs the orientation of the molecules can change to form a more closely packed system. Globular proteins (Fig. 3.1C) , which may adsorb in any orientation, making one or more points of contact, may undergo varying degrees of conformational change upon adsorption (Morrissey and Fenstermaker, 1976; Mitra and Chattoraj, 1978). As more protein adsorbs the orientation of protein molecules can change to form a more close-packed system. Further loss of native protein conformation may occur as the adsorbed layer becomes compressed (Morrissey and Fenstermaker, 1976). However, compact molecules such as globular proteins rarely unfold completely to form a loose, loop and tail-like adsorbed layer (Fig. 3.1A; *cf.* liquid/gas interface; Cumper and Alexander, 1951; James and Augensteun, 1966). In some instances, protein conformation does not appear to revert to their 'native' conformation upon desorption (Soderquist and Walton, 1980; Norde *et al.*, 1986).

To begin to understand the interaction between protein and sorbent, knowledge of certain properties of the surface of the sorbent is helpful. The chemical composition of the sorbent is important especially if groups are present that can react with the protein. Knowledge of whether the surface is homogenous (as in

Figure 3.1   <u>Schematic Diagram of the Adsorbed State</u>

<u>of the Three Protein "Classes" at the Solid/Liquid Interface</u>

Part A) Adsorbed state of class 1) proteins; highly flexible and solvated molecules.

Part B) Adsorbed state of class 2) proteins; molecules with highly regular structure.

Part C) Adsorbed state of class 3) proteins; globular molecules.

A

B

C

58
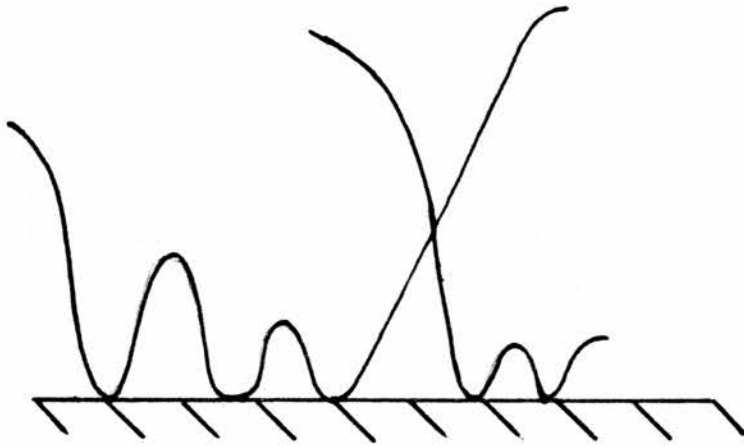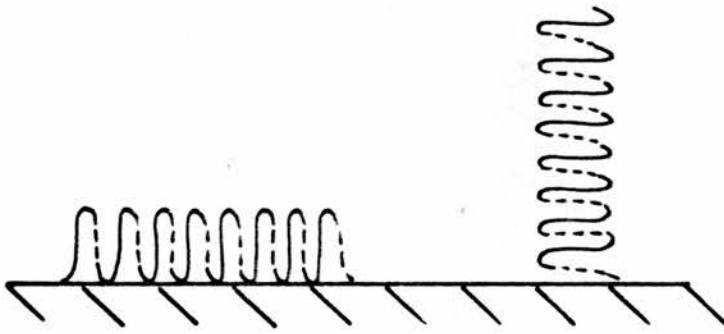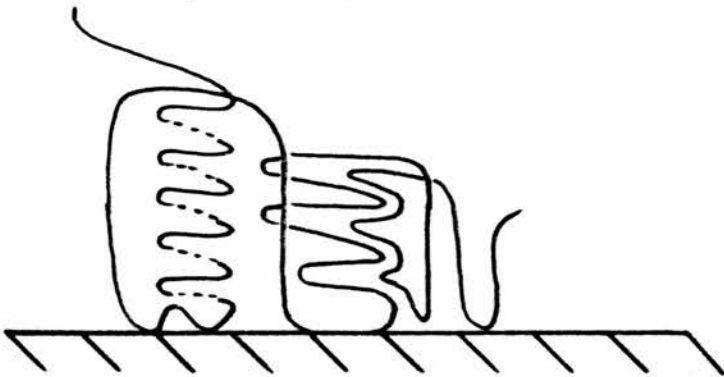
synthetic polymers) or heterogenous (as in inorganic crystals), or whether the surface is electrically charged or not is also important. In most cases both the protein and sorbent surface are charged and therefore electrostatic interactions play an important role in the adsorption process.

It appears that most proteins interact with most surfaces, but general conclusions regarding the interfacial behaviour of proteins and the actual mechanism by which they adsorb are difficult to deduce (discussed in section 3.1.9). One of the major reasons for this is that many studies have been performed under ill-defined conditions, making comparison between systems almost impossible (Norde, 1986). However, there are a few hypothetical models of adsorption that can be derived from existing experimental information (reviewed by Horbett and Brash, 1987). One, or a combination, of these proposed models may apply to any given protein/sorbent system.

3.1.3 Methods of Studying Protein Adsorption

The interactions of proteins at the solid/liquid interface have been investigated by various techniques: infra red spectroscopy (Lyman *et al.*, 1968; Morrissey and Stromberg, 1974; Matsui *et al.*, 1978), fluorescence spectroscopy (Watkins and Robertson, 1977; Walton and Maenpa, 1979), circular dichroism spectroscopy, radiolabelling (Grant *et al.*, 1977), electrochemical methods such as electrophoresis (Chattoraj and Bull, 1959) and proton titration (Kochwa *et al.*, 1967; Norde and Lyklema, 1978), optical techniques such as ellipsometry (Morrissey and Fenstermaker, 1976) and light scattering (Uzgiris and Fromageot, 1976; Morrissey and Han, 1978) and lastly "thermodynamic" methods such as surface tension (Mitra and Chattoraj, 1978) and contact angle (Vroman, 1967; van der Scheer and Smolders, 1978; Absolom *et al.*, 1987) measurements and calorimetry (Nyilas *et al.*, 1974; Koutsoukos *et al.*, 1983). All these methods have provided information on the type of binding, the thickness and structure of the adsorbed layer, the

reversibility of the adsorption process and the amount of protein adsorbed per unit area (Γ).

3.1.4 Adsorption Isotherms

If the amount of protein adsorbed per unit area, Γ, determined at constant temperature, is plotted as a function of the protein concentration in solution, c, then the resulting graph is called an adsorption isotherm. Γ is usually determined by depletion of protein from the solution but a sufficiently large sorbent surface area must be supplied to deplete the solution significantly.   This is usually achieved by use of a finely divided sorbent. Γ may also be determined directly, by labelling the protein with radioactive (Niemann and Hoffmann, 1964; Kozin and McCarty, 1977) or fluorescent (Beissinger and Leonard, 1982) chemicals, and by optical techniques such as ellipsometry (Morrissey and Fenstermaker, 1976).   However, radioactive and fluorescent labels can influence the adsorption of the protein (Grant *et al.*, 1977).

Protein adsorption differs from that of low molecular weight substances in that proteins tend to adsorb *via* several segments (multi-point adsorption; Morrissey and Fenstermaker, 1976).   Although the adsorption free energy per segment may be low, the adsorption free energy for the whole molecule is proportional to the number of segments adsorbed (Silberberg, 1971).   As a consequence most proteins have a large negative free energy of adsorption and do not readily desorb on diluting the system with solvent (*cf.* low molecular weight substances).   This large free energy of adsorption is reflected in the shape of the isotherm.   The various isotherm shapes were first classified by Giles and MacEwan (1957) but the majority of isotherms are of two types (see Fig. 3.2): "high" and "low" affinity.   High affinity isotherms (*viz.* the initial part of the isotherm is very steep; see Fig. 3.2A) are almost always observed with highly solvated and flexible molecules, reflecting the high number of segments adsorbed.   Also observed with highly solvated, flexible molecules is a continuously increasing value for Γ (*i.e.* no true adsoption plateau, Γ_p).   This

60

Figure 3.2   Schematic Diagram of the Two Types of Adsorption Isotherm Associated with Protein Adsorption at the Solid/Liquid Interface

Part A)   'High' affinity isotherms;   highly solvated and flexible molecules.

Part B)   'Low' affinity isotherms;   compact molecules.

Γ is the amount of protein adsorbed per unit area.

Reproduced from Norde *et al.*, 1986

A
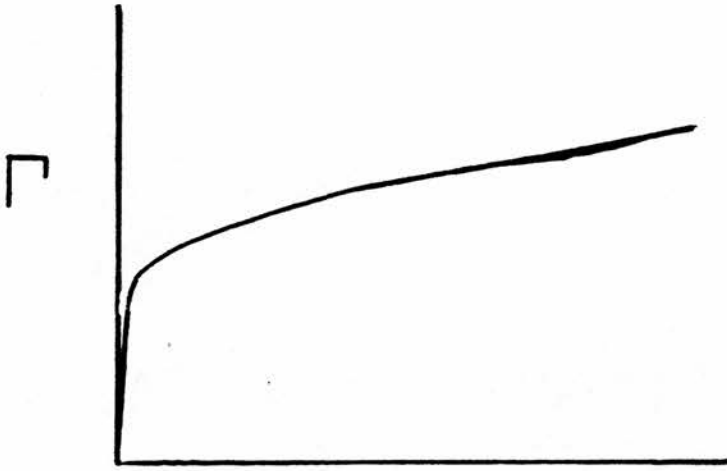
Equilibrium concentration

B
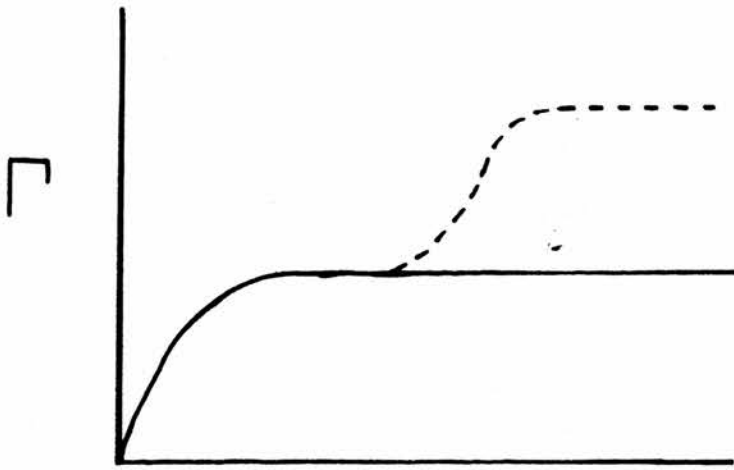
Equilibrium concentration

phenomenon is usually explained in terms of structural re-arrangements occurring in the adsorbed molecules as more molecules adsorb (Silberberg, 1971; Norde *et al.*, 1986). These re-arrangements can result in a decrease in the number of attached segments per adsorbed molecule with a larger proportion of the protein as loops and tails.

In contrast, the isotherms of compact molecules, such as globular proteins, develop well-defined adsorption plateaux (Γ_p) and the adsorption is not usually of such high affinity (see Fig. 3.2B). The plateau usually corresponds to a close-packed mono-layer of native molecules. However, with both "high" and "low" affinity adsorption isotherms, the corresponding desorption isotherms are usually of the high affinity type (Norde *et al.*, 1986). This suggests that upon adsorption, proteins undergo structural transitions and/or multi-point adsorption which enhances binding.

Another common feature of adsorption isotherms (observed with various proteins and surfaces) is the occurrence of a "kink" in the isotherm (Williams and Choppin, 1951; see Fig. 3.2B). This has been interpreted as the formation of a second layer of molecules (multi-layer adsorption; Williams and Choppin, 1951) or coagulation (MacRitchie and Owens, 1969; MacRitchie, 1972) or a structural transition in the adsorbed layer (Fair and Jamieson, 1980). The first interpretation can be evaluated by dilution experiments; if dilution leads to a high degree of desorption a multi-layer probably exists. However, multi-layer adsorption is to be expected only for nearly saturated solutions when (amorphous) phase separation is imminent (Hoeve, 1971). Coagulated protein at an interface will not desorb readily upon dilution (MacRitchie and Owens, 1969; MacRitchie, 1972; see Fig 3.2B). The structural transition model (third interpretation; Fair and Jamieson, 1980) which is called the model of "bimodal adsorption", has three putative regimes of adsorbed protein structure (see Fig 3.3). At low protein concentrations (region A of Fig. 3.3) the molecules adsorb randomly. At high protein concentrations (region C of Fig. 3.3) intermolecular nucleation occurs at the sorbent surface resulting in the

63

Equilibrium concentration
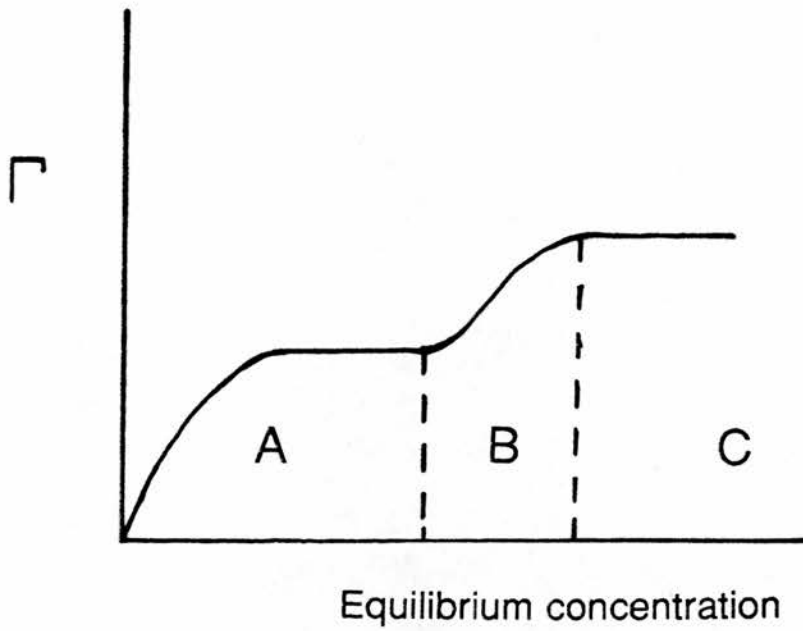
Figure 3.3   Schematic Diagram of the Adsorption Isotherm Associated with

the Structural Transition Model of Protein Adsorption

at the Solid/Liquid Interface

In region A protein molecules adsorb randomly.

In region C intermolecular nucleation occurs.

B is the region of transition between the above two states.

Γ represents the amount of protein adsorbed per unit area.

Reproduced from Norde *et al.*, 1986

formation of a two dimensional protein crystal. The kink in the isotherm represents the transition between these states (region B of Fig. 3.3) with the protein layer having a more or less unordered, glassy structure. Direct evidence of two-dimensional protein crystallisation and ordering is now available for the case of antibodies deposited on haptenated phospholipid monolayers (Uzgiris, 1985) and from electron diffraction studies of two-dimensional crystals of light harvesting complex -II from chloroplast membranes (Kuhlbrandt and Wang, 1991).

3.1.4.1 Description of Adsorption Isotherms

The adsorption isotherm is the most convenient form in which to plot experimental data, and it is the form in which theoretical treatments are most often developed (Adamson, 1983). In addition, the construction of an accurate adsorption isotherm allows calculation of the energy and entropy of adsorption. The following section deals with two theories (or models) for adsorption, the Langmuir model and the Brunauer, Emmett and Teller (or BET) model. Both of these theories were originally developed to describe the isotherms of gas adsorption to solids, but have proved adequate for the description of isotherms constructed from protein adsorption experiments at the solid/liquid interface.

The Langmuir Model

The adsorption of gasses onto solids was first described quantitatively by Langmuir (1916, 1918). This model is based on the following assumptions: that the surface contains a fixed number of adsorption sites, that each site holds only one molecule, that the free energy of adsorption is the same for all sites and does not depend upon the fraction of sites occupied and that there is no interaction between molecules on different sites (lateral interaction).

If the affinity constant, k, refers to the adsorption of a molecule at a single site, and the state of any such site is represented by its degree of association, θ, (*i.e.* the fraction of sites occupied is θ, and the fraction of unoccupied sites is $1 - \theta$) then at equilibrium

$$kc = \frac{\theta}{1 - \theta}$$

Where c is the equilibrium, free concentration. As $\Gamma = n\theta$, where n is the number of sites per unit area, the above equation can be re-arranged to give the Langmuir equation for adsorption,

$$\Gamma = \frac{nkc}{1 + kc}$$

Where Γ is the amount adsorbed per unit area. This theory is frequently used to describe protein adsorption at the solid/liquid interface as it is the simplest description of the isotherms obtained. This model can be expanded to account for further families of non-interacting adsorption sites on the same surface by adding further terms (Tanford, 1966), *i.e.*:

$$\Gamma = \frac{nkc}{1 + kc} + \frac{n'k'c}{1 + k'c} + \ldots \text{ etc.}$$

However, Norde (1980) argues that as a consequence of the prerequisites described above (*i.e.* reversible adsorption, a fixed number of adsorption sites and no lateral interaction), the thermodynamics of adsorption derived from a Langmuirian (or an analogous) analysis are without physical meaning. This argument is supported in part by the work of Mura-Galelli *et al.* (1991). However, Moreno *et al.* (1982) argue that thermodynamic quantities depend only on the initial and final states and are independent of the path of integration and that thermodynamic quantities are valid, whether the process is reversible or irreversible, provided a state of equilibrium exists. Therefore, the question remains as to whether the Langmuirian model of adsorption should be applied to protein adsorption at the solid/liquid interface.

66

The BET Model

The observation of adsorption isotherms which show no saturation and a marked increase in adsorption at higher equilibrium, free concentration are generally interpreted as multi-layer formation. Generally, these isotherms are described using the Brunauer, Emmett and Teller (BET) model (Brunauer *et al.*, 1938). Brunauer, Emmett and Teller extended Langmuir's approach to multi-layer adsorption by assuming that the Langmuir equation applies to each layer of adsorbed molecules. With the addition that the first layer of molecule's heat of adsorption may be some special value and that the succeeding layers' heat of adsorption is different from the first but are equal. The BET model can be represented by

$$\theta = \frac{cx}{(1 - x)\,[1 + (c - 1)\,x]}$$

where $x = c/c^o$ (c is the equilibrium, free concentration and c^o is the solubility of the adsorbate). Since the appearance of the BET model in 1938, the equation has become the standard one for surface area estimation, usually using nitrogen or krypton as the adsorbate.

Various modifications of the BET equation have been made in an attempt to correct certain approximations and so give a better fit. For example, if the number of layers formed is limited to n, the above equation becomes,

$$v = [v_m cx/(1 - x)][1 - (n +1)x^n + nx^{n + 1}]/[1 + (c - 1)x - cx^{n + 1}]$$

where v is the amount adsorbed per unit area (*i.e.* Γ) and v_m is the amount adsorbed per unit area at monolayer (*i.e.* Γ_p).

Cooperative Adsorption - The Hill Coefficient

In 1910, Hill showed that the sigmoidal dissociation curve of oxyhaemoglobin could be described by the equation

$$y = \frac{kx^h}{1 + kx^h}$$

where y is the percentage saturation of binding sites (*i.e.* θ), x is the oxygen tension in the solution (*i.e.* c, the equilibrium, free concentration), k is the affinity constant and h is also a constant. The constant, h, is now called the Hill coefficient. At highly cooperative binding sites (complete cooperation) h is approximately equal to the number of binding sites. At binding sites with some cooperativity the value of h indicates the degree of interaction between sites. Therefore, the Hill equation provides a semi-empirical means to describe a system where cooperative binding (or adsorption) occurs. A system which exhibits positive cooperativity (such as oxygen binding to heamoglobin) can be described by the above equation with h > 1 (in this case k denotes an average affinity constant). A value of h < 1 describes a system with either heterogeneity of binding sites or with negative cooperativity.

3.1.5 The Adsorbed Protein Layer

The attainment of a plateau in the adsorption isotherm (Γ_p) reflects a more or less close-packed layer of native molecules (Lyman *et al.*, 1968; Morrissey and Stromberg, 1974; Kamyshnyi, 1981). Kinks (or no Γ_p) observed in the isotherm are generally interpreted as a tilting or reorientation of non-spherical molecules (see Fig 3.4) or as surface nucleation which allow more protein molecules to adsorb. "Kinks" may also arise from changes in the structure of globular proteins (Norde *et al.*, 1986), although rarely does the protein completely unfold into a loose, loop and tail -like structure.

As mentioned earlier (see section 3.1.4), adsorption of proteins is rarely readily reversible. During adsorption studies the following anomalous features are

Figure 3.4   Schematic Diagram Representing the Reorientation of Non-spherical
              Protein Molecules at the Solid/Liquid Interface

         represents a non-spherical protein molecule.

         represents the adsorbent surface.

69

observed: 1) none or only a fraction of the adsorbed protein molecules desorb on diluting the system with solvent, 2) at Γ_p, changing the pH, ionic strength or temperature may result in additional adsorption whereas desorption on reversing these conditions is limited, 3) exchange of molecules from adsorbed to free states occurs, 4) adsorbed molecules can be exchanged/displaced by other (different) protein molecules, and 5) molecules that have undergone structural changes upon adsorption may not regain their native conformation upon desorption.

As the adsorbed molecule is attached *via* many segments and, once adsorbed, the protein may alter its conformation, the desorption process is not simply a reversal of the adsorption process. In order to desorb, the molecule has to overcome the sum of the free energies of adsorption and any subsequent conformational change. The following sections describe how electric charge, hydrophobicity, and temperature influence the adsorbed protein layer.

3.1.6 The Effect of Electric Charge on Protein Adsorption

In many systems, both the protein and the sorbent possess charged groups, the charge of each being dependant upon the pH of the solution. The cohesive stability of a protein is highest at its isoelectric point. Protein adsorption at a charged surface involves an overlap of electric double layers (Lyklema, 1985) which results in attraction of the protein to the sorbent if the signs oppose and repulsion if the signs are the same (Norde, 1986). Additionally, the charge of the molecule affects its cohesive stability which can influence its adsorption behaviour.

Maximum values of Γ_p frequently occur at pH's close to the isoelectric point of a protein molecule (MacRitchie, 1972; Morrissey and Stromberg, 1974; Mitra and Chattoraj, 1978; Kamyshnyi, 1981; Koutsoukos *et al.*, 1982). The reduction in Γ_p above and below the isoelectric point is thought to be due to structural re-arrangements in the adsorbing molecules as opposed to an increase in lateral replusion (Morrissey and Fenstermaker, 1976; Mitra and Chattoraj, 1978; Norde

70

et al., 1986). The extent of the reduction in Γ_p reflects the cohesive stability of the molecule (Norde *et al.*, 1986). However, such changes in Γ_p are not solely due to the instability of the protein; the charge carried by the sorbent surface plays an important role.

As stated above, when a protein approaches a like-charged surface adsorption is usually retarded but interaction between the like charges may be screened by low molecular weight electrolytes. However, increasing the ionic strength of the solution usually results in an increasing Γ_p regardless of whether the charges of protein and sorbent are like or opposed (Shastri and Roe, 1970; Mitra and Chattoraj, 1978; Susawa and Murakami, 1980; Kamyshnyi, 1981). This suggests that Γ_p is predominantly determined by intermolecular charge-charge interactions of protein molecules (Koutsoukas *et al.*, 1982; Norde, 1986). Furthermore, the adsorption process is sensitive to the type of ion present (McLaren, 1954; Mizutani, 1981; van Dulm *et al.*, 1981) indicating that the role of small ions in the adsorption process is more intricate than simple non-specific, screening of interacting charges.

3.1.7 The Effect of Hydrophobicity on Protein Adsorption

Most proteins have some hydrophobic regions that are exposed to the aqueous environment in addition to those in the interior of the protein. As the protein approaches an interface, dehydration of the hydrophobic parts of the protein, and of the sorbent surface, is "driven" by an entropy gain which promotes spontaneous adsorption. Adsorption is accompanied by a structural re-arrangement allowing internal hydrophobic regions to interact with the interface and, as noted by Birdi (1973), the greater the hydrophobicity of the protein, the greater the re-arrangement upon adsorption. The effect of the hydrophobicity of the sorbent has been much more difficult to ascertain because varying the hydrophobicity of the sorbent automatically involves varying its chemical composition. Generally sorbents of greater hydrophobicity result in greater values of Γ_p (MacRitchie, 1972).

3.1.8 The Influence of Temperature on Protein Adsorption

Very few studies have been undertaken to investigate the influence of temperature upon protein adsorption, consequently only generalisations can be made. The influence of temperature on Γ_p varies depending upon the system studied, in some systems (Kobamoto *et al.*, 1966; Dillman and Millar, 1973; Nyilas *et al.*, 1974; Norde and Lyklema, 1978) an increase has been reported and in others (Hummel and Anderson, 1965; Mitra and Chattoraj, 1978) a decrease on raising the temperature. Nevertheless, a greater value of k (and Γ_p) at a higher temperature implies an endothermic adsorption process with an increase in entropy being the driving "force" behind the adsorption process (Norde *et al.*, 1986)

3.1.9 Kinetics of Protein Adsorption

The mechanisms of protein adsorption at the solid/liquid interface are very complex. In any study of protein adsorption, but particularly when the reversibility and conformational aspects are being studied, it is important to know if an equilibrium has been reached. This information is obtained by studying the kinetics of the adsorption process. Kinetic constraints, due to proteins diffusing to the interface, contribute to the overall complexity of the mechanism of the adsorption of proteins at the solid/liquid interface. Additionally, the protein-surface interaction typically appears to show a large number of time-dependent effects (Horbet and Brash, 1987; Lundstrom and Elwing, 1990). Furthermore, adsorption may result in one or more two-dimensional phase transitions which result in a crystalline packing at the interface (see section 3.1.4).

The adsorption process can be broken down into five steps: 1) movement of the protein towards the interface, 2) binding of the protein to the interface, 3) re-arrangement of the protein structure in the adsorbed state, 4) desorption of the

72

protein from the interface and 5) movement of the protein away from the interface. Any one, or combination, of these steps can determine the rate of the overall adsorption process. The general aspects concerning these five steps are established, but the details of protein adsorption kinetics are still unresolved.

As discussed earlier (see section 3.1.4), proteins attach to the sorbent by several segments which results in very poor desorbability, so that desorption and retreat from the interface are not rate limiting for protein adsorption. Movement of the protein molecule towards the interface (step 1) occurs simply by diffusion. Therefore, it appears that under most experimental conditions, protein binding to the interface and structural re-arrangements (steps 2 and 3) are the rate limiting steps in protein adsorption. Several authors have proposed models that describe the kinetics of protein adsorption, some of which are illustrated in Fig 3.5.

All these models, including the Langmuir theory (see section 3.1.4 and Fig. 3.5A) make the assumption that the adsorption process is surface reaction limited. The Lundstrom model (Lundstrom, 1983; Fig. 3.5B) proposes that the protein adsorbs with a rate constant k_A into state A (adsorbed but in its native conformation) which may then change conformation to state B ("denatured"). This model was expanded to allow for protein desorption (Fig 3.5C). The Beissinger and Leonard (1982) model on the other hand accounts for desorption of both native and "denatured" adsorbed species (states A and B respectively; Fig. 3.5C).

A model was proposed by Soderquist and Walton (1980) which accounted for the time dependence of the surface reaction of protein adsorption (see Fig. 3.5D) and the re-sorption of desorbed material (Fig. 3.5D). In principle, this model takes into account the time dependence of the conformational changes of adsorbed proteins. Soderquist and Walton suggested that there are three distinct processes or states in the adsorption process:

Figure 3.5   <u>Kinetic Models of Single Protein Adsorption</u>

<u>at the Solid/Liquid Interface</u>

The models illustrated in Fig. 3.5 A to F assume that the adsorption process is surface reaction -limited (*i.e.* protein transport to the interface is not rate limitimg)

Part A) illustrates the Langmuir Model

Part B) illustrates the Irreversible Lundstrom Model

Part C) illustrates the Beissinger and Leonard Model

Part D) illustrates the Soderquist and Walton Model

Part E) illustrates the Sevastianov *et al.* Model

Part F) illustrates the Andrade and Hlady Model

The nomenclature for the diagrams is as follows:

t   Time

C_O Bulk solution concentration

$C_S(t)$ Adsorbed surface concentration at time t

$(C_S)_\infty$ Plateau surface concentration at time $\gg$ t

k_i Rate constants

A, B and C represent the different adsorbed states of the protein.

D represents centres of irreversible desorption.

P represents centres of reversible adsorption.

D

C

C (t)

C (t=∞)

k_A k_D

k'_D k'_A

k''_D → O

t

t

A

B

C

Soderquist and Walton

E

k_A

k_D

k_A

D

P

Sevastianov *et al.*

F

C

FAST

FAST

k_A k_D

$k'_D(t)$

$k''_D(t)$

C(t)

k_r

k_r

t-0

t=t

t=∞

t ⟶

Andrade and Hlady

76
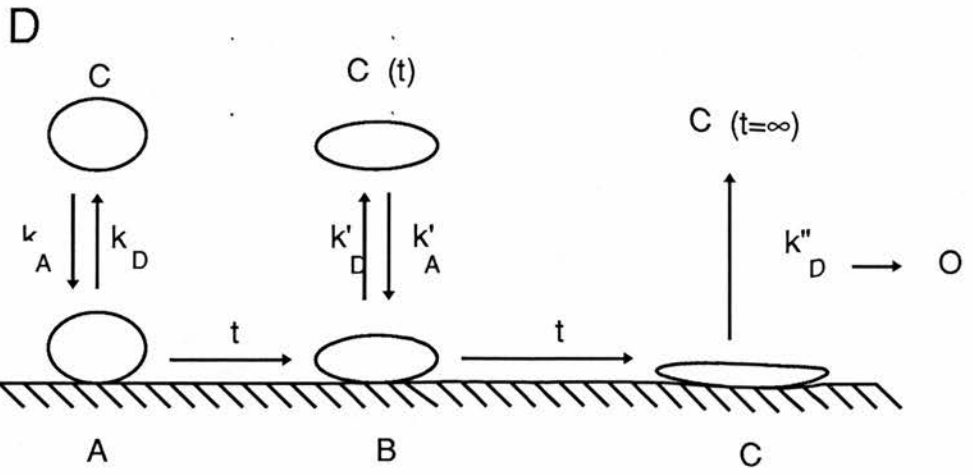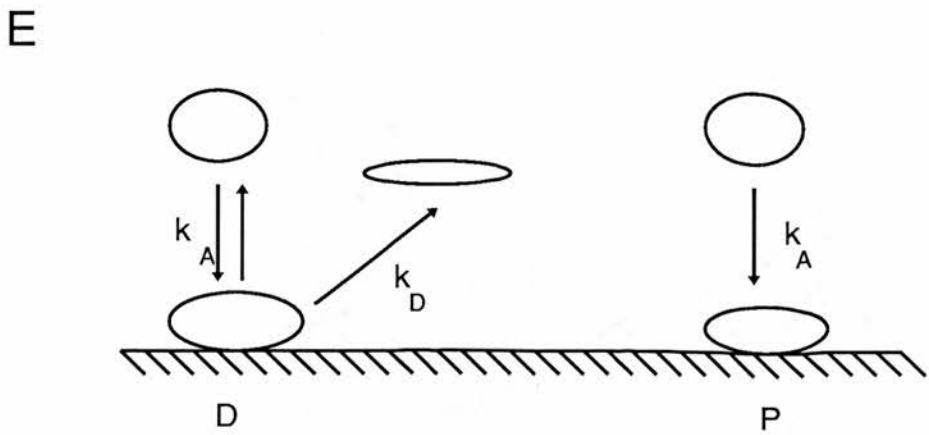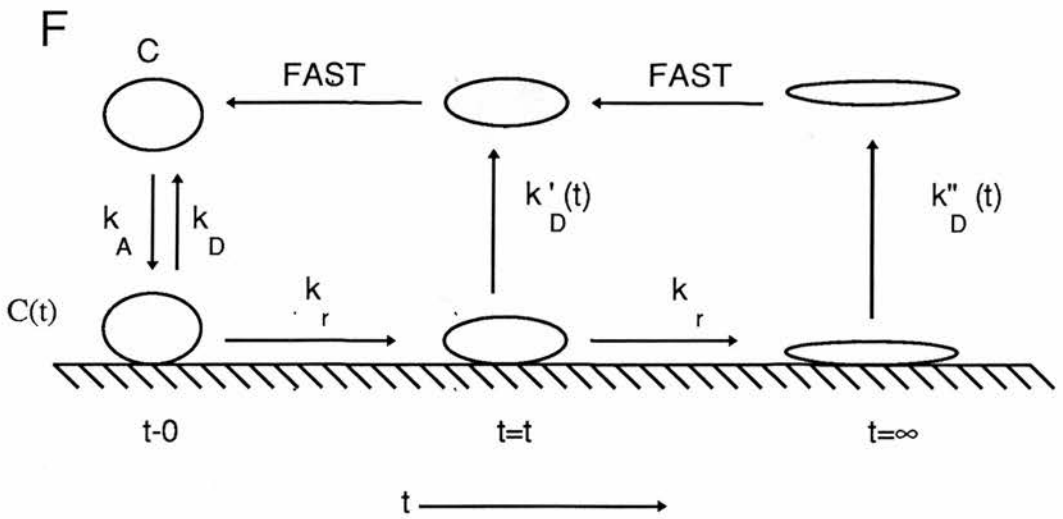
State A) First, a rapid and reversible adsorption takes place that reaches a pseudo-equilibrium during the first minute (Langmuir type adsorption).

State B) Then there is a surface-induced change in conformation that optimises protein-surface interactions and so decreases the probability of desorption.

State C) As time elapses adsorbed protein is fully "denatured" and, if desorption does occur, protein cannot readsorb (*i.e.* desorption from state C is irreversible).

Serastianov *et al.* (1983; 1984) developed a model in which the effect of surface heterogeneity on the adsorption process is described. They defined two centres, P and D; P centres were of reversible adsorption and D centres were of irreversible adsorption (see Fig. 3.5E). Serastianov *et al.* (1984) argued that desorbed material is conformationally changed and thus cannot resorb (hence desorption is irreversible). Andrade and Hlady (1986) proposed a more general kinetic model (Fig. 3.5F). This model is essentially a simplified version of the Soderquist and Walton model, with the additional assumption that desorbed protein rapidly "re-natures" in solution and is therefore available for adsorption.

All of these models tend to fit specific experimental data reasonably well, but relating such models to other systems is not always possible. Also, some of the assumptions made are not entirely reasonable and some important phenomena that take place are neglected (Andrade and Hlady, 1986; Horbet and Brash, 1987; Lundstrom and Elwing, 1990). For example, it is reasonable to assume that although proteins do undergo time-dependant, conformational changes at the interface, they probably "re-nature" in solution and therefore become indistinguishable from the proteins in free solution. Additionally, possible lateral

interaction and binding cooperativity between molecules is neglected as well as the influence of conformational changes within the molecule upon the rate constants (Lundstrom and Elwing, 1990).

3.2 The Human Salivary Acidic Proline-Rich-Phosphoproteins

The relationship of the acidic proline-rich-phosphoproteins (acidic PRP's) of human saliva with calcium ions and calcium minerals is one of the most extensively characterised biological systems where phosphoprotein/calcium mineral interactions occurs.

3.2.1 Introduction

The concentration of inorganic ions in human saliva indicates a state of supersaturation with respect to basic calcium phosphates, such as hydroxyapatite (Moreno *et al.*, 1979).   However, spontaneous precipitation does not normally occur. The stability of saliva is attributed to the phosphoproteins statherin (Hay and Schlesinger, 1977; Schlesinger and Hay, 1977; Hay *et al.*, 1979) and the acidic PRP's.

The acidic PRP's and statherin (along with other salivary constituents) are adsorbed from saliva onto the tooth enamel to form the precursor molecules of the acquired enamel pellicle (Kousvelari *et al.*, 1980). The acquired enamel pellicle is thought to have several functions. It is thought to act as a reservoir of calcium ions which buffers the free calcium ion activity in saliva and therefore helps to maintain a state of supersaturation with respect to calcium phosphates and carbonates (Bennick *et al.*, 1981; Saitoh *et al.*, 1985).   In addition, it is thought to retard enamel demineralisation (Propas *et al.*, 1977; Juriaanse, 1979) and to prevent crystal growth on the enamel surface from the supersaturated saliva (Hay *et al.*, 1979; Moreno

78

et al., 1979). Finally, it affects the attachment of oral micro-organisms to the tooth surface (Gibbons *et al.*, 1976).

The acidic PRP's, which are a closely related group of proteins, constitute approximately 30% of the protein in human parotid and submandibular saliva. The primary amino acid sequences of four of the acidic PRP's (PRP's 1 - 4) are known (Wong *et al.*, 1979; Wong and Bennick, 1980; Hay *et al.*, 1988; the Mr for PRP1 and 2 is 16,000, the Mr for PRP3 and 4 is 11,320). PRP1 has 150 amino acids containing 2 phosphoseryl residues at positions 8 and 22. The first 30 amino acids (known as the TX peptide) are highly acidic and hydrophilic, with the remainder of the molecule being hydrophobic. This gives the molecule a polar character, like β-casein. PRP2 differs from PRP1 in the substitution of an asparagine for an aspartyl residue at position 4. PRP3 consists of the first 106 amino acid residues of PRP1, and PRP4 the first 106 residues of PRP2. It is thought that PRP3 and PRP4 may be the result of proteolytic cleavage of PRP1 and PRP2 respectively, by the action of kalikrein (Wong and Bennick, 1980). However, it is argued (Schlesinger and Hay, 1986) that partial gene duplication is responsible, rather than proteolysis; an argument which is supported when genetic polymorphism is considered (Azen, 1978).

Circular dichroism spectra of the acidic PRP's suggest the presence of very little secondary structure (Bennick, 1975). Two calcium binding sites, of different affinity, have been identified, which involve the phosphoseryl and aspartyl residues of the N-terminal (TX peptide; Bennick *et al.*, 1979; 1981). However, amino acid residues from the remainder of the protein are thought to interact with the calcium binding site (Braulin *et al.*, 1986).

3.2.2 The Adsorption of the Human acidic Proline-Rich-Phosphoproteins
to Apatites

Human acidic PRP's (and statherin) inhibit seeded crystal growth of calcium phosphate phases (Hay *et al.*, 1979; Oppenheim *et al.*, 1982). However, they do not inhibit precipitation of basic calcium phosphate phases from a solution which is supersaturated with respect to physiological concentrations. The acidic PRP's are thought to inhibit seeded growth by adsorption to the crystal, the phosphorylated TX peptide being of prime importance in the adsorption process (Hay *et al.*, 1979, 1987). The behaviour of the acidic PRP's is similar to that of the caseins (see section 3.3.2) except that they do not inhibit precipitation of calcium phosphate phases.

The adsorption of the acidic PRP's has been investigated using two different approaches: firstly by examining their adsorption to apatites and then constructing adsorption isotherms and secondly by examining their inhibition of seeded crystal growth. Most of this work was performed by E. C. Moreno and co-workers. They investigated extensively the adsorption thermodynamics of PRP's 1 - 4 and the TX peptide to hydroxyapatite and to fluorapatites (Moreno *et al.*, 1978; 1982; 1984). The data obtained were fitted to a Langmuir model for adsorption (Moreno *et al.*, 1978; see sections 3.1.4 and 3.1.9).

These adsorption studies revealed that the four acidic PRP's adsorb to hydroxyapatite and exhibit distinct differences in adsorption affinity despite their similarity in primary structure. Moreno *et al.* (1982) showed that the affinity constant of adsorption is determined by the N-terminal region alone, as the values for the TX peptide, PRP1 and PRP3 are essentially the same (25.3, 26.7 and 26.0 x 10^6 lmol^{-1} respectively) despite the large differences in size. In addition, the adsorption affinity constants for PRP2 and PRP4 are similar (18.1 and 21.0 x 10^6 lmol^{-1} respectively), but are lower than those of PRP1 and PRP3 because of the substitution of an asparagine for an aspartyl residue at position 4. However, the two

phosphoseryl residues (at positions 8 and 22) were also shown to play a vital role in adsorption to hydroxyapatite (Moreno *et al.*, 1984). Moreover, the role of the phosphoseryl residues was shown to be of prime importance in inhibition of seeded crystal growth as dephosphorylation of the acidic PRP's resulted in a reduction in inhibition to 1% of the original activity (Hay and Moreno, 1979).

The areas occupied per molecule (A) for acidic PRP adsorbed to hydroxyapatite at 37°C and 4°C are listed below (Table 3.1; Moreno *et al.*, 1982):

	A (nm^2/molecule) 37°C	A (nm^2/molecule) 4°C
PRP1	8.3	9.71
PRP2	8.3	-
PRP3	10.38	11.07
PRP4	9.22	-
TX-peptide	5.9	-

The values for the two homologous pairs are quite similar, but in both cases, the area occupied is larger for the smaller molecule. This is unexpected, as if the area occupied is related to the packing of molecules on the surface, the smaller the molecule, the lower the value of A (as examplified by the TX-peptide). PRP3 has a calculated net negative charge of eight (Wong *et al.*, 1979), whereas PRP1 has a calculated net negative charge of five (Wong and Bennick, 1980). Therefore Moreno *et al.*, (1982) suggested that adsorption of PRP3 (with a higher charge density) onto one adsorbent site may induce polarisation in the neighbouring sites to a larger extent than PRP1. Which results in a lower adsorption of PRP3, thus explaining the lower value of A.

Moreno *et al.* (1982) proposed the following model for acidic PRP adsorption to apatites. The adsorption of the acidic PRP's is an endothermic process and adsorption is therefore "driven" by an increase in entropy. Most of the entropy increase originates from the adsorbing molecules, probably through disruption of internal ion pairs and hydrogen bonds and by displacement of water molecules from

both protein and sorbent surface. The acidic PRP's have a higher affinity for fluorapatites than for hydroxyapatite, this being ascribed to the lower surface energy of fluorapatites, which results in a decrease in the sorbent's affinity for water and, as a consequence, an enhanced interaction between protein and adsorbent (Moreno *et al.*, 1982).

3.3 Milk Phosphoproteins: The Caseins

The biological function of milk, as well as providing a source of amino acids for the suckling, is to provide a means of transporting calcium and phosphate, in a readily assimilable form, from dam to young. Milk performs these functions by virtue of the caseins. Other proposed functions of the caseins include protection of the mammary gland from ectopic calcification (Holt and Sawyer, 1988) and the production of biologically active peptides (*e.g.* the casomorphins; Maubois and Leonil, 1989) during digestion.

3.3.1 Introduction

The caseins in cows' milk, and all other milks so far studied, are found in colloidal spherical particles known as casein micelles. Bovine micelles range in size from 20 to 600 nm in diameter and consist of about 93% casein (by dry weight) and 7% calcium phosphate. The latter is called colloidal calcium phosphate (CCP) and plays an important role in maintaining micelle integrity.

The precise structure and dynamics of the casein micelle is unknown. A typical micelle contains in the order of 10,000 polypeptide chains, but they are variable in size, molecular weight and composition. There are two main schools of thought concerning the substructure of casein micelles; the first supports the submicelle model (proposed by Schmidt, 1982) and the second proposes that the substructure results from aggregation of protein around calcium phosphate granules.

82

Native casein micelles have a high voluminosity and are more-or-less spherical, colloidal particles that contain the four casein types in an approximate weight ratio of 3 : 0.8 : 3 : 1 (casein of α_{s1}-, α_{s2}-, β- and κ-; Schmidt, 1982). Dispersed throughout the micelle, and forming an intergral part of it, are small granules of an amorphous calcium phosphate. The number frequency of micelle sizes decreases steadily with increasing diameter up to 200 nm (Schmidt *et al.*, 1973; Dewan *et al.*, 1974). Holt *et al.* (1978) and Kimber *et al.* (1978) observed a small, second maximum in the size distribution at a diameter of 80 to 100 nm, and also found a long 'tail' of size distribution which extended to a particle diameter of 600 nm.

Most of the casein monomers appear to be held in the micelle *via* links to calcium phosphate ion clusters. Electron microscopy (Knoop *et al.*, 1979) indicated that the ions are distributed throughout the protein matrix as clusters of ions a few nanometers in diameter. The caseins are thought to interact with the ion clusters, *via* their phosphoseryl residues, although most of the evidence is indirect (Aoki *et al.*, 1987; Farrell and Thompson, 1988; Schmidt and Poll, 1989) and possibly *via* the carboxyl groups of glutamyl and aspartyl residues (Byler and Farrell, 1989). The milk salt system has been divided, historically, into micellar calcium phosphate (MCP), which is in fact a mixture of calcium phosphate and casein derived phosphopeptides, and colloidal calcium phosphate (CCP) which refers only to the small ion clusters found within the micelle. A full description of the methods and results of the chemical and physical characterisation of the calcium phosphate of milk is beyond the scope of this discussion, and the reader is referred to Holt *et al.* (1981, 1982) and Holt (1992).

The casein micelle is described as an almost spherical particle and is proposed to possess substructure. This substructure, first recognised by electron microscopy (Rose and Colvin, 1966; Carrol *et al.*, 1968; Schmidt *et al.*, 1973; Kalab *et al.*, 1982) and ultracentrifugation investigations (Morr, 1967; Slattery and Evard, 1973), and later confirmed by small angle neutron scattering work (Stothart

and Cebula, 1982; Stothart, 1989), has been ascribed to the existence of submicelles of 8 to 20 nm in diameter (Buchheim and Welsch, 1973; Farrell, 1973; Creamer and Berry, 1975; Schmidt, 1982). The existence of substructure led Morr (1967) to postulate the submicelle model for casein micelle structure, which was later modified by Slattery and Evard (1973) and then by Schmidt (1980).

The modified submicelle model (Schmidt, 1982) proposes that the submicelles have a hydrophobic core, covered with a hydrophilic coat in which the polar moieties of the κ-casein molecule are accumulated in one or more areas on the submicelle surface. The remaining parts of the submicelle surface are composed of the polar parts of the other caseins, notably the phosphoseryl residues. The submicelles are then assumed to aggregate into micelles by interaction of the phosphoseryl residues with finely divided colloidal calcium phosphate (CCP). Submicelles with low levels of or no κ-casein are buried in the interior of the micelle. As the κ-casein content of the surface "shell" of the submicelles increases, with a concomitant decrease in phosphoseryl residues, micelle growth will ultimately come to an end. The weak point of this model is the requirement of the κ-casein to be unevenly distributed on the surface of the submicelle (Schmidt, 1982).

A second model, argued for by Holt and Hukins (1991) and Holt (1992), proposes that the substructure results from casein adsorbing to small calcium phosphate ion clusters. As more casein monomers associate, either with other caseins or with ion clusters, the casein micelle forms. The advantage of this model is that κ-casein does not have to be located at specific surface sites of the submicelle.

3.3.2 The Caseins

Mammary epithelial cells are responsible for the synthesis and secretion of milk proteins. Messenger RNA's encoding the secretory proteins are translated by polysomes bound to the rough endoplasmic reticulum (Palade, 1975; Blobel, 1980) and the polypeptides enter the Golgi apparatus for further post-translational

modification and eventual secretion.   As the caseins travel through the rough endoplasmic reticulum and on to the Golgi apparatus, the α_{s1}-, α_{s2}-, β- and κ-caseins are post-translationally modified by phosphorylation (Mercier and Gaye, 1983) and κ-casein is glycosylated.   From the distal face of the Golgi apparatus secretory vesicles break off and begin to migrate to the apical membrane.   It is at this stage that the micelles are thought to form.   Once the vesicles arrive at the apical membrane, exocytosis occurs and the micelles are released into the mammary gland alveolus.

Phosphorylation of the caseins is necessary for their major biological function of calcium and phosphate transport from dam to young.   Caseins interact with colloidal calcium phosphate and in doing so maintain the integrity of the casein micelle.   At least two different protein kinases are involved in phosphorylation of the caseins (Bingham, 1987).   The casein kinases of the mammary gland are highly specialised and specific: they phosphorylate seryl residues and, to a much lesser extent, threonyl residues at primary recognition sites that invariably have the sequence Ser/Thr-X-Y.   Where Y is either a glutamyl or sometimes an aspartyl residue and X is any amino acid.   However, if X is particularly basic or bulky it may reduce the extent of phosphorylation (Mercier, 1981).   Glycosylation is conferred upon κ-casein only. κ-Casein is glycosylated *via* the O-glycosyl mechanism, probably in the golgi apparatus (Takeuchi, 1984).

Knowledge of the physico-chemical properties of the caseins is of great relevance to our understanding of the interactions of caseins with calcium phosphate. The subject matter of this section has been comprehensively covered in several reviews (Payens and Vreeman, 1982; Schmidt, 1982; Swaisgood, 1982; Farrell and Thompson, 1988; Holt, 1992), to which the reader is referred for an account of the physico-chemical properties of the caseins.

The caseins form a family of proteins with a high degree of genetic divergence.   The most conserved regions of the casein genes are the sequences encoding the "5'-untranslated regions" of the messenger RNA's and the sequences

encoding the signal peptides and phosphorylation sites of the proteins. Caseins fall into four main categories; α_{s1}-, α_{s2}-, β- and κ-casein. Bovine caseins, and probably all other caseins, can be separated into the calcium-sensitve (α_{s1}-, α_{s2}-, β-) and the calcium-insensitive (κ-) caseins. There follows a brief review of the physico-chemical properties of β-casein, as it was this casein which was used throughout my investigation.

There is a total of seven known genetic variants of β-casein: the three "A" variants predominate in western breeds of cattle. Typically β-casein accounts for 33.6% (molar) of casein in milk, but this varies, especially at the onset of lactation and during involution. The complete primary sequences of the major β-casein variants have been determined (Mercier *et al.*, 1971) and five phosphoseryl residues have been identified; four in a cluster at positions 15, 17, 18 and 19 and the fifth at position 35. The primary structure of β-CN A[1] is as follows:

^{1}RELEELNVPG-EIVESLSSSE-ESITRINKKI-EKFQSEEQQQ-40

^{41}TEDELQDKIH-PFAQTQSLVY-PFPGPIPNSL-PQNIPPLTQT-80

^{81}PVVVPPFLQP-EVMGVSKVKE-AMAPKHKEMP-FPKYPVQPFT-120

^{121}ESQSLTLTDV-ENLHLPPLLL-QSWMHQPHQP-LPPTVMFPPQ-160

^{161}SVLSLQSQKV-LPVPEKAVPY-PQRDMPIQAF-LLYQQPVLGP-200

^{201}VRGPFPIS^{208}

The amino acid sequence of β-casein is such that the molecule has a hydrophilic head (the acidic N-terminal peptide containing four of the five phosphoseryl residues) and a hydrophobic tail, thus giving the molecule a polar character, somewhat like a surfactant. At near-neutral pH, β-casein possesses a net negative charge of about -12, which largely resides in the N-terminal 47 residues (the hydrophilic head).

In free solution β-casein behaves as an expanded coil of low axial ratio with a radius of gyration (assuming a "random coil" structure) of about 5.1 nm (Payens and

Vreeman, 1982). This value is only a little larger than the value found from low angle X-ray scattering (4.6 nm) and is not apparently changed in the presence of 6 M guanidium chloride. However, there is experimental evidence for some regular secondary structure within the β-casein molecule. Investigation by optical rotatory dispersion and circular dichroism spectroscopy indicates that the β-casein primary sequence is composed of 7 % α-helix, 33 % β-strand and 19 % β-turn (Andrews *et al.*, 1979; Graham *et al.*, 1984). When the temperature is raised from 25 to 60°C a decrease in the magnitude of the circular dichroism band at 220 nm results (Graham *et al.*, 1984). This might be interpreted as an increase in β-strand content at the expense of aperiodic structure with a constant proportion of α-helix. In addition, some secondary structure in the presence of high concentrations of urea or guanidium chloride appears to persist (Creamer *et al.*, 1981; Graham *et al.*, 1984). Secondary structure prediction methods have also been applied to β-casein, which suggest a structure with a similar degree of order (Creamer *et al.*, 1981; Graham *et al.*, 1984; Holt and Sawyer, 1988; Kumosinski *et al.*, 1991a,b).

A high degree of side chain mobility in the β-casein molecule is indicated by both ^{1}H- and ^{31}P-n.m.r. spectroscopy. The ratio of the intensities of the aliphatic and aromatic protons agrees fairly closely with that expected from the amino acid composition (Andrews *et al.*, 1979; Sleigh *et al.*, 1983). However, the absolute intensities are lower in 8 M urea than in trifluoroacetic acid solution and lower still in ^{2}H$_2$O solution. The latter indicates that a proportion of the amino acid side chains are in fairly fixed conformational states (Andrews *et al.*, 1979).

In solution, β-casein monomers associate to form micelles above a critical micelle concentration of 0.5g/l (at 21°C, ionic strength 0.2 M in the absence of calcium ions). The β-casein molecules behave like simple surfactants, to form spheroidal, soap-like micelles (Payens and Vreeman, 1982). Various findings support a monomer/polymer equilibrium model, with the number of monomers being fairly large. For example, in the analytical ultracentrifuge there is good separation between monomer and micelle peaks (Payens and Vreeman, 1982).

87

This peptide has a calculated net charge of -12 at pH 6.6, and circular dichroism spectral analysis indicates no regular secondary structure. Lack of α-helix is attributed to the structure-breaking properties of the prolyl residue at position 9 and to charge repulsion by the four phosphoseryl residues at positions 15, 17, 18 and 19 (Creamer et al., 1981; Chaplin et al., 1988).

3.3.3 Casein Interaction with Calcium Phosphate Minerals

At the pH of milk, 37°C and at free calcium and phosphate concentrations similar to those in milk, but without magnesium ions, rapid precipitation of amorphous calcium phosphate occurs (van Kemenade and de Bruyn, 1987, 1989). Addition of whole casein at very low concentrations ($< 10^{-8}$ M) results in a dramatic increase in the time that elapses before the onset of precipitation. However, the rate of crystal growth thereafter is hardly affected by casein. At casein concentrations exceeding 5×10^{-8} M, octacalcium phosphate forms instead of hydroxyapatite (van Kemenade, 1988).

The inhibitory effects of casein on the precipitation kinetics can be understood in terms of adsorption of casein onto the active growth sites of the crystal surface, using the Langmuirian theory of adsorption (van Kemenade, 1988). For whole casein, this model of adsorption indicates a very high adsorption affinity and virtually complete site occupancy. In addition, for most of the caseins (α_{s1}-, β- and κ-) there is a linear relationship of increasing affinity for apatite crystals as phosphoserine content increases. When the phosphoserine content was decreased (by partial dephosphorylation of β-casein) the ability of casein to inhibit apatite precipitation was also decreased (Holt and van Kemenade, 1989) indicating the importance of the phosphoseryl residues. However, at very low casein concentrations there was a reduction in the time taken for precipitation to occur indicating that casein stimulated nucleation *in vitro* which suggests a possible role for casein as a nucleation centre in milk. Similar experiments showed that

phosphoserine also markedly reduced the time for amorphous calcium phosphate precipitation to occur (van Kemenade, 1988) but, at the same time, this amino acid (at higher concentrations) also inhibited crystal growth by adsorption at the growth sites (Schmidt, 1987; Schmidt *et al.*, 1987).   These studies suggest that the phosphoseryl residues of casein may act as nucleation centres for calcium phosphate crystals.

This observation led Holt and van Kemenade (1989) to propose the hypothesis for casein micelle formation in the Golgi apparatus, that calcium phosphate can precipitate directly onto the casein in a controlled way so that a highly dispersed, large surface area, amorphous calcium phosphate is produced.   Further casein interactions could then result in micelle formation.   Alternatively, nucleation of calcium phosphate occurs (without casein), then casein rapidly adsorbs preventing further growth of the mineral phase, resulting in the same highly dispersed calcium phosphate phase found in micelles.

Stabilisation of thermodynamically unstable calcium phosphate phases is commonly observed in biological mineralisation processes.   This phenomenon is believed to be the result of adsorption of ions or macromolecules on the growth sites of such crystalline phases.   The effect of α_{s1}-, β- and κ-casein on the seeded growth of hydroxyapatite, octacalcium phosphate and dicalcium phosphate dihydrate crystals has been studied (van Kemenade, 1988).   In carefully controlled, seeded crystal growth experiments, all three caseins, at pH values 7.4, 6.4 and 5.5, reduced the growth rate of calcium phosphate crystals in the order hydroxyapatite < octacalcium phosphate < dicalcium phosphate dihydrate.   The growth of the thermodynamically most stable phase (hydroxyapatite) was least affected.   The order of the degree of inhibition was the order of phosphoseryl residue content of the casein (*i.e.* κ- < β- < α_{s1}-casein) for all mineral phases studied.   Complete suppression of crystal growth at much less than monolayer coverage was also observed.

3.3.3.1 Interaction of Caseins with Dicalcium Phosphate Dihydrate Crystals

Large, near perfect dicalcium phosphate dihydrate (DCPD) crystals can be grown by diffusion in acid solution (Legeros and Legeros, 1972; Legeros *et al.*, 1983). A representation of a single crystal of DCPD is given in Fig. 3.6 which shows its typical "platey" habit with well developed (010) faces whereas the fast growing (121) and (110) faces are hardly developed at all. The crystal structure of DCPD is known (Curry and Jones, 1971): DCPD contains compact, corrugated sheets, consisting of parallel chains (each composed of alternating anions and cations) normal to the (010) face, in which calcium ions are coordinated by six oxygen atoms of the anions and by two oxygen atoms of the water molecules. Electron micrographs of the DCPD crystals used throughout this study are shown in Fig. 3.7.

The crystal habit of DCPD is affected by the method of growth, by temperature and by the presence of impurities such as fluoride, magnesium, strontium, CO_3^{2-} and $P_2O_3^{4-}$ ions (Marshall and Nancollas, 1969; Legeros and Legeros, 1972).

Crystal habit can also be influenced by macromolecules (Addadi and Weiner, 1985; Addadi *et al.*, 1985) which are thought to adsorb selectively to certain crystal faces present during growth and therefore to alter the crystal's habit. When DCPD crystals are grown in the presence of whole casein, the morphological importance of the edge faces in the (010) zone increases markedly, indicating a preferential adsorption at these planes (van Kemenade, 1988). In addition to enlarging these faces, casein has the effect of producing sawtoothed structures on the edges of the crystal (van Kemenade, 1988). van Kemenade (1988) also examined the influence of β-CN A on the rate of seeded growth of DCPD crystals. The fractional reduction in relative growth rate of DCPD crystals in the presence of β-CN A (10^{-7} to 10^{-6} M) could be interpreted in terms of the blocking of active growth sites through a
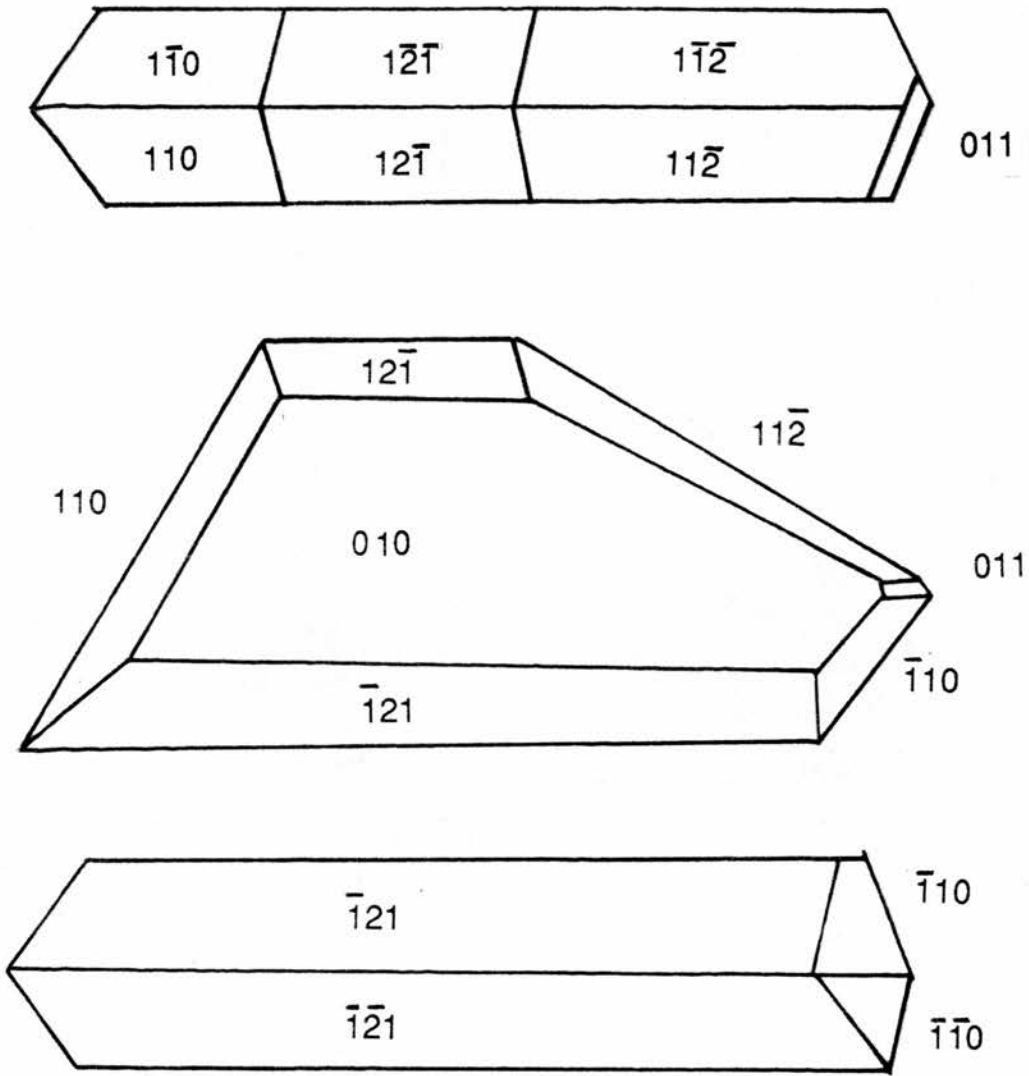
Figure 3.6   Sketch of a Perfect, Single Crystal
of Dicalcium Phosphate Dihydrate (DCPD)

Each crystal face is given its Miller index.

Figure 3.7   <u>Electron Micrographs of the Dicalcium Phosphate Dihydrate Crystals</u>
               <u>used Throughout this Investigation</u>

DCPD crystals were prepared as described in section 3.4.3.   A sample was
prepared for electron microscopy and the micrographs were kindly prepared by Mr. J.
Findlay (Science Faculty - E.M. Facility, University of Edinburgh)

93
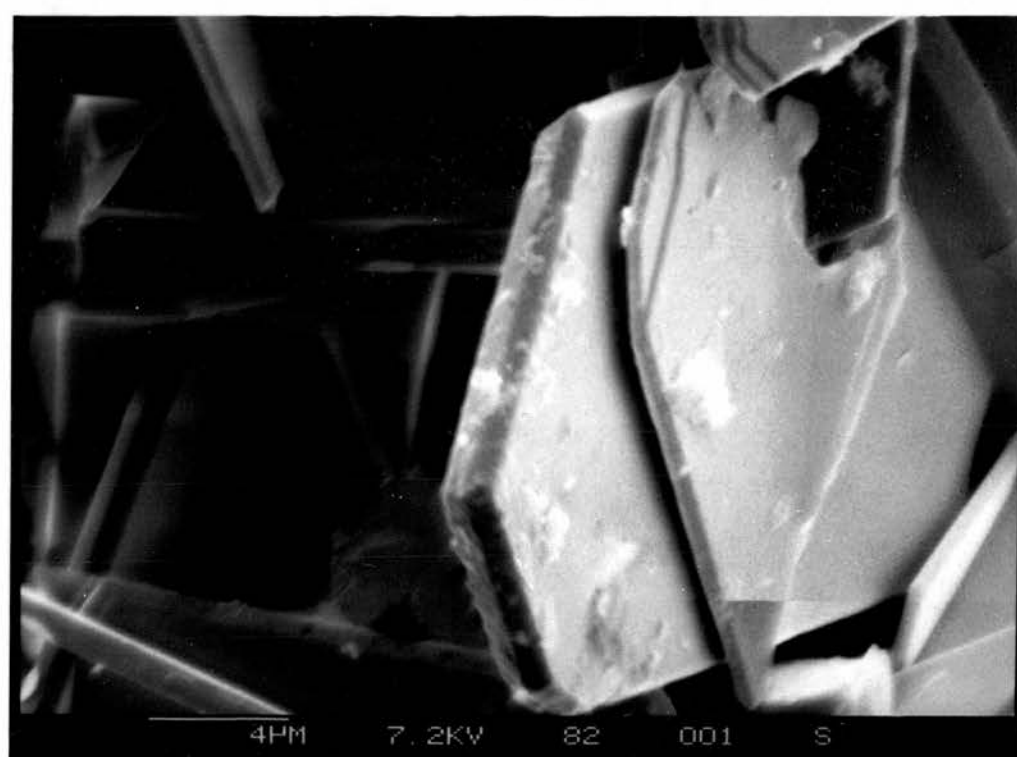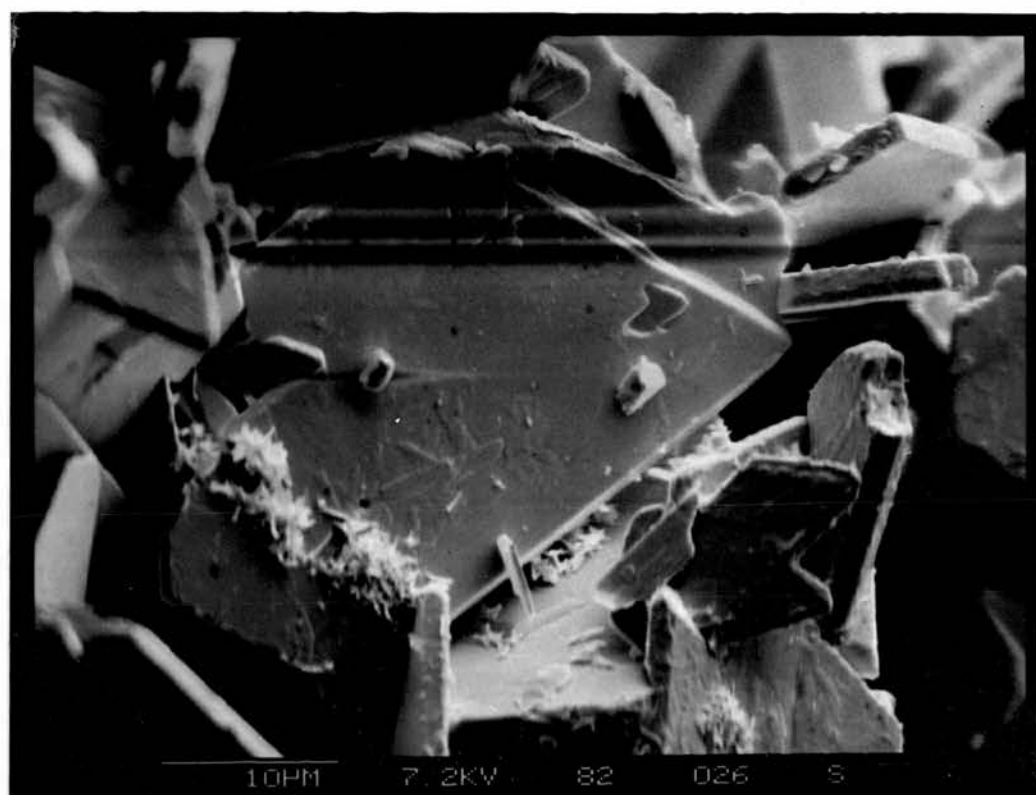
Langmuirian adsorption model. The affinity constant of β-CN A at pH 5.5 and 37°C for DCPD crystals was 2.1 x 10^{-8} M.

3.4 General Methods

All chemicals were of "Analar" grade and were purchased from BDH Ltd. unless otherwise stated. All solutions were made with de-ionised water and the pH was measured with a Radiometer combination glass electrode type GK 2401C. Free calcium ion concentrations were determined using a Radoimeter selective calcium ion electrode, type 93-3209, calibrated with freshly-prepared standard solutions having the same ionic strengh as the unknowns. [^{14}C]Formaldehyde was purchased from Sigma Chemical Company, Poole, Dorset (1 mCi/ml with a specific activity of 51.1 mCi/mmol).

Pure bovine β-casein A (β-CN A) was prepared using the method of Aschaffenburg (1963) by Mrs. E. Little (Hannah Research Institute). Crude β-CN (f1-25) was prepared from bovine β-CN A by tryptic digestion, essentially as described by Manson and Annan (1971), by Dr. C. Holt and Mrs E. Little. Concentrations of bovine β-CN A and β-CN (f1-25) were determined spectrophotometrically by the bicinchoninic acid protein assay (BCA assay; Pierce Ltd.) in accordance with the manufacturer's instructions. The assay was calibrated with standard solutions of β–CN A or β–CN (f1-25) as appropriate.

Specific surface areas of DCPD samples were determined by the multi-point 'BET' method (krypton adsorption) performed by MCA Services, Melbourn Science Park, Cambridge. Amino acid analyses were kindly performed by Dr. J. Leaver (Hannah Research Institute) and amino acid sequencing by the WELMET Protein Sequencing Service, University of Edinburgh.

3.4.1 The Purification of Bovine β-CN (f1-25)

Purification of the phosphopeptide β-CN (f1-25) was a two step process; first, ion-exchange chromatography and secondly de-salting of the purified phosphopeptide.

3.4.1.1 Purification of β-CN (f1-25) by Ion-Exchange Chromatography.

The peptide was purified by ion-exchange chromatography using DEAE Sephadex A50 (Pharmacia Ltd.) equilibrated in 0.1mM sodium dihydrogen phosphate (pH 2.6). Elution was effected by a linear pH gradient (pH 2.6 to 1.6) using 0.1mM potassium chloride (pH 1.6) of 1 litre volume.

Crude phosphopeptide (500 mg) was applied to the column (dimentions 26 x 230 mm), the flow rate being 9.0 $mlh^{-1}cm^{-2}$, and 10 ml fractions were collected. The absorbance of each fraction was measured at 230 nm (A_{230nm}) in 2.0 mm optical path length silica cuvettes and two peaks were detected (see Fig. 3.8). Pooled fractions (as indicated in Fig. 3.8) were lyophilised and a total amino acid analysis performed as a means of identification. Peak 1 was found to be β-CN (f1-25) and peak 2 to be either β-CN (f2-25) or β-CN (f1-24).

3.4.1.2 De-salting of β-CN (f1-25)

Contaminating salt was removed from peak 1 by gel filtration using Sephadex G-10 (Pharmacia Ltd.) equilibrated with de-ionised water. A column of dimensions 12 x 260 mm was prepared and packed according to the manufacturer's instructions. A flow rate of 21.0 $mlh^{-1}cm^{-2}$ was used and 1.0 ml fractions were collected. The absorbance of each fraction was measured at $A_{230\ nm}$ instead of $A_{280\ nm}$ as the peptide contains no tyrosine, tryptophan or phenylalanine residues. A single peak was observed (see Fig. 3.9). To ensure complete removal of salt, the
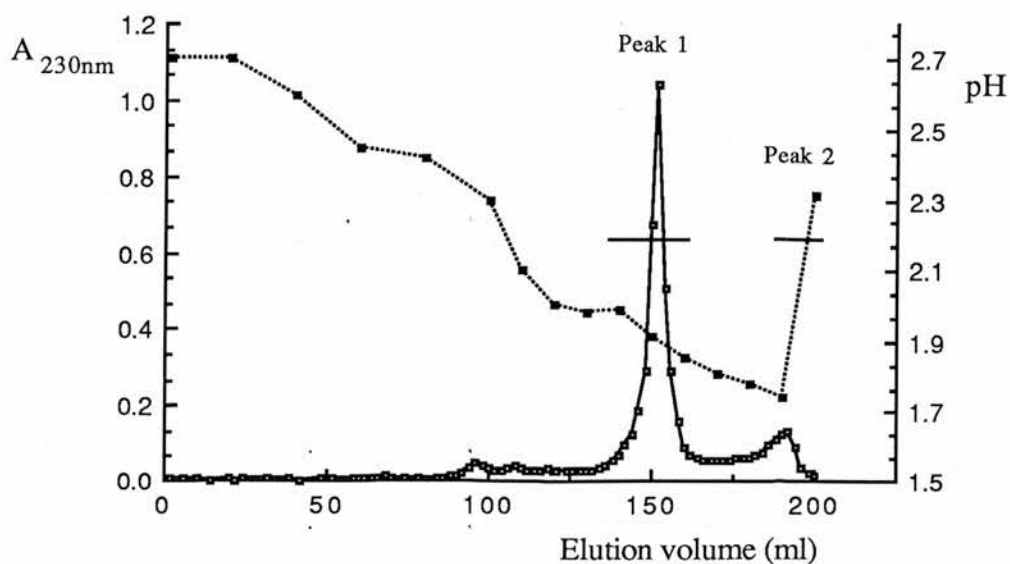
Figure 3.8   Elution Profile from the DEAE A50 Ion-Exchange Column

for the Purification of ß-CN (f1-25)

Crude ß-CN (f1-25) was applied to the ion-exchange column as described in section

3.4.1.1.   The absorbance of the fractions was measured at $A_{230\ nm}$, pH of the

fractions was measured with a Radiometer combination glass electrode type GK

2401C.

> indicates absorbance at $A_{230\ nm}$
>
> indicates the pH gradient
>
> The horizontal bar indicates pooling of fractions.
>
> Peak 1 = ß-CN (f1-25)
>
> Peak 2 = ß-CN (f2-25) or ß-CN (f1-24)
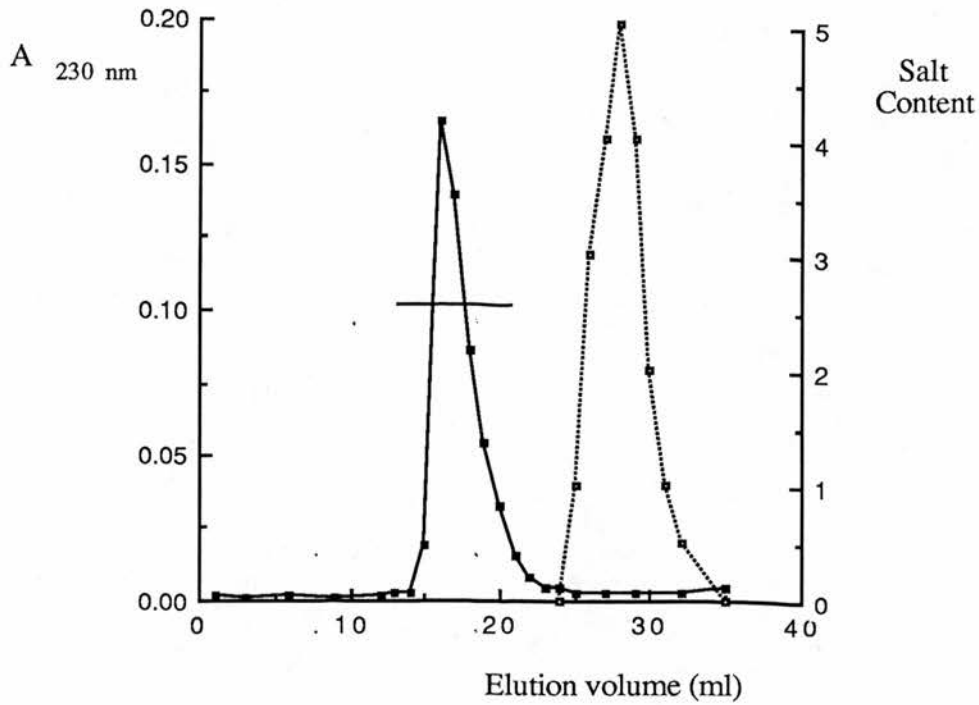
Figure 3.9   Elution Profile from the Sephadex G-10 De-Salting Column

for ß-CN (f1-25)

Peak 1 (ß-CN (f1-25)) from the DEAE A50 ion-exchange column (see section 3.4.1.1) was de-salted as described (in section 3.4.1.2). The absorbance of the fractions was measured at $A_{230 \text{ nm}}$ and the presence of salt was determined by the turbidity (estimated by eye and then rated on a scale of 0 to 5) resulting from the addition of silver nitrate solution (see section 3.4.1.2).

———■——— indicates absorbance at $A_{230 \text{ nm}}$.

·········■········· indicates turbidity.

The horizontal bar indicates pooling of fractions absorbing at $A_{230 \text{ nm}}$.

97

salt eluting from the column was detected by the turbidity (estimated by eye) resulting from the addition of 1 drop of a silver nitrate solution (1% w/v; see Fig. 3.9).

The peak absorbing at A_{230nm} was collected as indicated (Fig. 3.9) and lyophilised to give pure β-CN (f1-25). A second total amino acid analysis was performed on the de-salted, lyophilised phosphopeptide and as a final check the sequence of the first five amino acids was determined (Welmet Protein Sequencing Service, University of Edinburgh). The β-CN (f1-25) was then lyophilised and stored at -15°C.

3.4.2 The Radiolabelling of β–CN A and β-CN (f1-25)

As an alternative, and more sensitive, means of estimating protein concentration both β–CN A and β-CN (f1-25) were ^{14}C-radiolabelled by the reductive methylation of their primary amino groups.

3.4.2.1 β-CN (f1-25)

β-CN (f1-25) was radiolabelled by reductive alkylation following the method used by Dottovio-Martin and Ravel (1978). This method utilises [^{14}C]formaldehyde and sodium cyanoborohydride as reducing agent.

To 56 μl of a 10 mg/ml solution of β-CN (f1-25) (in 40 mM phosphate buffer pH 7.0) was added 18 μl of [^{14}C]formaldehyde (0.35 μmol, 18 μCi). To this mixture was added 36 μl of a freshly-made solution of sodium cyanoborohybride (6.0 mg/ml; in 40 mM phosphate buffer pH 7.0), the solutions were mixed and the reaction allowed to proceed at room temperature for 2 hrs. Below is a chemical equation for the reaction:

$$R\text{-}NH_2 + HCHO + NaBH_3CN \longrightarrow R\text{-}NH(CH_3) + HCN + NaH_2BO_3$$

The reaction mixture was de-salted by gel filtration using a Bio-Gel P2 gel filtration column (Bio-Rad Ltd.) of dimensions 13 x 460 mm, which was prepared and packed according to the manufacturer's instructions. A flow rate of 8.6 mlh^{-1}cm^{-2} was used and the absorbance of each 1.0 ml fraction was measured at $A_{230\ nm}$ (see Fig. 3.10). Radioactivity in the fractions was determined by liquid scintillation spectrometry (in a Beckman LS 2800 counter) using 10 µl of each fraction in 5.0 ml of "Emulsi-safe" scintillation fluid. Fractions were pooled as indicated (see Fig. 3.10), lyophilised, and prepared for adsorption assays as described (see section 3.4.5).

3.4.2.2 Radiolabelling of β-CN A

β-CN A was also radiolabelled by the method of Dottovio-Martin and Ravel (1978). Briefly, to 3.39 ml of a 10 mg/ml solution of β–CN A (in 40 mM phosphate buffer pH 7.0) was added 72 µl of [^{14}C]formaldehyde (1.411 µmol, 72 µCi). To this mixture was added 148 µl of a freshly-made solution of sodium cyanoborohydride (6.0 mg/ml; in 40 mM phosphate buffer pH 7.0), the solutions were mixed and the reaction was allowed to proceed at room temperature for three hours. Then a further 148 µl of sodium cyanoborohydride was added, the solutions mixed and the reaction allowed to proceed for a further 2 hrs. The reaction mixture was then dialysed extensively against de-ionised water for 2 days at 4°C to remove any unreacted [^{14}C]formaldehyde and sodium cyanoborohydride. The specific activity of the ^{14}C-β-CN A product was then determined by liquid scintillation spectrometry. Radioactivity was determined by liquid scintillation spectrometry (in a Beckman LS 2800 counter) by using two 100 µl aliquots of the dialysed protein (1 in 4 dilution of the non-dialysable material) added to 5.0 ml of "Emulsi-safe" scintillation fluid.
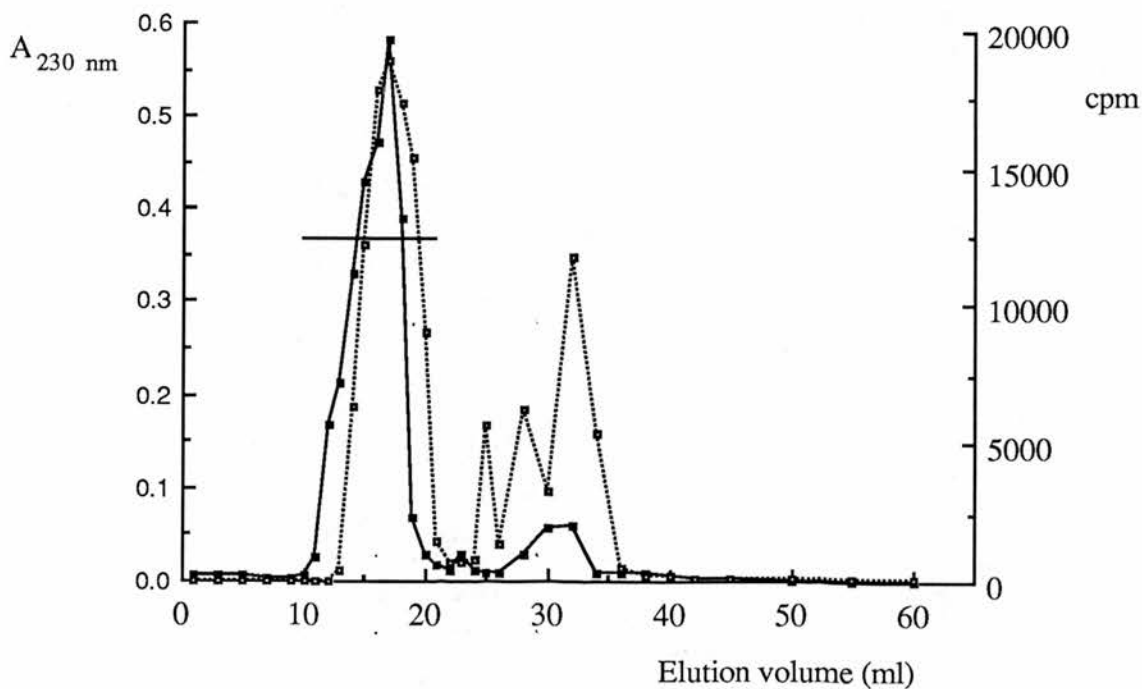
Figure 3.10   Elution Profile from the Bio-Gel P2 De-Salting Column

for ^{14}C-ß-CN (f1-25)

^{14}C-ß-CN (f1-25)) was prepared and de-salted as described (in section 3.4.2.1). The

absorbance of the fractions was measured at $A_{230\,nm}$ and associated radioactivity was

determined by liquid scintillation spectrometry as described (in section 3.4.2.1).

———■——— indicates absorbance at $A_{230\,nm}$

········□········· indicates associated radioactivity as cpm

The horizontal bar indicates pooling of fractions absorbing at $A_{230\,nm}$.

	cpm	Protein concentration (mg/ml)	Specific radio-activity μCi/mg
^{14}C-ß-CN A	4.3×10^5	1.5	1.3
^{14}C-ß-CN A with 20% (w/v) TCA	700	-	-
^{14}C-ß-CN (f1-25)	9.03×10^6	0.43	2.558

Table 3.2   Radioactivity associated with ^{14}C-ß-CN A1 and ^{14}C-ß-CN (f1-25)

Radioactivity associated with ^{14}C-ß-CN A1 and ^{14}C-ß-CN (f1-25) was determined by liquid scintilation spectrometry as described (in sections 3.5.2.1 and 3.5.2.2). Protein estimations were performed using the BCA assay (see section 3.5).

To confirm that radioactivity was associated with β–CN A, a 300 μl aliquot was mixed with 300 μl of trichloroacetic acid (20% w/v) to precipitate the β–CN A and then centrifuged for ten minutes in a bench top micro-centrifuge at full speed to pellet the precipitated protein. Two 100 μl aliquots were subsequently added to two 5.0 ml aliquots of "Emulsi-safe" scintillation fluid and their radioactivity (see Table. 3.2) determined as above. These results indicate that the radioactivity is associated with the protein fraction.

3.4.2.3 Dilution of ^{14}C-β–CN A for Adsorption Experiments

To 45.37 mg of un-radiolabelled β–CN A, 4.63ml of a 1.5mg/ml solution of ^{14}C-β–CN A was added. This mixture was dialysed against 1.0 litre of adsorption assay buffer (see section 3.4.4) for 16 hours at 20°C and was used as the stock protein solution.

3.4.3 Preparation of Dicalcium Phosphate Dihydrate Crystals (DCPD)

Two preparations of DCPD, designated A and B, both prepared by the method of Jensen and Rathley (1953), were used for the adsorption experiments. Briefly, 1 litre of 0.5 M disodium hydrogen orthophosphate and 0.037 M potassium dihydrogen orthophosphate, and 1 litre of 0.5 M calcium chloride were added slowly to 0.5 litre of 0.147 M potassium dihydrogen orthophosphate at room temperature with rapid mechanical stirring over a period of approximately three hours. The DCPD crystals were harvested by collection onto filter paper (Whatman No. 1) and then washed three times with 330 ml portions of phosphoric acid (0.16 ml of 45 % orthophosphoric acid in 1 litre of water) and then once with 250 ml of ethanol. The crystals were then dried *in vacuuo* over silica gel in a dessicator. The identity of DCPD from each preparation was verified by infrared spectroscopy (by Dr. C. Holt, Hannah Research Institute) and the yield of DCPD from each was 96%. The

specific surface areas of the two DCPD preparations were determined by the multipoint 'BET' method and were found to be:

Preparation A = 0.684 m^2g^{-1}

Preparation B = 0.919 m^2g^{-1}

3.4.4 Preparation of Buffers to be used in Adsorption Experiments

It is essential with all adsorption experiments that the environment of the system (*i.e.* that of the solid and the liquid phases) is fully defined so that meaningful results can be obtained. The buffers used in these adsorption experiments were chosen to have properties in common with milk. They were carefully designed to ensure that their ionic strength, pH and free calcium ion activities were similar to those found in bovine milk serum (Holt *et al.*, 1981). A free calcium ion concentration of approximately 4.0 mM was selected for the reason above and because free calcium ions are essential for caseins to bind to calcium phosphate phases (Holt *et al.*, 1986). As DCPD is slightly soluble (Moreno *et al.*, 1960a,b), buffers saturated with respect to DCPD must be used during experimentation to avoid crystal dissolution and the concomitant change in surface area and calcium ion activity. Buffers had an ionic strength of approximately 80 mM and a free calcium ion concentration of approximately 4.0 mM (see Table 3.3). Buffers were saturated with respect to DCPD after 48 hour's equilibration with excess of the salt at the appropriate temperature.

Four different buffers were prepared (summarised in Table 3.3) using calcium and potassium nitrate stock solutions. Their pH's were checked and adjusted with nitric acid before dilution with deionised water to their final concentrations. Buffers were equilibrated with 2.0 g/litre of DCPD, at the temperature intended for the adsorption experiments, in a water bath for 48 hours. Then the excess DCPD was removed by filtration through a Buchner funnel. The

Temperature of incubation (°C)	pH	Free calcium ion concentration after incubation (mM)	Imidazole concentration (mM)	Potassium nitrate concentration (mM)	Urea concentration (M)
20	6.5	4.02	20	60	0.0
20	7.0	3.91	20	60	0.0
3.0	7.0	3.76	20	60	0.0
20	7.0	4.78	20	60	6.0

Table 3.3   Composition of Buffers used in Adsorption Experiments

buffers were then stored (in a water bath) again at the temperature intended for the adsorption experiments (either 20°C or 3°C). Free calcium ion concentrations were measured, after equilibration with the DCPD crystals, using the selective calcium ion electrode and were found to be approximately 4.0 mM (see Table 3.3).

During the equilibration period the initial calcium ion concentration rose from 3.0 mM to approximately 4.0 mM due to dissolution of a portion of the DCPD crystals. Equilibration for 48 hours was found to be sufficient as no further increase in calcium ion activity was observed when equilibration was continued for a further five days (results not shown).

3.4.5 Preparation of Stock β-CN A and β-CN (f1-25) Solutions

Stock solutions of β-CN A and β-CN (f1-25) were prepared, just prior to each adsorption experiment, as follows.

3.4.5.1 β-CN A

A 10.0 mg/ml stock solution of β-CN A was prepared using the appropriate buffer for the conditions of each adsorption experiment (see Table 3.3). After passing each stock solution through a filter of pore size 0.8 μm (Millipore S.A., Molsheim, France), it was diluted with buffer to its final concentration used for adsorption experiments.

3.4.5.2 β-CN (f1-25)

A 20.0 mg/ml solution, of 10 ml volume, of β–CN (f1-25) was made using the appropriate buffer for the conditions of each adsorption experiment (see Table 3.3). The free calcium ion activity was measured with a freshly-calibrated, selective calcium ion electrode and was found to be negligeable. Calcium nitrate solution

105

(100 mM) was then added dropwise until the mV reading of the electrode was the same as that of a solution with 4.0 mM calcium nitrate and an ionic strength of 80 mM. The pH of this stock solution was adjusted to pH 7.0 with 1.0 M sodium hydroxide. It was then diluted to a total volume of 20 ml with fresh buffer, giving a 10 mg/ml stock solution. The stock solution was then passed through a filter of pore size 0.8 μm and diluted to the final concentrations to be used in the adsorption experiment.

As expected upon addition of (10.0 mg/ml, 6.4×10^{-6} M) β–CN (f1-25) to the buffer the initial concentration of free calcium ions fell to very low levels (as indicated by the fall in mV reading of the selective calcium ion electrode) because of calcium ions binding to the peptide (Baumy et $al.$, 1989). β–CN (f1-25) has the potential to bind 4 mol of calcium ions per mol of peptide. Therefore the addition of 6.4×10^{-6} mol of peptide per ml of buffer, containing 4×10^{-6} mol of calcium ions, will result in the binding of most of free calcium ions. As I wished to have similar calcium ion concentrations, so that results between experiments could be compared, and because free calcium ions are required for binding to calcium phosphate minerals, it was essential that the calcium ion concentration be restored to 4.0 mM. This was achieved by addition (as described above) of calcium nitrate solution.

Addition of β–CN A also resulted in a decrease in free calcium ion concentration, but to a much lesser extent. β–CN A has the potential to bind 5 mol of calcium ions per mol of protein. Therefore addition of 4.17×10^{-7} mol of protein per ml of buffer, containing 4×10^{-6} mol of calcium ions, will result in a decrease in calcium ion concentration but to a much lesser extent than addition of the β–CN (f1-25) solution. However, upon dilution to 3.0 mg/ml (the most concentrated solution used during adsorption assay) only a very small proportion (approximately 7%) of the free calcium ions will be bound to the protein (as indicated by the mV reading of the selective calcium ion electrode). As the fall in free calcium ions was

106

minimal it was not considered pertinant to restore the free calcium ion concentration as this would cause an unnecessary perturbation of the buffer system.

3.4.6 Adsorption Experiments

In order to examine the binding of β–CN A and β–CN (f1-25) to DCPD an adsorption assay was developed so that adsorption isotherms could be constructed. The adsorption assay had to fulfill certain requirements: it had to be simple to perform, accurate and be easily adaptable to other phosphoproteins.

Portions of DCPD were accurately weighed (100 mg or 200 mg) into ten screw cap bottles (20 ml volume). To each bottle was added an accurately measured volume (by micro-pipette) of stock protein or stock peptide solution (see section 3.4.5). The contents of the bottles were then mixed thoroughly, to disperse the DCPD, and incubated in a rocking water bath at the appropriate temperature (see Table 3.4 for 1 hour. Reference assays, without DCPD, were prepared and performed in parallel with each adsorption assay. Adsorption isotherms were determined at each of two DCPD / buffer ratios: 100 mg / 3.0 ml and 200 mg / 2.0 ml. For any given set of conditions (see Table 3.4) the resulting adsorption isotherms for each of the two ratios were similar.

After each incubation, a 1 ml aliquot was taken from each bottle and centrifuged in a bench-top micro-centrifuge at full speed for 2 minutes (x1000 g) to pellet any suspended DCPD. The supernatant was then collected and protein estimations performed using the bicinchoninic acid protein assay (BCA assay). The amount of β–CN A or β–CN (f1-25) adsorbed to the DCPD was calculated by subtraction as follows:

β–casein A or β–phosphopeptide 1-25 in reference assay supernatant	-	β–casein A or β–phosphopeptide 1-25 in "test" assay supernatant	=	Amount adsorbed to DCPD

107

Experimental Conditions			Number of experiments performed with ß-CN A		Number of experiments performed with ß-CN (f1-25)	
Temperature of incubation ($^\circ$C)	pH	Urea concentration (M)	DCPD preparation A	DCPD preparation B	DCPD preparation A	DCPD preparation B
20	6.5	0.0	3	-	-	-
20	7.0	0.0	5	3	9	4
3	7.0	0.0	-	-	-	3
20	7.0	6.0	-	3	-	-

Table 3.4   Summary of the Adsorption Experiments:

Experimental Conditions and the Number of Experiments Performed

for each set of Conditions

Experimental conditions were achieved as described in the text (section 3.4.6).

3.4.7 Adsorption Equilibrium Determinations

In order to ensure that adsorption in the above experiments had reached equilibrium within the one hour incubation period, a time course experiment was performed for each set of conditions (see Table 3.4) resulting in a graph of time of incubation *versus* amount adsorbed (see Fig. 3.11). DCPD (100 mg) was accurately weighed into glass screw cap bottles (20 ml volume). To each was added 3.0 ml of a 1.0 mg/ml protein or peptide solution. The contents of the bottles were thoroughly mixed and incubated for a fixed time (15, 30, 60, 120 and 240 min.). Appropriate reference assays (no DCPD) were performed in parallel with each adsorption assay. After incubation each bottle was treated as previously described (section 3.4.6).

3.5 Results and Discussion

In order to examine the adsorption of the milk phosphoprotein β-CN A and its tryptic phosphopeptide β-CN (f1-25) a binding assay was developed (see section 3.4.6). DCPD was the mineral chosen for these studies because it is considered to be closely related to the amorphous calcium phosphate mineral that forms colloidal calcium phosphate in milk (Holt *et al.*, 1982). In addition, DCPD can be easily prepared as well-formed (large) crystals with perfect stoichiometry. DCPD was prepared using the standard method for bulk preparation (see section 3.4.3) and its purity confirmed by infra-red sprctroscopy. Contamination of the DCPD by other calcium phosphate phases was not expected as care was taken to ensure that the pH was kept well below 7.0 during crystal growth. Above pH 7 the crystal growth solution may become saturated with respect to other calcium phosphate phases such as octacalcium phosphate (Moreno *et al.*, 1960a,b).

(Boratynski, 1985; Krystal *et al.*, 1985; Krystal, 1987) and the modified Lowry assay (Polacheck and Cabib, 1981); none of which was found to be suitable. Eventually the BCA assay (Smith *et al.*, 1985; Redinbaugh *et al.*, 1986) was adopted because it was sensitive within the protein/peptide concentration range used and was found to be unaffected by the assay buffers (results not shown).

The time required for adsorption equilibrium to be reached was determined for each set of adsorption conditions used (see Table 3.4) and the results obtained are shown in Fig. 3.11. These results indicate that equilibrium was reached within 15 minutes. Therefore, adsorption experiments were incubated for 1 hour, at least four times the time required to reach equilibrium, to ensure that equilibrium was well established. Later experiments with β-CN A, performed by Mrs. E. Little (Hannah Research Institute), confirmed that adsorption was complete within 1 min. In addition, desorption experiments (by dilution) indicated that there was no significant desorption of β-CN A after 2 hr.

During these time course, adsorption assays, and in subsequent experiments, it was found that the protein solution added to the DCPD crystals was only just depleted sufficiently. This was a result of the relatively small specific surface area of the DCPD crystals (see section 3.4.3). Therefore, the fact that DCPD forms large crystals was a disadvantage. This problem was circumvented to some extent by using a low buffer/mineral ratio so that the standard errors of the assays became acceptable.

To increase the sensitivity and accuracy of the adsorption assay, an alternative method of protein estimation was assessed; that of radiolabelling (see section 3.4.2). Methylation of the lysine residues was chosen as it has little or no effect on the size, shape, charge or secondary structure of β-casein (Evans *et al.*, 1971a,b). Specific activities of radiolabelled β-CN A and β-CN (f1-25) were 1.3 mCi/g and 2.558 mCi/g respectively. Knowing the specific activity of the [^{14}C]formaldehyde (51.1 mCi/mmol) the number of mol of ^{14}C atoms per mol of protein or peptide can be calculated and hence the average level of labelling (table

Figure 3.11   <u>Determination of the Time Taken to Reach Adsorption Equilibrium</u>

A time course experiment was performed as described (in section 3.4.7) for each set of adsorption experiment conditions (see Table 3.4) using the buffers described (in Table 3.3).   All these experiments were performed with DCPD preparation A.

Γ = x 10^{-7} moles of ß-CN A or ß-CN (f1-25) adsorbed per m^2 of DCPD.

—o—   indicates ß-CN A adsorption at pH 6.5 and 20°C.

—□—   indicates ß-CN A adsorption at pH 7.0 and 20°C.

—▲—   indicates ß-CN (f1-25) adsorption at pH 7.0 and 20°C.

—●—   indicates ß-CN (f1-25) adsorption at pH 7.0 and 3°C.

Values are the means ± half the range of duplicate determinations of an experiment. The half the range of the determination not shown are smaller than the symbol.

Γ (x10^{-7} moles ß-CN A or ß-CN (f1-25) adsorbed per m^2 DCPD)

Time of incubation (min.)
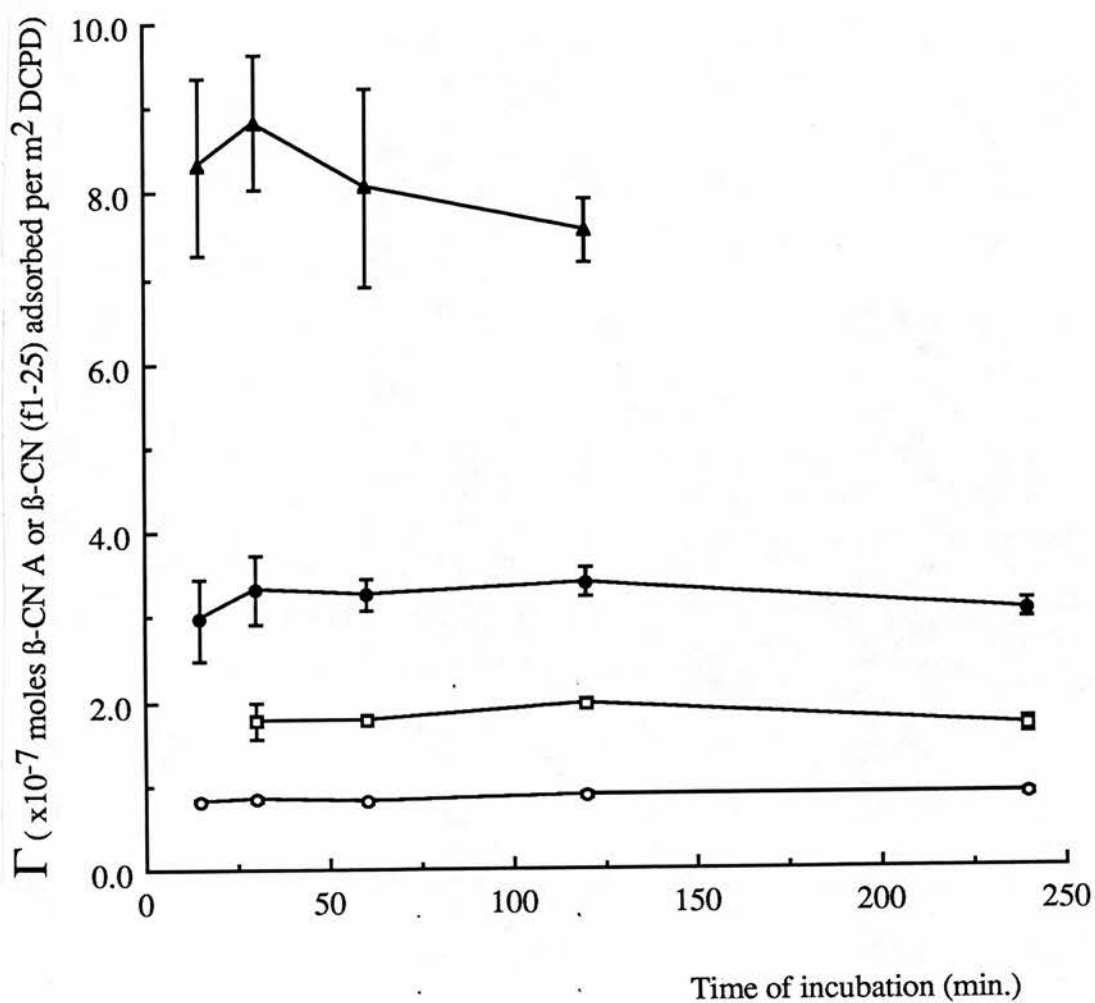
3.2): 0.155 mol/mol for β-CN (f1-25) and 0.61 mol/mol for β-CN A. These low levels of radiolabelling were desired (β-CN A has the potential to be labelled by 21 carbon atoms) to minimise the effects that radiolabelling can have on protein adsorption (Grant *et al.*, 1977).

The adsorption isotherms obtained using the BCA assay and by using ^{14}C-β-CN A both at pH 7.0, 20°C and using DCPD preparation B are compared in Fig 3.12. The adsorption isotherm obtained using the BCA assay is typical of those obtained for highly-solvated and flexible molecules such as β-CN A (discussed in section 3.1.4). The steep gradient of the initial part of the isotherms reflects a relatively high adsorption affinity (see Table 3.5) which is approximately 80 fold less than those of the acidic PRP's (see section 3.2.2 and Table 3.5). The adsorption isotherm obtained using ^{14}C-β-CN A shows a similar high adsorption affinity. The most striking difference between the two isotherms (see Fig. 3.12) is in the positions of Γ_p. When radiolabelled β-CN A was used, the adsorption plateau (measured at 6×10^{-5} molar free β-CN A) was approximately 25% lower than when the BCA assay was used in spite of the low average level of radiolabelling. This implies that methylation perturbs the structure of the adsorbed layer of β-CN A.

The lower Γ_p suggests that the ^{14}C-β-CN A molecules do not pack as closely together at the interface, possibly due to disruption of intermolecular interactions or by inducing a conformational change in the protein. However, with such a low average level of radiolabelling it is difficult to explain such a large decrease in Γ_p (approximately 25%) by disruption of intermolecular interactions and/or conformational changes alone. In view of the observed effect of radiolabelling on the adsorption isotherm (see Fig. 3.12) further use of the radiolabelled protein/peptide in binding studies was considered unsuitable for our purposes and was therefore discontinued.

Figure 3.12   Comparison of the Adsorption Isotherms obtained for ß-CN A

using the BCA assay and by using ^{14}C-ß-CN A

Two methods of protein estimation were used to determine the amount of protein adsorbed: the BCA assay and the use of ^{14}C-ß-CN A. They were compared in the adsorption experiments described (in section 3.4.6) performed at pH 7.0 and 20°C using DCPD preparation B. ^{14}C-ß-CN A was prepared as described (in section 3.4.2.2) and diluted for use in adsorption experiments as described (in section 3.4.2.3). Radioactivity of ^{14}C-ß-CN A was determined by liquid scintillation spectrometry as described (in section 3.4.2.2). Curves were fitted to the results using the computer program REGRESSION as described (see section 3.5.2) and the parameters of the curve are summarised in Table 3.5. Results are plotted as Γ (amount adsorbed per unit area; $\Gamma = x10^{-7}$ moles ß-CN A adsorbed per m^2 DCPD) *versus* C (equilibrium, free concentration x 10^{-5} M).

—o—   indicates ß-CN A determined by BCA assay.

—□—   indicates ^{14}C-ß-CN A determined by liquid scintillation spectrometry of ^{14}C-ß-CN A.

Values for ß-CN A determined by BCA assay are the mean $\pm$ S.E.M. of duplicate determinations of three separate adsorption experiments. Values for ^{14}C-ß-CN A determined by liquid scintillation spectrometry are the mean $\pm$ half the range of duplicate determinations of an experiment. The S.E.M. not shown are smaller than the symbol.

114

Γ (x10^{-7} moles ß-CN A adsorbed per m^2 DCPD)

C (x 10^{-5} M)
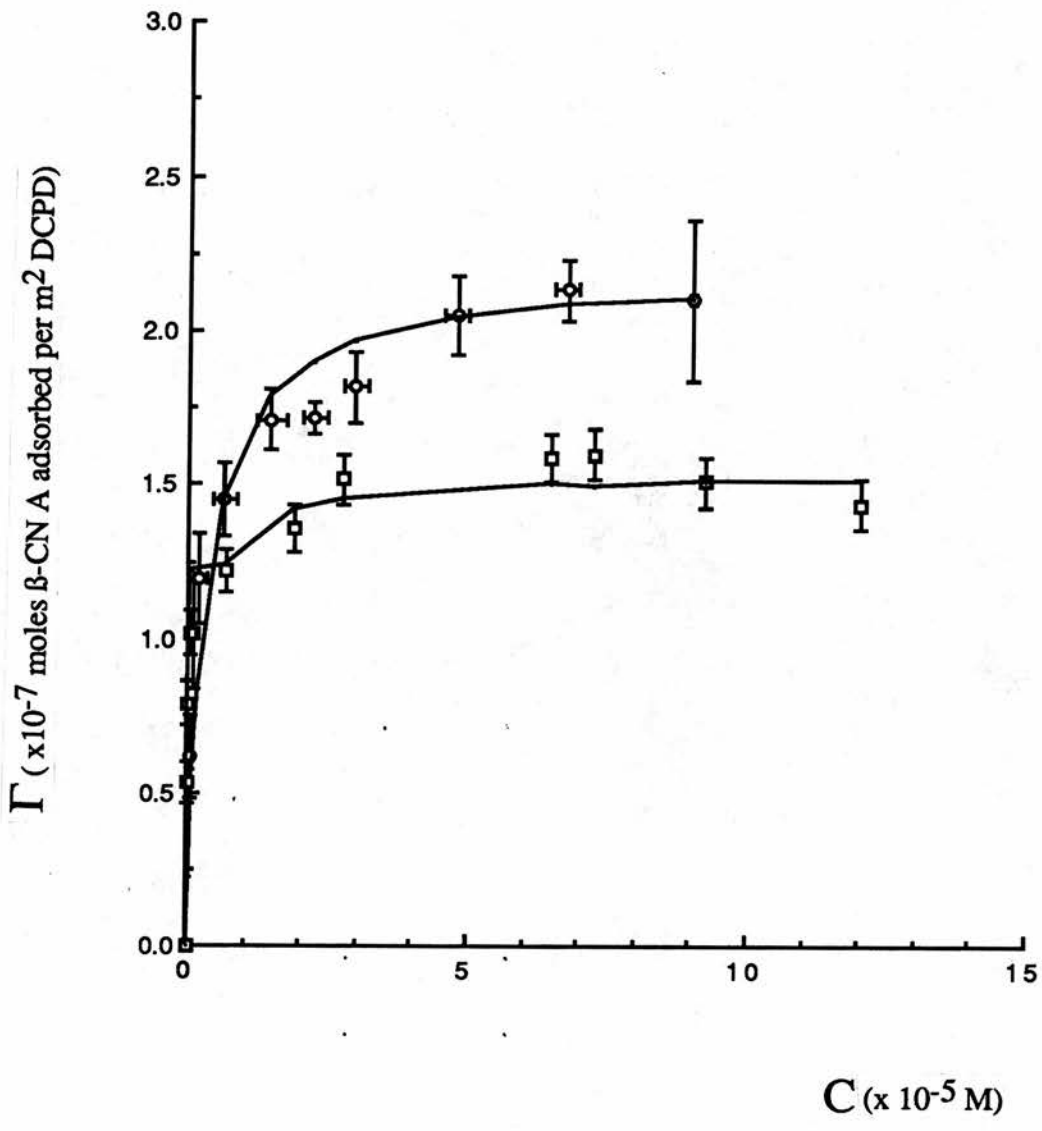
3.5.2 Differences between DCPD Preparations
with respect to Adsorption of β-CN A and β-CN (f1-25)

In the present study two preparations of DCPD were used, designated A and B, with specific surface areas of 0.684 and 0.919 m^2g^{-1} respectively. The adsorption isotherms for β-CN A and β-CN (f1-25), measured at pH 7.0 and at 20°C, for the two DCPD preparations are shown in Figs. 3.13 and 3.14. As expected for β-CN A, both isotherms (Fig. 3.13) show the typical pattern observed for highly solvated and flexible molecules (see section 3.1.4), but there is a difference of approximately 25% in the adsorption plateau (Γ_p; measured at 4×10^{-5} M free β-CN A) between preparations A and B. The isotherms for β-CN (f1-25) have a plateau (see Fig. 3.14; at about 2×10^{-4} M free β-CN (f1-25)) followed by an upward curvature from about 3×10^{-4} M free β-CN (f1-25). Again there is a difference of approximately 25% in Γ_p for the β-CN (f1-25) isotherms between preparations A and B.

A model was sought to describe the isotherms mathematically. The Langmuir model has been used to describe protein adsorption at the solid/liquid interface (discussed in sections 3.1.4, 3.1.9 and 3.2.1). The Langmuir theory can be expressed by the equation:

$$\Gamma = \frac{nkc}{1 + kc} \qquad (1)$$

Where Γ is the adsorbed amount per unit area, n is the number of binding sites per unit area, k is the affinity or association constant for a site and c is the equilibrium, free concentration. This one-site model proved adequate for describing the isotherms obtained with β-CN A but inadequate for describing β-CN (f1-25) adsorption isotherms and therefore a two-site model was developed by Dr. C. Holt (Hannah Research Institute). This model was adopted because it is the simplest explanation of the upward curvature observed in the β-CN (f1-25) adsorption isotherm. Alternative reasons for this upward curvature, such as multi-layer

116

Figure 3.13   Comparison of the Adsorption Isotherms for ß-CN A

for DCPD Preparations A and B

The adsorption isotherms were prepared from the results of experiments (see section 3.4.6) performed at pH 7.0 and 20°C (see Table 3.4).   Curves were fitted to the results using the computer program REGRESSION as described (in section 3.5.2) and

the parameters of the curve are summarised in Table 3.5.   Results are plotted as Γ

(amount adsorbed per unit area; $\Gamma \times 10^{-7}$ moles ß-CN A adsorbed per m^2 DCPD) *versus* C (equilibrium, free concentration $\times 10^{-5}$ M).

  —o— indicates ß-CN A adsorption isotherm for DCPD preparation B

  —□— indicates ß-CN A adsorption isotherm for DCPD preparation A

The amount of protein adsorbed at each equilibrium concentration was determined in duplicate.

Plotted points are the mean ± S.E.M. of four separate adsorption experiments.   The S.E.M. not shown are smaller than the symbol.
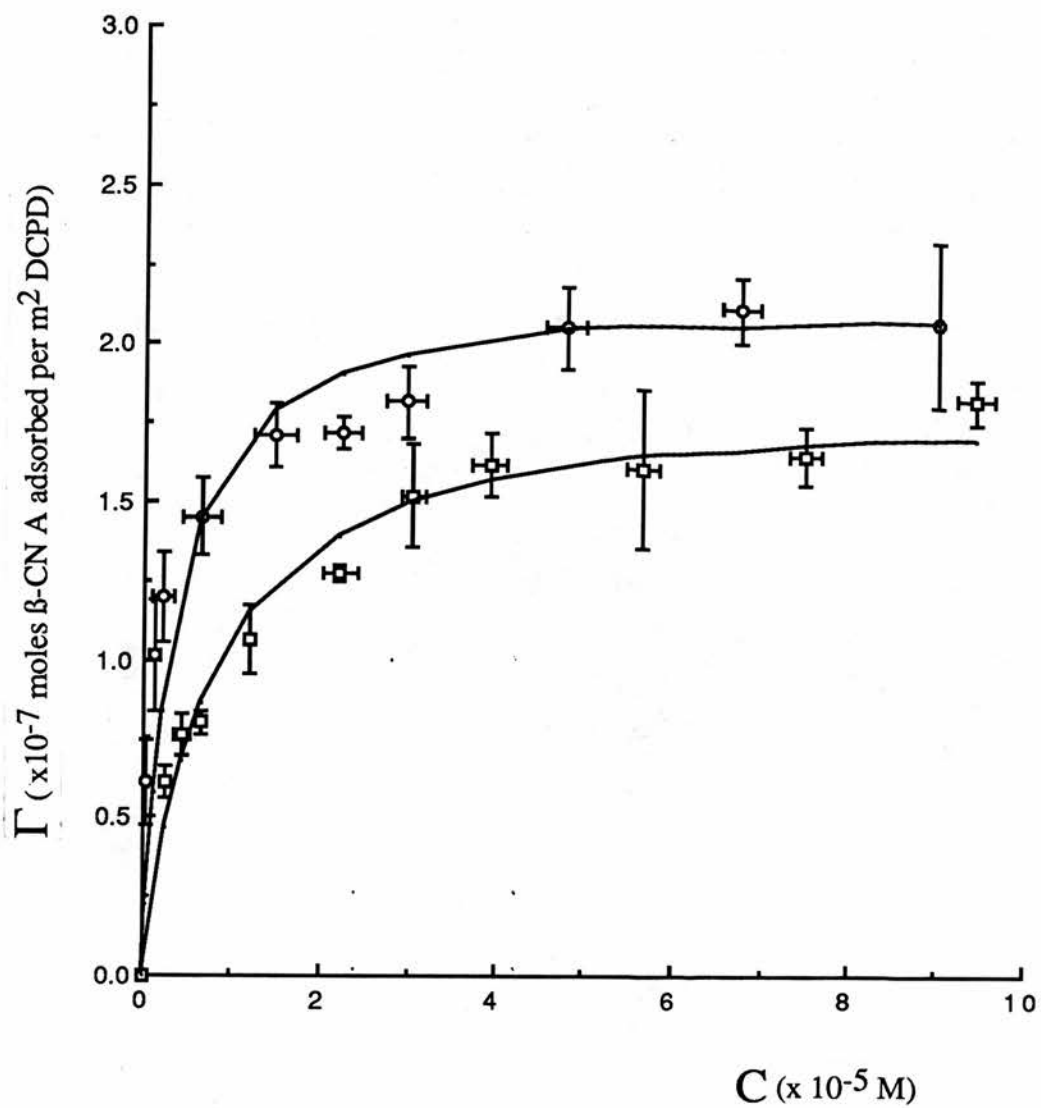
Figure 3.14 <u>Comparison of the Adsorption Isotherms for ß-CN (f1-25)</u>

<u>for DCPD Preparations A and B</u>

The adsorption isotherms were prepared from experiments (see section 3.4.6)

performed at pH 7.0 and 20°C (see Table 3.4). Curves were fitted to the results

using the computer program REGRESSION as described (in section 3.5.2) and the

parameters of the curve are summarised in Table 3.5. Results are plotted as Γ

(amount adsorbed per unit area; Γ x 10^{-7} moles ß-CN (f1-25) adsorbed per m^2

DCPD) *versus* C (equilibrium, free concentration x 10^{-4} M).

—o— indicates ß-CN (f1-25) adsorption isotherm for DCPD preparation B

—□— indicates ß-CN (f1-25) adsorption isotherm for DCPD preparation A

The amount of protein adsorbed at each equilibrium concentration was determined in

duplicate. Plotted points are the mean ± S.E.M. of of four separate adsorption

experiments. The S.E.M. not shown are smaller than the symbol.

formation or coagulation, are not expected for β-CN (f1-25) as it shows no tendency to associate and is very hydrophilic.

Examination of the adsorption isotherms appeared to show a small number of high affinity binding sites and a larger number of intrinsically lower affinity binding sites. The simplest model that describes this situation is one of two sets of non-interacting binding sites with the following relationship:

$$\Gamma = \frac{nkc}{1 + kc} + \frac{mlc}{1 + lc} \qquad (2)$$

Where m is the number of low affinity binding sites and l their affinity constant. However, as lc << 1 (within the concentration range used) equation (2) reduces to:

$$\Gamma = \frac{nkc}{1 + kc} + p.c \qquad (3)$$

Where $p = ml$

To represent cooperative, low affinity binding, a type of Hill coefficient was introduced, hence equation (3) becomes:

$$\Gamma = \frac{nkc}{1 + kc} + (p.c)^\gamma \qquad (4)$$

provided p.c << 1.

The four parameters n, k, p and γ, were determined using the non-linear, least squares procedure using the computer program REGRESSION (Blackwell Scientific Publications) which employs a simplex minimisation algorithm. Curve fitting was tested by using different initial estimates of the parameters. Parameters were eliminated if the F statistic of the fitted curve changed by a significant amount (p< 0.001) when γ or p were removed from the model. The results of curve fitting, using the theoretical equations (1) and (4), are summarised in Table 3.5.

The curves fitted to the isotherms (for β-CN A and β-CN (f1-25); see Fig. 3.13 and 3.14 and Table 3.5) indicate that, under comparable conditions, the number

121

	VARIABLE PARAMETERS				
EXPERIMENTAL CONDITIONS	n $\times 10^7$ mol g^{-1}	k $\times 10^{-5}$ lmol^{-1}	p mol$^{(1-\gamma)/\gamma}$ lm$^{-2/\gamma}$	γ -	A nm^2
ß-CN A, pH 7.0 20°C, DCPD-A	1.282 ± 0.046	1.31 ± 0.19	-	-	8.86 ± 0.33
ß-CN A, pH 7.0 20°C, DCPD-B	1.95 ± 0.130	3.0 ± 1.03	-	-	8.50 ± 0.128
^{14}C-ß-CN A, pH 7.0, 20°C, DCPD-B	1.411 ± 0.040	6.31 ± 1.17	-	-	10.8 ± 0.30
ß-CN A, pH 6.5 20°C, DCPD-A	0.741 ± 0.032	5.21 ± 1.30	-	-	15.3 ± 0.70
ß-CN A, pH 7.0 20°C, 6 M urea, DCPD-B	0.644 ± 0.046	375 ± 1400	-	-	23.7 ± 1.70
ß-CN (f1-25) pH 7.0, 20°C, DCPD-A	1.460 ± 0.110	2.50 ± 1.80	2.42 ± 0.24	1.89 ± 0.26	7.8 ± 0.60
ß-CN (f1-25), pH 7.0, 20°C, DCPD-B	2.316 ± 0.069	17.1 ± 14.2	1.88 ± 0.12	1.72 ± 0.20	6.60 ± 0.20
ß-CN (f1-25), pH 7.0, 3.0°C, DCPD-B	2.75 ± 0.100	2.92 ± 0.59	2.12 ± 0.15	1.58 ± 0.41	5.60 ± 0.20

Table 3.5   Parameters for the Adsorption Isotherms for ß-CN A and
ß-CN (f1-25) Calculated using the Program REGRESSION

Parameters for the adsorption isotherms were calculated as described in section 3.5.2

n represents the number of adsorption sites per unit area

k represents the affinity constant

p represents the product term, where p=m.l

γ represents the Hill type coefficient

A represents the area occupied per molecule

of high affinity sites was approximately the same for both crystal preparations (A and B), whether β-CN A or β-CN (f1-25) was the adsorbate.

If the protein molecules had adsorbed to DCPD in a uniform monolayer the isotherms, resulting from the two DCPD preparations, would be superimposable. The observed difference in Γ_p of 25% suggests therefore, that crystal shape is an important factor. As discussed in section 3.3.3.1, DCPD crystals have a thin, platy habit and therefore, as their size increases the edge faces account for proportionally less of the total surface area. These results suggest that the adsorption sites for β-CN A and β-CN (f1-25) may be concentrated on the edge faces of the DCPD crystals. The selective adsorption of proteins to specific crystal faces is not a unique observation (Addadi and Weiner, 1985). Selective adsorption is also observed to organic crystals, accompanied by a concomitant change in crystal morphology (Addadi *et al.*, 1985). In addition, selective adsorption of proteins (and also nucleic acids and nucleotides) to specific hydroxyapatite crystal faces has been reported (Kawasaki *et al.*, 1990). The theory that adsorption sites are concentrated on the edge faces is supported by the work of van Kemenade (1988). She observed an increase in the morphological importance of the edge faces of the crystals when they are grown in the presence of whole casein, indicating a preferential adsorption to these planes (see section 3.3.3).

There is an apparent difference in the adsorption affinity of β-CN A between the two DCPD preparations. However, determination of the affinity constant (k) is dependant on two or three data points (the average of four adsorption assays) at the lowest concentration of β-CN A used. From curve fitting experiments (see section 3.5.2; results not shown) it was found that the affinity constant could be varied between 1.31 - 8.3 x 10^5 lmol^{-1} and the curve would still fit within one standard deviation of the experimental points.

From Γ_p the area occupied by each adsorbed molecule can be calculated. The area of occupancy for β-CN A and β-CN (f1-25) for each isotherm is listed in Table 3.5. The area of occupancy is calculated as an average area assuming

monolayer coverage of the whole crystal. If the adsorption sites are concentrated on the edge faces, the actual areas of occupancy would be considerably less than those calculated.

β-CN A molecules, under the buffer conditions used during this study, will probably associate to form micelles. It is impossible, however, to calculate the extent of polymerisation, but it is likely to be high (see section 3.3.2). Adsorption of β-CN A may therefore occur as whole micelles, resulting in a rapid dissociation of the micelle at the crystal surface with a concomitant spreading of β-CN A monomers over the crystal surface. Alternatively, β-CN A adsorption may occur as monomers from solution, resulting in a shift in the equilibrium of monomer/polymer causing a gradual dissociation of micelles. From the results presented here it is impossible to determine the balance between these processes. The shape of the isotherm will not be influenced by the processes described above because equilibrium is already established when the isotherms are measured.

There is no tertiary, structural information for β-caseins (see section 3.3.2) but from the radius of gyration (Rg) in solution, estimated to be about 5.1 nm (Payens and Vreeman, 1982), and the assumption that the molecule is a uniform sphere, the cross-sectional area of β-casein is about 136 nm^2. This is considerably greater than the calculated area per molecule from Γ_p of the adsorption isotherm, suggesting that only a fraction of the β-CN A molecule binds to the crystal. The area per molecule (calculated from the plateau region of the isotherm; 2×10^{-4} M free β-CN (f1-25), see Fig. 3.14) for β-CN (f1-25) is about the same as that for β-CN A (see Table 3.5) despite the difference in size. This suggests that the N-terminal region is the fraction of the molecule that binds to the DCPD crystal with the remainder of the molecule dangling free in solution. If the affinity constants for β-CN A and β-CN (f1-25) are compared (see Table 3.5), there is no significant difference, supporting the conclusion that adsorption occurs *via* the N-terminal segment, with the C-terminal segment playing only a minor role.

124

affinity binding sites. In the light of the present results it is not possible to confirm which of these is the case. However, it is unlikely that a highly acidic and hydrophilic phosphopeptide such as β-CN (f1-25) would associate to form multilayers and the condition associated with coagulation at the interface (*e.g.* very high concentrations) are not encountered. Structural transitions may occur upon adsorption, but β-CN (f1-25) has so little secondary structure that changes to its conformation would not be expected to cause such a dramatic effect. Therefore it is proposed that the upward curvature (see Fig. 3.14) is a result of adsorption to a second family of intrinsically lower affinity adsorption sites.

If the upward curvature of the β-CN (f1-25) isotherm is due to a second family of adsorption sites, such sites may be present on other crystal faces or may be the result of non-specific binding. Curve fitting was performed using the two-site model (see section 3.5.2). The number and affinity of this putative second family of adsorption sites could not be determined separately (see section 3.5.2), and therefore, the product term $(p.c)^\gamma$ was used. However, this type of binding site appears to be more abundant than the high affinity sites. A Hill-type coefficient was calculated and found to be much greater than unity, indicating cooperative interaction between binding sites. The presence of lower affinity adsorption sites for β-CN A on DCPD crystals could not be tested as the isotherms did not cover a wide enough concentration range (see Fig. 3.15).

3.5.3 The Effect of pH
upon the Adsorption of β-CN A to DCPD Crystals

In Fig. 3.16, the isotherm obtained at pH 6.5 is compared with that obtained at pH 7.0 for the adsorption of β–CN A to DCPD preparation A at 20°C. An increase in pH from 6.5 to 7.0 is within the range of the pK's of the phosphoseryl residues of β–CN A, as these range from 6.4 to 6.95 (Shrager*et al.*, 1972; Humphrey and Jolley, 1982; Baumy *et al.*, 1989). As the phosphoseryl residues of

Figure 3.15   Comparison of the Adsorption Isotherms

for ß-CN A and ß-CN (f1-25)

The adsorption isotherms were prepared from experiments (see section 3.4.6) performed at pH 7.0 and 20°C using DCPD preparation B (see Table 3.4). Curves were fitted to the results using the computer program REGRESSION as described in section 3.5.2 and the parameters of the curves are summarised in Table 3.5. Results are plotted as Γ (amount adsorbed per unit area; $\Gamma = x \ 10^{-7}$ moles ß-CN A or ß-CN (f1-25) adsorbed per m^2 DCPD) *versus* C (equilibrium, free concentration x 10^{-4} M).

—o—   indicates ß-CN A adsorption isotherm.

—□—   indicates ß-CN (f1-25) adsorption isotherm.

The amount of protein adsorbed at each protein concentration was determined in duplicate. Plotted points are the mean ± S.E.M. of four separate adsorption experiments. The S.E.M. not shown are smaller than the symbol.

Γ (x10^{-7} moles ß-CN A or ß-CN (f1-25) adsorbed per m^2 DCPD)

C (x 10^{-4} M)
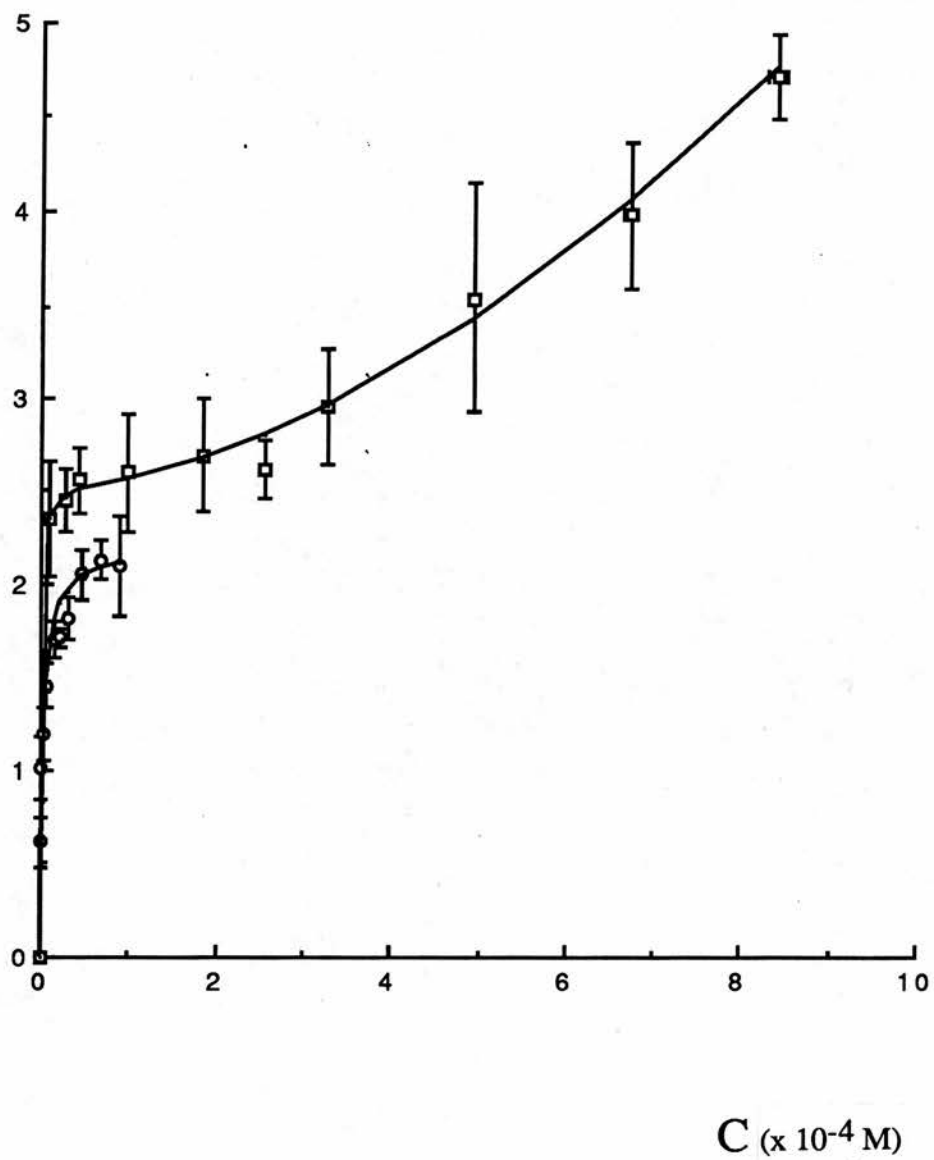
Figure 3.16   Comparison of the Adsorption Isotherms

at pH 6.5 and pH 7.0 for ß-CN A

The adsorption isotherms were prepared from adsorption experiments (see section 3.4.6) performed at 20°C using DCPD preparation A (see Table 3.4).   Curves were fitted to the results using the computer program REGRESSION as described (in section 3.5.2) and the parameters of the curves are summarised in Table 3.5.   Results are plotted as Γ (amount adsorbed per unit area; $\Gamma = x \ 10^{-7}$ moles ß-CN A adsorbed per m^2 DCPD) *versus* C (equilibrium, free concentration x 10^{-5} M).

—o—   indicates ß-CN A adsorption isotherm at pH 6.5.

—□—   indicates ß-CN A adsorption isotherm at pH 7.0.

The amount of protein adsorbed at each equilibrium concentration was determined in duplicate.   Plotted points are the mean $\pm$ S.E.M. of of three separate adsorption experiments performed at pH 6.5 and four adsorption experiments performed at pH 7.0.   The S.E.M. not shown are smaller than the symbol.

Γ (x10^{-7} moles ß-CN A adsorbed per m^2 DCPD)

C (x 10^{-5} M)
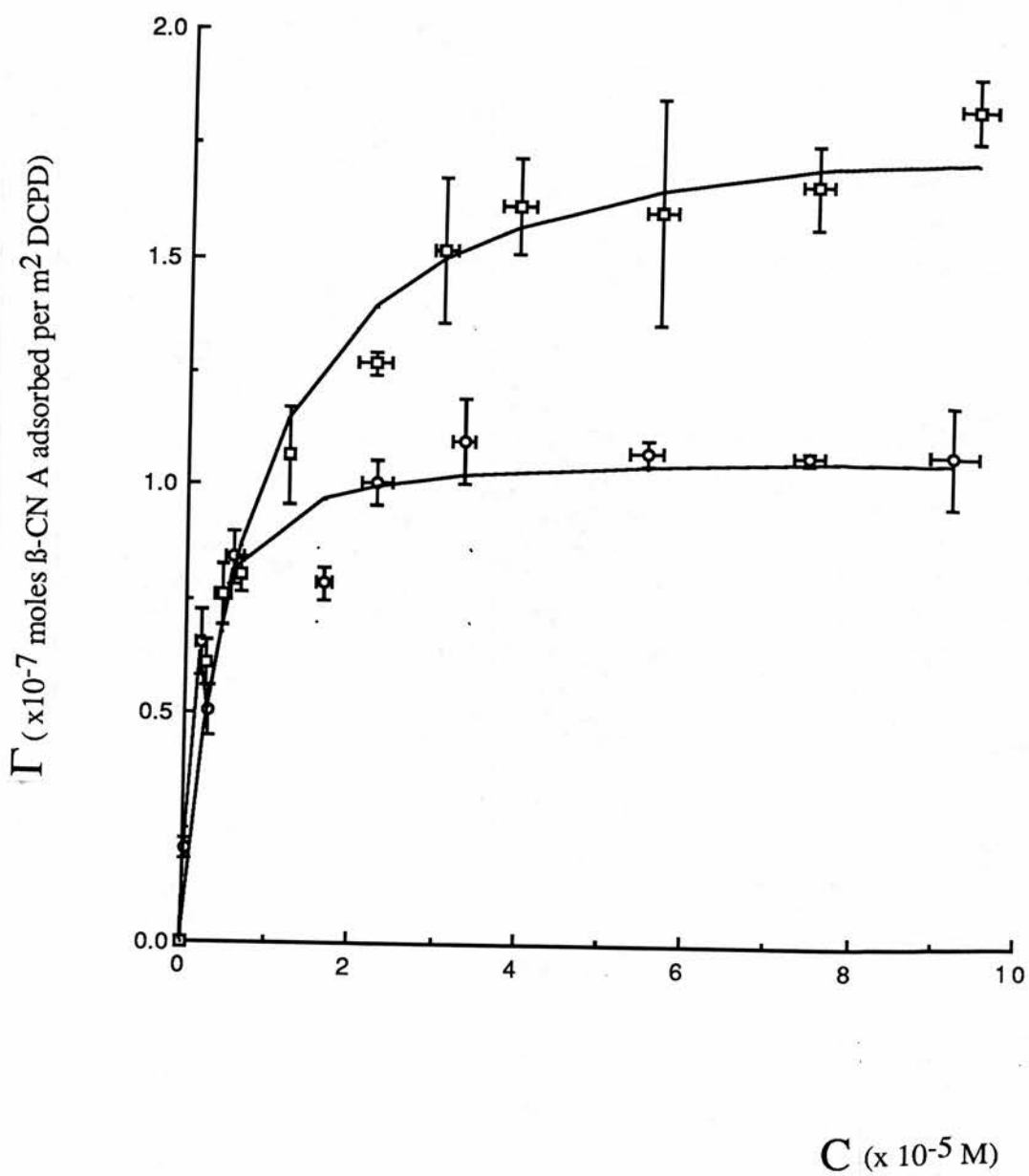
phosphoproteins are generally considered to play a major role in calcium ion and calcium mineral adsorption (see section 3.3.3) this increase in net negative charge should contribute to an increase in adsorption. This expected increase was observed in the adsorption isotherm (see Fig. 3.16), with an increase in Γ_p of some 20% (measured at 5×10^{-5} molar free β–CN A). The results of curve fitting, using the one site model are summarised in Table 3.5. The apparent number of binding sites is less at pH 6.5 than at pH 7.0, and the area of occupancy for β–CN A molecules is greater. The increase in Γ_p demonstrates that electrostatic interactions play an important role in adsorption of molecules at the solid/liquid interface (see section 3.1.6). The surface charge of the DCPD may also be altered, the surface being less likely to be protonated at pH 7.0 than 6.5, possibly making adsorption sites more available to the adsorbing molecule. In the above curve fitting experiments the lower number of binding sites, at pH 6.5, is accompanied by a greater affinity. However, examination of the fitted curves indicated that both curves could be described by a single affinity constant and still be within one standard deviation of the experimental results. To confirm whether a change in pH results in a change in affinity, adsorption isotherms would have to be constructed which include more data points below 1×10^{-5} M free β–CN A.

3.5.4 The Effect of Urea
upon the Adsorption of β-CN A to DCPD Crystals

The effect of urea on the adsorption of β-CN A to DCPD crystals was investigated by performing adsorption experiments with buffers containing 6.0 M urea (see section 3.4.4). Urea totally disrupts the hydrophobic interactions that occur between β-CN A monomers so preventing the formation of micelles (see section 3.3.2), by increasing the aqueous solubility of the hydrophobic portions of the polypeptide chain (Nozaki and Tanford, 1963; Wetlaufer et al., 1964; Franks and England, 1975). This effect is observed in the dissociation of casein aggregates

130

in 4.0 M urea (Ono *et al.*, 1976). In addition, the secondary structure of β-CN A molecules will be disrupted almost completely by 6.0 M urea. Therefore, the adsorption of β-CN A to DCPD in the presence of urea will occur only *via* electrostatic interactions, with hydrogen bonds and van der Waals bonds being the only intermolecular interactions.

The adsorption isotherms for β-CN A, measured at pH 7.0 and 20°C, in the presence or absence of 6.0 M urea are compared in Fig. 3.17. In the presence of urea the value of Γ_p is 50% less than in the absence of urea. In addition, the adsorption sites are completely saturated throughout the concentration range used. Therefore, intermolecular hydrophobic interactions may play an important role in the process by which β-CN A adsorbs to DCPD. However, protein adsorption is proposed to be "driven" by the entropy gain as water molecules leave the sorbent surface and the protein, and from disruption of secondary and tertiary protein structure (see section 3.1.4). As urea will disrupt the hydration state of both DCPD and β-CN A, and the structure of the β-CN A molecule, the entropy gain will be reduced in the presence of urea thus making adsorption less favourable.

3.5.5 The Effect of Temperature
on the Adsorption of β-CN (f1-25) to DCPD Crystals

The influence of temperature on an adsorption isotherm can give an insight into the adsorption process through a consideration of the thermodynamics involved (see section 3.1.8). A determination of the effect of temperature on an isotherm can, by application of the Gibbs-Helmholtz equation, determine the enthalpy of binding of the system (Tanford, 1966). Therefore, a final study was performed on β-CN (f1-25), in which the effect of temperature upon adsorption was investigated. In Fig. 3.18 the isotherms for β-CN (f1-25) obtained at 3°C and 20°C (measured at pH 7.0 on DCPD preparation B) are compared. At 20°C the isotherm is as previously described: initially a high affinity adsorption followed by a plateau at

Figure 3.17   Comparison of the Adsorption Isotherms

for ß-CN A in the Presence and Absence of 6.0 M Urea

The adsorption isotherms were prepared from experiments (see section 3.4.6) performed at pH 7.0 and 20°C using DCPD preparation B (see Table 3.4). Curves were fitted to the results using the computer program REGRESSION as described (in section 3.5.2) and the parameters of the curves are summarised in Table 3.5. Results

are plotted as Γ (amount adsorbed per unit area; $\Gamma = x \ 10^{-7}$ moles ß-CN A adsorbed

per m^2 DCPD) *versus* C (equilibrium, free concentration, $x \ 10^{-5}$ M).

       —o—   indicates ß-CN A adsorption isotherm in the absence of 6.0 M urea.

       —□—   indicates ß-CN A adsorption isotherm in the presence of 6.0 M urea.

The amont of protein adsorbed at each equilibrium concentration was determined in duplicate. Plotted points are the mean $\pm$ S.E.M. of of three separate adsorption experiments. The S.E.M. not shown are smaller than the symbol.

132
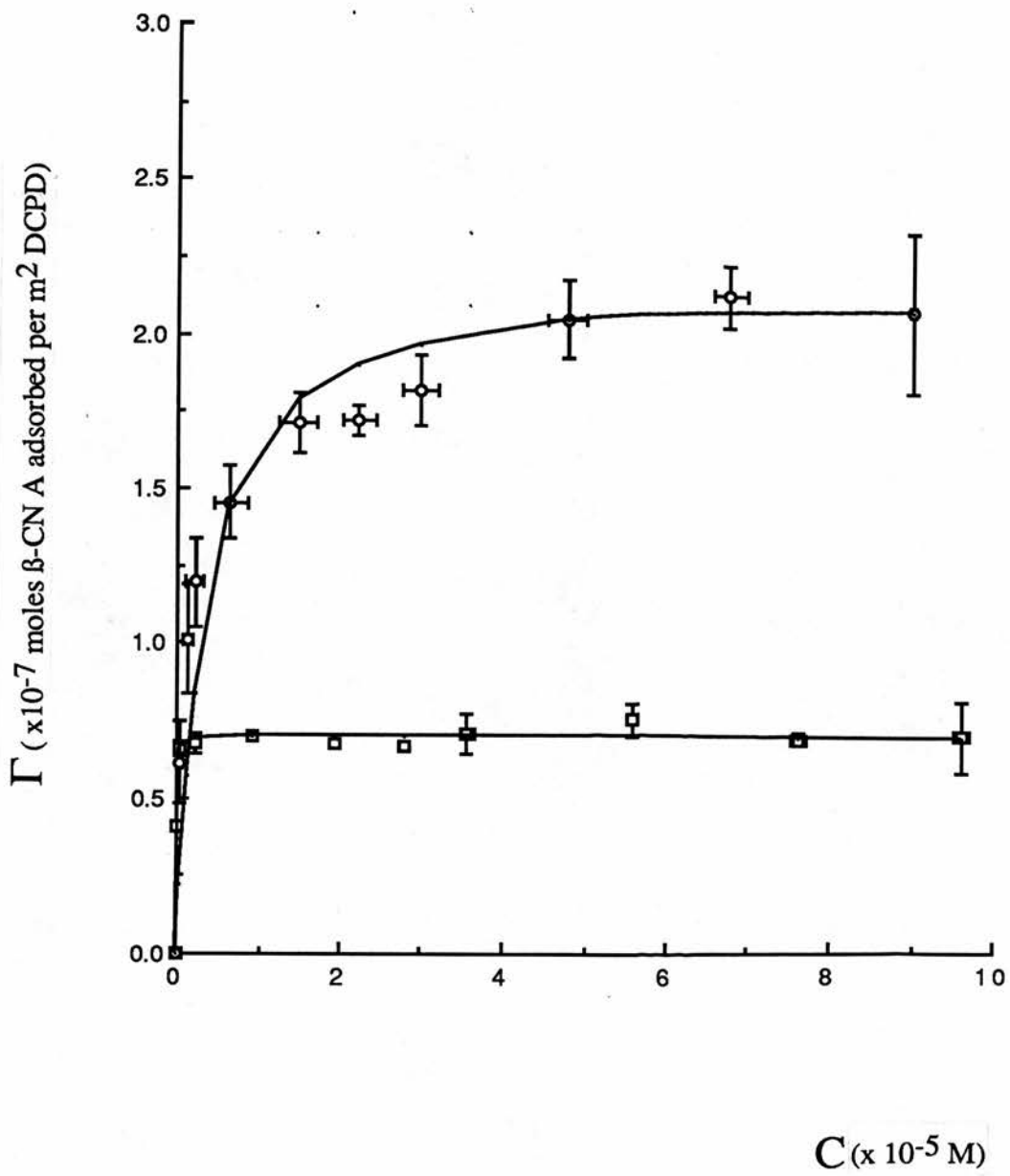
Figure 3.18   Comparison of the Adsorption Isotherms

at 20°C and at 3°C for ß-CN (f1-25)

The adsorption isotherms were prepared from experiments (see section 3.4.6)

performed at pH 7.0 using DCPD preparation B (see Table 3.4). Curves were fitted

to the results using the computer program REGRESSION as described (in section

3.5.2) and the parameters of the curves are summarised in Table 3.5. Results are

plotted as Γ (amount adsorbed per unit area; $\Gamma = x\ 10^{-7}$ moles ß-CN (f1-25)

adsorbed per m^2 DCPD) *versus* C (equilibrim, free concentration, $x\ 10^{-5}$ M).

—o—   indicates ß-CN (f1-25) adsorption isotherm at 20°C.

—□—   indicates ß-CN (f1-25) adsorption isotherm at 3°C.

The amount of protein adsorbed at each equilibrium concentration was determined in

duplicate. Plotted points are the mean $\pm$ S.E.M. of of three separate adsorption

experiments performed at 3°C and of four separate determinations performed at

20°C. The S.E.M. not shown are smaller than the symbol.

134

Γ (x10⁻⁷ moles ß-CN (f1-25) adsorbed per m² DCPD)

C (x 10⁻⁴ M)
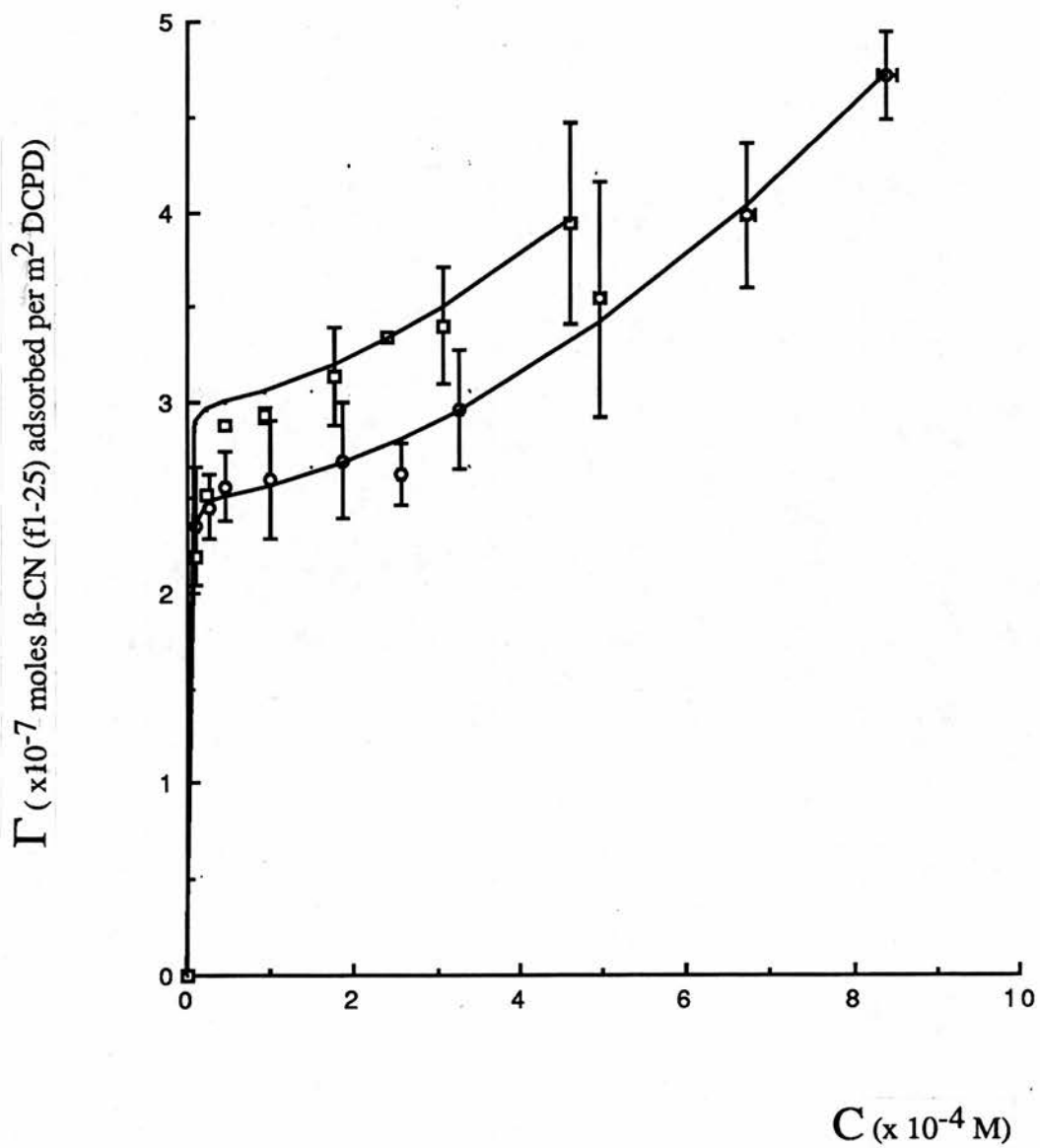
as the error bars from the two isotherms overlap. This implies that the adsorption process for β-CN (f1-25) is athermal and is "driven" by an entropy gain.

However, all the data points for the adsorption isotherm obtained at $3^\circ C$ are higher than those obtained at $20^\circ C$ (see Fig. 3.18). If the errors were random, and there was no effect of temperature upon adsorption, this would not be observed. Therefore the adsorption of β-CN (f1-25) may be exothermic, but further experimentation would be required to confirm this.

Summary

Adsorption of β-CN A occurs to high affinity sites which may be concentrated on the edge faces of the DCPD crystals (see section 3.5.2). Adsorption probably occurs *via* the N-terminal region of the molecule (first 25 amino acids; β-CN (f1-25) segment) with the remainder of the molecule dangling free in solution. Inclusion of urea in the adsorption assay buffers results in a dramatic decrease in Γ_p (see section 3.5.4). This may indicate that either intermolecular, lateral interactions occur between adsorbed molecules or that adsorption is "driven" by an entropy gain (see section 3.5.4).

Adsorption of β-CN (f1-25) appears to be very similar to that of β-CN A. However, at higher peptide concentrations (above 3×10^{-4} M free β-CN (f1-25)) an increase in adsorption is observed (see section 3.5.2). This increase in adsorption is attributed to a second family of intrinsically lower affinity adsorption sites. Adsorption of β-CN (f1-25) to these lower affinity sites is cooperative, as demonstrated by a Hill coefficient (γ) much greater than unity (see Table 3.5). Adsorption of β-CN (f1-25) is not significantly affected by temperature, indicating that adsorption is "driven" by an entropy gain (see section 3.5.5).

CHAPTER FOUR

CO-CRYSTALLISATION OF PHOSPHOSERINE
WITH CALCIUM IONS,
AND THE DETERMINATION OF THE STRUCTURES
OF TWO SMALL MOLECULES
BY X-RAY CRYSTALLOGRAPHIC METHODS

Much of our knowledge of the architecture of many types of molecules (*e.g.* drugs, peptides, hormones and enzymes) comes from the technique of X-ray crystallography. Molecules in crystals can have their precise structure determined; by understanding the relationship between the arrangement of the molecule within the crystal and the diffraction pattern obtained as the paths of X-rays are altered by passing through the crystal.

Prior to X-ray crystallographic analysis it is necessary to grow a single crystal of minimum dimensions (typically 0.1 mm). A crystal is a regular, repeating array of atoms or molecules in three dimensions. For the purpose of X-ray crystallography it is convenient to describe a crystal with the aid of a lattice. A crystal lattice is a regular, three dimensional arrangement of "points", such that the view in a given direction from each point in the lattice is identical with the view in the same direction from any other lattice point. The lattice can be defined by three axes with three angles between them, along each axis a point will repeat at a distance referred to as the unit translation or unit cell repeat. The axes are labelled a, b and c and the angles between b and c, a and c and a and b are called α, β and γ respectively. The crystal is composed of billions of identical unit cells and a description of the contents of any one unit cell is all that is required to describe the complete crystal structure. To aid the description of the diffraction process, and hence the determination of the contents of the unit cell, it is convenient to be able to divide the lattice into a series of planes. These lattice planes intersect the crystal lattice in a regular, uniform way and have an integral number of repeats per unit cell.

In order to "see" the individual atoms of the molecule, radiation of similar wavelength to the interatomic distances (typically 0.15 nm) is required. Radiation of this wavelength lies in the X-ray region of the electromagnetic spectrum. The way X-rays are scattered by the electrons of the atoms (i.e. diffraction) is conveniently described by the Bragg equation:

$$n\lambda = 2d\sin\theta \qquad\qquad (1)$$

In the equation, λ is the radiation wavelengh, n is an integer, d is the perpendicular spacing between the lattice planes and θ is the angle the X-ray beam makes with the lattice plane. Fig. 4.1 gives a diagrammatic representation of the Bragg equation. The crystal lattice is represented by a row of points A, B and C. For the scattered X-rays from row B to enhance those scattered from row A there must be an integral number of wavelengths difference. Bragg's law (equation 1) represents the relationship between the lattice spacing d, the wavelength λ and θ, the angle the emergent beam makes relative to the direction of the rows. Provided there is a large enough number of lattice planes contributing (that enhance the scattered X-ray beam), the position in space at which the scattered beam is observed is highly defined.

The scattered (or diffracted) X-ray radiation emerging from the crystal produces a diffraction pattern, which can be observed as a series of spots on photographic film. The symmetry and positions of the spots of the diffraction pattern give the dimensions and symmetry of the unit cell in the crystal. The intensities of the spots are related to the arrangment of the atoms within the unit cell.

It is convenient to use the analogy of the light (and electron) microscope when trying to understand the principle of X-ray diffraction. In an ordinary optical microscope the radiation (light) scattered by the object can be recombined by the lens system of the microscope to give a magnified image. In a similar way X-rays are scattered by the electrons of the molecule, but X-rays cannot be recombined as in the light microscope to give a magnified image of the molecule. Therefore, the diffracted X-rays are recombined mathematically, by use of Fourier syntheses. The lens system of the light microscope collects all the scattered light waves and, using the amplitudes and phases of the waves, recombines them to form a magnified image. In the same way, the Fourier synthesis uses the position, intensity and the
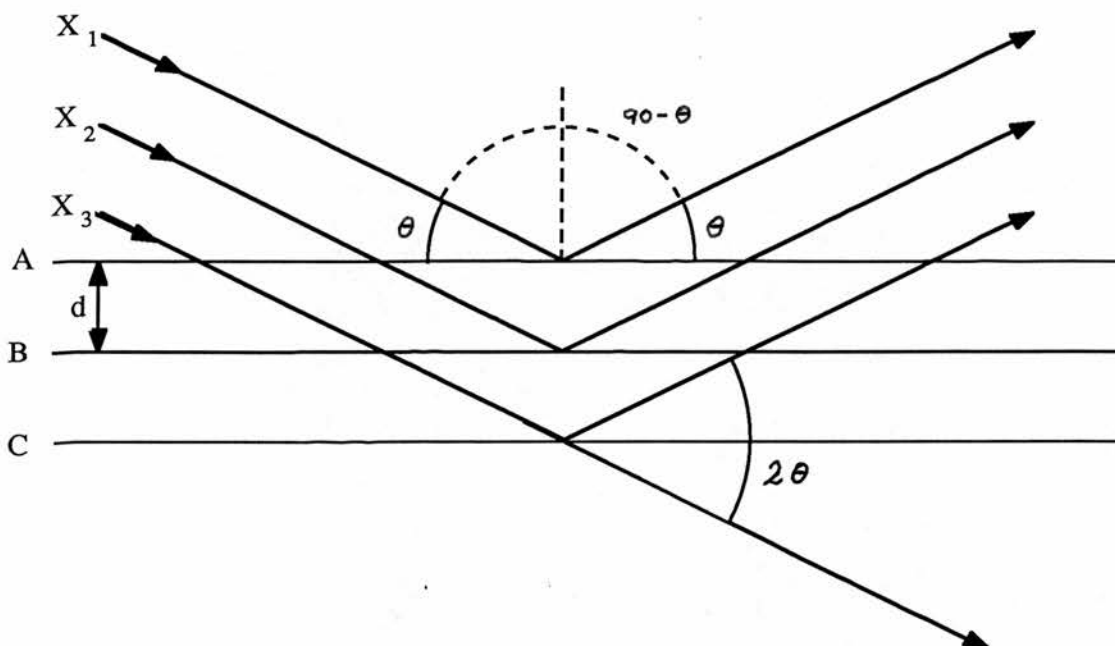
Figure 4.1   Diagrammatic Representation of the Bragg Equation

The diagram illustrates the fulfilment of the conditions required to satisfy the

Bragg equation.   The lattice planes A, B and C are separated by the

perpendicular distance d.   X-rays X_1, X_2 and X_3 are incident at an angle of θ

with respect to the lattice planes.   The X-rays, scattered from plane A (X_1),

are enhanced by those from plane B (X_2) provided that the extra distance

travelled by X_2 is a integer number of wavelengths (n).

calculated phase (as the actual phase cannot be recorded directly) of the diffracted X-ray waves to calculate a three dimensional electron density map of the molecule (the magnified picture of the object) and hence determine its structure.

4.2 Co-crystallisation Experiments with Phosphoserine and Calcium ions

The binding of calcium ions by the phosphoseryl residues of phosphoproteins is well documented (Holt *et al.*, 1986; Aoki *et al.*, 1987; Farrell and Thompson, 1988; Schmidt and Poll, 1989). However, no precise structural information about this interaction is available. The crystal structures of the calcium salts of phospho-amino acids (*i.e.* Ser(P) and Thr(P)) and short phosphopeptides would give this information. Therefore, co-crystallisation trials of phosphoserine and calcium salts were initiated.

4.2.1 Materials and Methods

All chemicals were purchased from Sigma (Poole, Dorset) unless otherwise stated. All solutions were made with distilled water and their pH's (measured with a Gallenkamp combination glass electrode) adjusted with 2.0 M sodium hydroxide, potassium hydroxide or hydrochloric acid. Finally, solutions were passed through 0.2 μm filters (Millipore, USA).

4.2.1.1 Co-crystallisation Experiments of Phosphoserine with Water-Soluble Calcium Salts

Growth of co-crystals of phosphoserine and calcium ions was attempted using the simplest method, that of slow solvent evaporation. Crystal trials were performed in plastic 24 (flat bottomed) well tissue culture plates (Flow Laboratories, Inc., USA). Table 4.1 summarises the conditions used and the results of the

Ser-(P)/Ca ion Ratio	pH																										
	2.0	2.5	3.0	3.5	4.0	4.5	5.0	5.1	5.2	5.3	5.4	5.5	5.6	5.7	5.8	5.9	6.0	6.1	6.2	6.5	7.0	7.5	8.0	8.5	9.0	9.5	10.0
20 : 1	P	P	P																								
18 : 1	P	P	P																								
16 : 1	P	P	P																								
14 : 1	P	P	P																								
12 : 1	P	P	P																								
11 : 1	P	P	P																								
10 : 1	P	P	P																								
9 : 1	P	P	P																								
8 : 1	P	P	P																								
7 : 1	P	P	P																								
6 : 1	P	P	P																								
5 : 1	P	P	P																								
4 : 1	P	P	P	N	N	N	T	T																			
3 : 1	P	P	P	N	N	N	T	T	*	*	*	*	*	*	*	*	*	*	*	T	T	T					
2 : 1	P	P	P	N	N	N	T	T	*	*	*	*	*	*	*	*	*	*	*	T	T	T	T	T	T	T	T
1 : 1	P	P	P	N	N	N	T	T	*	*	*	*	*	*	*	*	*	*	*	T	T	T	T	T	T	T	T
1 : 2	P	P	P	N	N	N	T	T	*	*	*	*	*	*	*	*	*	*	*	T	T	T	T	T	T	T	
1 : 3	P	P	P	N	N	N	T	T	*	*	*	*	*	*	*	*	*	*	*	T	T	T					
1 : 4	P	P	P	N	N	N	T	T																			
1 : 5	P	P	P	N	N	N	N	N	N	N	T	T	T	T	T	T	T	T	T	T	T	T	T	T	T	T	T
1 : 6	P	P	P																								
1 : 7	P	P	P																								
1 : 8	P	P	P																								
1 : 9	P	P	P																								
1 : 10	P	P	P																								
1 : 12	P	P	P																								
1 : 14	P	P	P																								
1 : 16	P	P	P																								
1 : 18	P	P	P																								
1 : 20	P	P	P																								

Table 4.1   Summary of Co-Crystallisation Experiments
using Phosphoserine and Water-Soluble Calcium Salts.

Trials were conducted with various combinations of pH and Phosphoserine/Calcium ion ratio.

Conditions under which crystals composed entirely of phosphoserine formed are indicated P.

Conditions under which non-crystalline precipitates formed are indicated T.

Conditions under which neither crystals nor precipitate formed are indicated N.

Conditions under which micro-crystals of a phosphoserine : calcium complex formed are indicated *.

co-crystallisation trials. All trials were performed at three different temperatures (3.0, 10.0 and 20.0°C) using three different calcium salts: calcium chloride ($CaCl_2.2H_2O$; 6.0 M), calcium nitrate ($Ca(NO_3)_2.4H_2O$; 2.0 M) and calcium hydroxide ($Ca(OH)_2$; 0.2 M). Each optical isomer of phosphoserine was tested (*i.e.* L-Ser(P) and D-Ser(P)) as well as the racemic mix, each at six different concentrations: 17.0 mM, 20.0 mM, 25.0 mM, 100 mM, 130 mM and 150 mM. Crystal trials were conducted at various pH's (see Table 4.1). The pH's of the phosphoserine solutions were adjusted, in separate trials, with sodium hydroxide and with potassium hydroxide, except when calcium hydroxide was used as calcium salt when no pH adjustment was necessary.

The crystal trials were constructed as follows. To 1 ml of a phosphoserine solution at the appropriate pH was added, dropwise, a solution of the calcium salt such that the desired phosphoserine : calcium ion ratio was obtained. The pH of the resulting solution was measured and re-adjusted as necessary (with either sodium hydroxide or potassium hydroxide). The solution was then left undisturbed at either 3.0, 10.0 or 20.0°C to crystallise.

4.2.1.2 Co-crystallisation Experiments of Phosphoserine with Calcium Carbonate

Addition of base to acid (in solution) causes a reaction resulting in the formation of the corresponding salt and water. Therefore, addition of calcium carbonate (base) to a solution of phosphoserine (acid; pH 2.0) should result in the formation of the corresponding phosphoserine/calcium salt and water with the liberation of carbon dioxide gas. Briefly, to a 0.1 M solution of phosphoserine (25 ml) was added an excess of solid calcium carbonate (3 g), the solution was then stirred for 12 hr at room temperature. The solid calcium carbonate remaining was removed by filtration (Whatman No. 1) and the resulting solution then left undisturbed at either 3.0, 10.0 or 20.0°C to crystallise. The pH of the final solution was 4.2.

4.3 Results and Discussion

In order to determine a molecule's structure a well-formed, single crystal is required.   The co-crystallisation trials failed to yield any such crystals.   Therefore the determination of the structure of the calcium salt of phosphoserine by X-ray diffraction techniques was not possible.

The results of the co-crystallisation trials using the water-soluble calcium salts are summarised in Table 4.1.   At pH's between 2.0 and 3.5 crystals grew but when they were analysed by X-ray powder diffraction, they were found to be composed entirely of phosphoserine regardless of the calcium salt concentration. Between approximately pH 3.5 and 5.0 neither crystals nor precipitate formed and, upon complete evaporation of the solvent (after 9-12 months), a white non-crystalline (determined by X-ray powder diffraction) solid was observed. Between pH 5.1 and 6.2, and approximately 30 min after the addition of the calcium salt, a rapid crystallisation process began which was complete within 4 hr and resulted in the formation of micro-crystals.   These micro-crystals had approximate dimensions of 0.05 x 0.01 x 0.01 mm, were needle-shaped and tended to form spherules.   The crystals remained stable for up to 12 hr at room temperature and up to 24 hr at 4°C.   After this time the crystal lattice had decayed to such an extent that the crystals no longer diffracted X-rays.   The crystals were characterised using X-ray powder diffraction techniques immediately after their growth and were shown to consist not only of phosphoserine (see Fig. 4.2).   It is therefore likely that they were co-crystals of calcium and phosphoserine.   Unfortunately, the powder diffraction data collected were unsuitable for structure determination because of the poor quality of the crystals. An elemental analysis for "C, H, N" and calcium was performed upon the micro-crystals which formed between pH 5.1 and 6.2, the results of which are reported in Table 4.2.   By use of the molar percentage of carbon and

144

ORIGIN

A

B
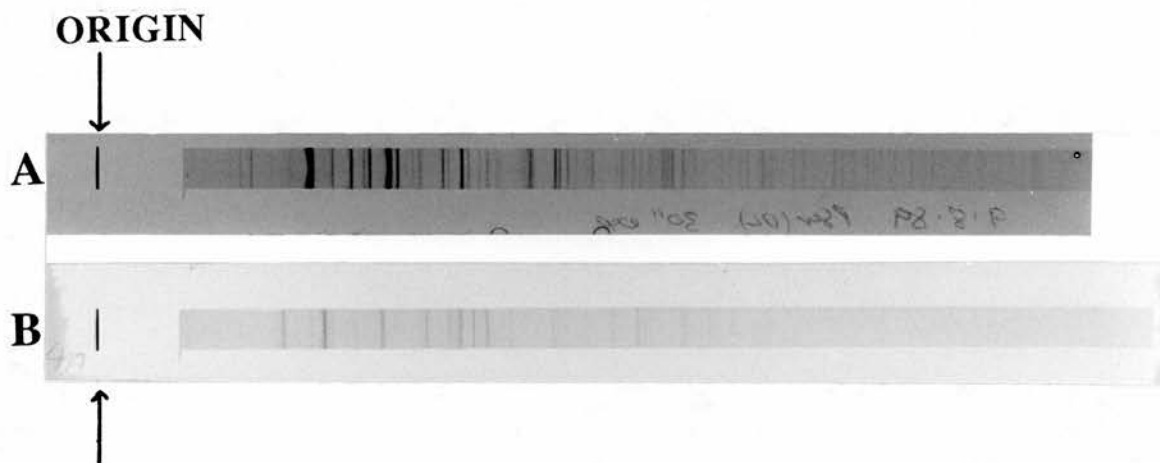
Figure 4.2   X-ray Powder Diffraction Patterns of D,L-Phosphoserine and
              the Phosphoserine/Calcium Complex

A Hagg-Guinier camera was used to obtain the powder diffraction photographs.

A) X-ray powder diffraction pattern of D,L-Ser(P) crystals grown at 20°C.
Exposure time (to X-rays) was 30 minutes.

B) X-ray powder diffraction pattern of the D,L-Ser(P)/Calcium complex.   These
micro-crystals were grown at pH 5.6 and 20°C.   Exposure time (to X-rays) was
30 minutes.

145

ELEMENT	Molar Percent ± s.e.m	Calculated molar percent for the theoretical empirical formula $Ser(P) : Ca : 2H_2O$
Carbon	13.88 ± 0.04	13.84
Hydrogen	3.60 ± 0.02	3.87
Nitrogen	5.355 ± 0.005	5.38
Calcium	10.0 ± 3.0	15.40

Table 4.2   Elemental Analysis of Micro-Crystals

of a Phosphoserine/Calcium Complex

The trials which yielded the micro-crystals are described in section 4.2.1.1.

The molar percentages resulting from "C, H, N" analysis and from Calcium

analysis of the micro-crystals are presented.

The calculated molar percentages for a theoretical complex possessing the

empirical formula Ser-(P) : Ca : $2H_2O$ are shown in the column on the right.

molar percentage of nitrogen it is possible to propose a tentative empirical formula for this calcium salt of phosphoserine:

$$Ser(P) \; : \; Ca \; : 2H_2O$$

However, the molar percentage of calcium (10 ± 3 %) is less than the theoretical 15.4% required for this complex (see Table 4.2). This could be due to the presence of other ions contaminating the sample, such as sodium, chloride or hydroxyl ions. It was not possible to determine the structure of these crystals using standard X-ray diffraction techniques because of their small size and their instability. However, use of a synchrotron radiation source might allow a crystal structure to be elucidated from the powder diffraction pattern. When the pH was above 6.2 a white, non-crystalline (by X-ray powder diffraction studies) precipitate formed quickly after addition of the calcium salt.

A structural investigation into the theory of the intermolecular chelation of phosphoserine and calcium ions has been performed by Gresh (1980). Gresh inferred that the (calculated) two most stable complexes were Ser(P):Ca and Ser(P):Ca:Ser(P). The more stable complex was Ser(P):Ca, in which calcium ions interact simultaneously with the four anionic oxygens of the ligand (*i.e.* two oxygens from the phosphate group and two oxygens from the carboxyl group). This work is in agreement with the empirical formula (above) suggested in this work.

Co-crystallisation trials using calcium carbonate as calcium ion source instead of the water-soluble calcium salts resulted in no crystals forming. Upon complete evaporation of the solvent a white, non-crystalline (determined by X-ray powder diffraction) solid remained.

If co-crystals of phosphoserine/calcium and Ser(P)-Ser(P)/calcium had been grown the geometric information obtained could be useful in understanding phosphoprotein/calcium mineral interactions. At present, no information is available for calcium ion/phosphate group interaction. For example, bond lengths

Summary

The results obtained with both soluble and insoluble calcium salts may be interpreted as follows. The complex between calcium ions and phosphoserine begins to form above pH 5.0. As no solid complex is observed at a pH less than 5.0 and as the pK value of the phosphate group of phosphoserine is 5.65 (Osterberg, 1957), it is likely therefore that the phosphate group must be ionised for calcium ion binding to occur with sufficient "strength" for a solid complex to form. Once the complex has formed in solution, rapid precipitation/crystallisation occurs (depending upon pH), the solid complex being very insoluble in water, methanol and in ethanol once formed. Elemental analysis indicates that each calcium ion is chelated by one phosphoserine molecule.

4.4 The Solving of Two Small Molecule Structures
by X-ray Crystallographic Methods

The following section describes the elucidation of the structures of two small molecules of pharmacological importance (see Fig. 4.3). These structures were solved as an exercise in familiarisation with the crystallographic process.

4.4.1 1-(2-Methoxyphenyl)-4-[4-(2-phthalimido)but-2E-ynyl]piperazine. HBr (1-MPP)

The 5-hydroxytryptophan (5-HT$_{1A}$) receptor is believed to be involved in thermoregulation, adenylate cyclase modulation and in the control of blood pressure (Peroutka, 1988). 1-(2-methoxyphenyl)-4-[4-(2-phthalimido)butyl]piperazine (NAN-190) is a partial agonist of the 5-HT$_{1A}$ with a high affinity (Ki = 1.0 nM; Glennon et al., 1988a,b). Alkenyl and alkynyl derivatives of NAN-190 have been synthesised interalia (Dawson et al., 1991), by appropriate replacements

148
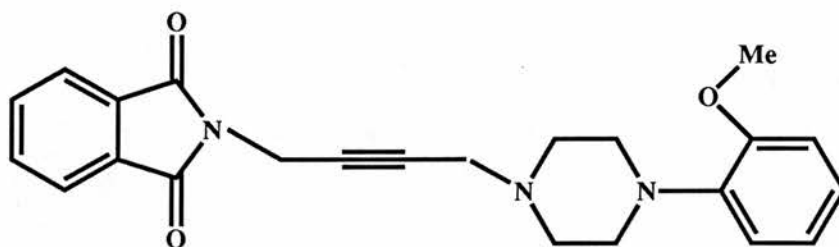
1-(2-methoxyphenyl)-4-[4-(2-phthalimido)but-2E-ynyl]piperazine . HBr   (1-MPP)
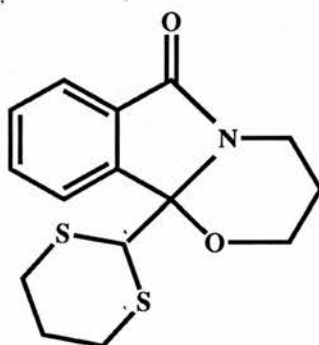
1-aza-5-oxa-6-(1',3'-dithianyl)-7,8-benzo-9-oxobicyclo[4.3.0]nonane   (1-ATN)

Figure 4.3   Structural Diagrams of the Two Small Molecules of
              Pharmacological Importance whose Structures were Solved
              by X-ray Crystallographic Techniques.

of the 4-bromo-1-phthalimido butane synthon in the reaction with 1,4(2'-methoxyphenyl)piperazine, in an attempt to increase the affinity of NAN-190 for the 5-HT$_{1A}$ receptor. However, the binding affinities for the alkenyl and alkynyl ligands were 10.0 nM and 270.0 nM respectively. Therefore the change in geometry and rigidity of the phthalimido side chain as a result of the modifications does not confer a higher affinity for the 5-HT$_{1A}$ receptor. Below is the crystallographic structure determination of the alkynyl derivative 1-(2-methoxyphenyl)-4-[4-(2-phthalimido)but-2E-ynyl]piperazine . HBr (1-MPP).

4.4.1.1 Method of Structure Solution and Refinement

Crystals (supplied by Dr. I Dawson, Department of Pharmacology, University of Edinburgh) of 1-MPP were prepared by diffusion of ether into a methanolic solvation of the hydrobromide salt at 293 K. A crystal of dimensions 0.2 x 0.5 x 0.1 mm was used for data collection. The crystals were characterised by Weissenberg photography, which revealed the likely space group as C 2/c, and then data was collected on a Stoe STADI-4 diffractometer (with the help of Dr. A. J. Blake, Dept. of Chemistry, University of Edinburgh). An orientation matrix was calculated using 7 reflections in the 2θ range of 10 to 20 degrees. Accurate cell dimensions were determined using 28 reflections at $\pm$ ω in the same 2θ range. Data were collected over -26 < h ≥ 26, 0 < k ≥ 16, 0 < l ≥ 16 (excluding h+k = odd as the space group was C 2/c) with 7 reflections being measured every 2 hours to check for crystal decay or movement. During data reduction, 3107 reflections of the 4988 measured were rejected as they had I < 2σ(I) and were therefore considered unobserved. During refinement 1881 reflections were used out of the 4988 measured during data collection.

A trial position for the Bromine atom was located using a Patterson synthesis, phases obtained from this atom were sufficient to reveal all non-hydrogen atoms. The structure was then refined using the program SHELX76 (Sheldrick, 1976).

Atoms were refined anisotropically before the addition of hydrogen atoms, which were further refined with fixed isotropic temperature factors and site occupancies. These were allowed to ride on the atoms to which they were attached. The maximum atom shift on the final refinement cycle was 0.002 Å. A weighting scheme was not adopted in the structure refinement because it gave no improvement. A total of 295 parameters were refined resulting in a final R factor of 0.048. The final difference map gave maximum and minimum values of 0.435 and -0.291 eÅ^{-3} respectively and the maximum $\sin\theta/\lambda$ was 0.5946 Å^{-1}.

Final atomic parameters are given in Table 4.3. Table 4.4 gives a summary of the data collected and the structure solution. The program CALC (Gould and Taylor, 1983) was used to provide the molecular geometry data presented in Tables 4.5, 4.6 and 4.7. Crystal structure diagrams (Fig. 4.4) were prepared using the program ORTEP (Johnson, 1965; Mallinson and Muir, 1985), and crystal packing diagrams (Fig. 4.5) were prepared using the program PLUTO (Motherwell, 1972).

4.4.1.2 Discussion

The crystal structure of 1-MPP is shown in Fig. 4.4, the bond lengths and angles for this structure are as expected (see Tables 4.5, 4.6 and 4.7). The molecular packing (see Fig. 4.5) indicates few close contacts between molecules. The aromatic rings of the molecules appear to overlap, the A ring of one overlapping with the B ring of another, in a translation along the b axis. There are two significantly short carbon carbon intermolecular distances which may indicate weak intermolecular interactions between the stacked aromatic rings. Two of the latter occur between carbon 6A of one molecule and carbon 5B of another and carbon 3B of one molecule and carbon 5A of another (these being 3.469(18) and 3.719(16) Å respectively) related by the symmetry operations x,1+y,z and x,-1+y,z respectively.
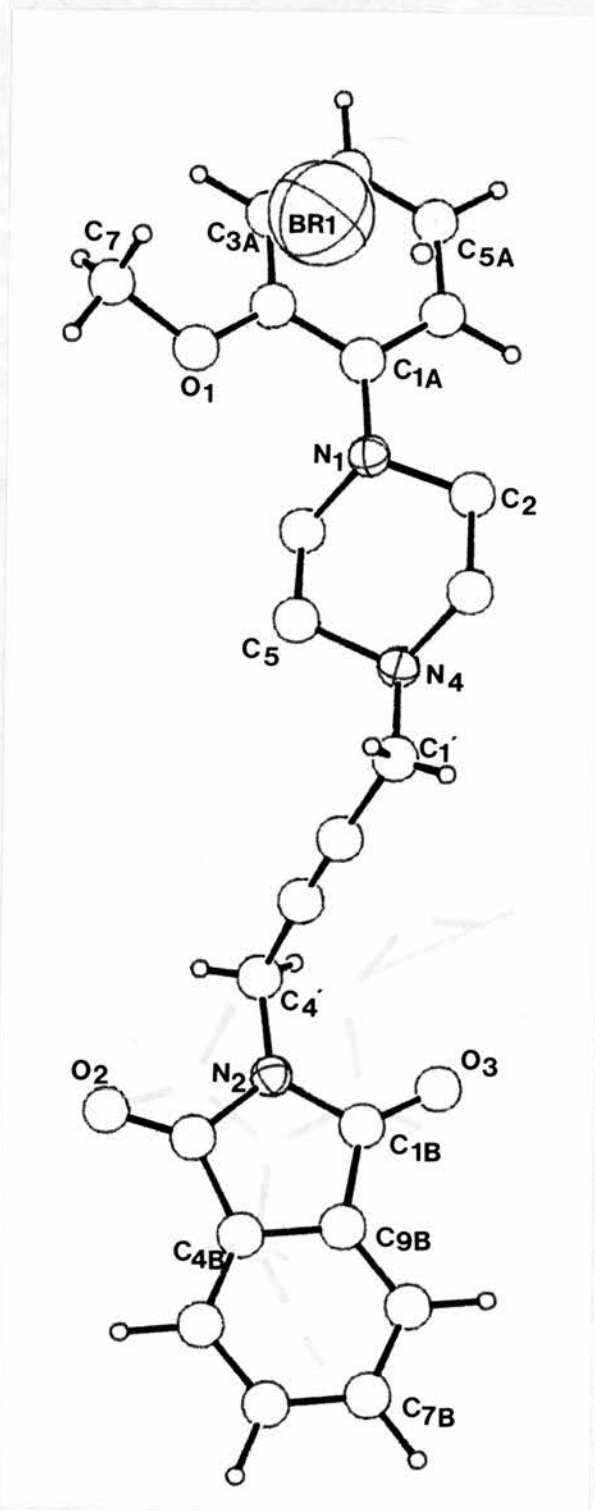
Figure 4.4   Crystal Structure of the Pharmacological Compound 1-MPP

The crystal structure diagram was prepared using the computer program ORTEP. Nitrogen (small) and Bromine (large) atoms are shaded.

152
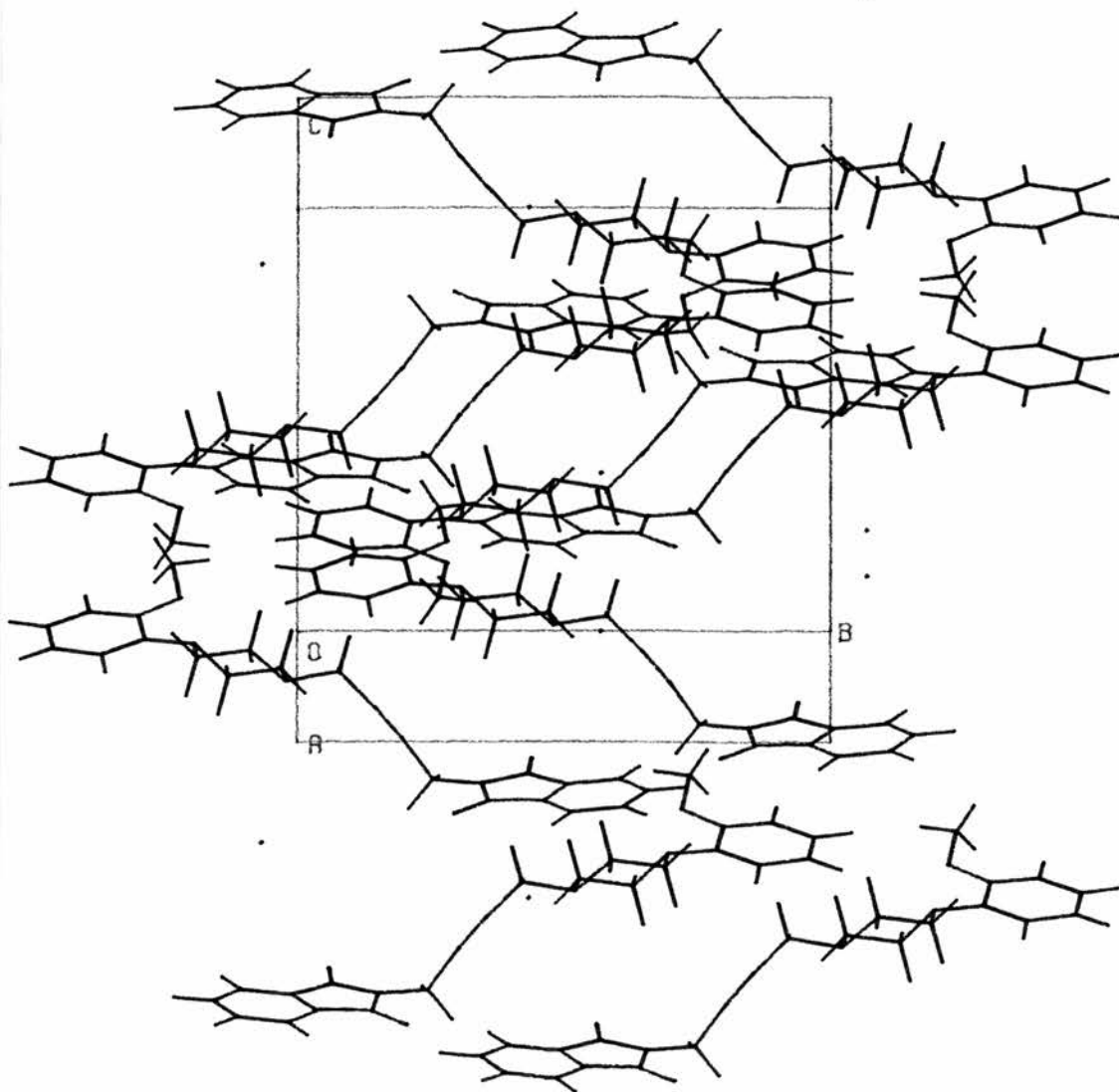
Figure 4.5   Crystal Packing Diagram of the Pharmacological Compound 1-MPP

The packing diagram was generated using the computer program
PLUTO.   The view is taken down the a axis

Fractional Coordinates of Atoms with Standard Deviations

	x	y	z	Ueq
Br(1)	0.08045(4)	-0.06717(9)	0.61856(6)	0.0675(6)
N(4)	0.1032(3)	0.0193(5)	0.9058(5)	0.046(4)
O(1)	0.2619(3)	0.2199(5)	0.7839(4)	0.071(5)
C(1')	0.0807(4)	-0.0799(6)	0.8852(6)	0.056(6)
N(2)	0.1217(4)	-0.3453(6)	1.1037(5)	0.064(6)
N(1)	0.1544(3)	0.1938(5)	0.8470(5)	0.054(5)
O(3)	0.0319(3)	-0.2939(6)	1.1418(5)	0.092(6)
O(2)	0.2001(3)	-0.4394(7)	1.0716(5)	0.109(6)
C(3B)	0.1495(5)	-0.4324(9)	1.0901(6)	0.073(7)
C(1A)	0.1782(4)	0.2864(7)	0.8436(6)	0.055(6)
C(5)	0.1688(3)	0.0294(6)	0.8977(6)	0.058(6)
C(4B)	0.1040(5)	-0.5075(9)	1.0998(7)	0.067(7)
C(2)	0.0913(3)	0.1884(7)	0.8599(6)	0.058(6)
C(2A)	0.2347(4)	0.2997(7)	0.8115(6)	0.057(6)
C(3')	0.1275(4)	-0.1965(7)	1.0188(6)	0.063(6)
C(6A)	0.1480(5)	0.3678(8)	0.8663(7)	0.079(8)
C(3A)	0.2578(5)	0.3901(8)	0.8084(7)	0.070(7)
C(9B)	0.0524(5)	-0.4619(8)	1.1193(7)	0.066(7)
C(2')	0.1082(4)	-0.1464(7)	0.9571(7)	0.061(6)
C(7B)	0.0041(8)	-0.6115(12)	1.1206(9)	0.105(12)
C(4')	0.1503(5)	-0.2548(8)	1.1008(7)	0.077(8)
C(6)	0.1890(4)	0.1289(6)	0.9156(6)	0.053(6)
C(1B)	0.0636(4)	-0.3587(8)	1.1238(6)	0.065(7)
C(7)	0.3114(4)	0.2347(8)	0.7311(8)	0.086(8)
C(5A)	0.1720(6)	0.4581(8)	0.8592(8)	0.093(9)
C(5B)	0.1055(7)	-0.6048(11)	1.0906(9)	0.100(11)
C(8B)	0.0016(6)	-0.5135(11)	1.1304(8)	0.087(9)
C(4A)	0.2267(6)	0.4690(9)	0.8305(9)	0.089(9)
C(6B)	0.0547(9)	-0.6554(11)	1.1014(9)	0.112(13)
C(3)	0.0687(3)	0.0892(6)	0.8419(6)	0.055(6)

Anisotropic Vibration Parameters with Standard Deviations

	U11	U22	U33	U23	U13	U12
Br(1)	0.0579(5)	0.0959(8)	0.0486(5)	-0.0046(7)	0.0134(3)	-0.0121(7)
N(4)	0.0337(35)	0.0611(47)	0.0424(38)	0.0037(36)	0.0093(29)	0.0018(34)
O(1)	0.0547(39)	0.0709(50)	0.0870(48)	-0.0010(38)	0.0195(34)	-0.0064(35)
C(1')	0.0647(60)	0.0561(68)	0.0466(48)	-0.0004(50)	0.0057(40)	-0.0067(53)
N(2)	0.0617(51)	0.0702(63)	0.0579(46)	0.0042(46)	0.0062(40)	0.0120(49)
N(1)	0.0482(43)	0.0630(53)	0.0507(40)	0.0078(38)	0.0092(33)	0.0035(39)
O(3)	0.0777(51)	0.0976(63)	0.0995(55)	-0.0108(48)	0.0197(42)	0.0362(48)
O(2)	0.0684(46)	0.1454(75)	0.1122(56)	-0.0133(62)	0.0169(42)	0.0409(57)
C(3B)	0.0803(71)	0.0828(80)	0.0527(51)	-0.0016(66)	-0.0056(48)	0.0257(78)
C(1A)	0.0475(52)	0.0759(74)	0.0408(45)	0.0001(48)	0.0026(38)	-0.0104(53)
C(5)	0.0385(47)	0.0728(70)	0.0617(56)	0.0175(48)	0.0147(41)	0.0110(46)
C(4B)	0.0823(80)	0.0679(82)	0.0472(57)	-0.0042(56)	0.0008(52)	0.0211(67)
C(2)	0.0422(50)	0.0761(74)	0.0563(52)	0.0047(55)	0.0161(41)	0.0161(52)
C(2A)	0.0658(62)	0.0501(64)	0.0499(56)	0.0080(50)	-0.0139(45)	-0.0117(53)
C(3')	0.0740(66)	0.0605(68)	0.0532(55)	0.0044(54)	0.0153(49)	-0.0035(54)
C(6A)	0.0922(83)	0.0734(82)	0.0730(69)	-0.0014(64)	0.0307(61)	0.0024(69)
C(3A)	0.0577(62)	0.0752(79)	0.0749(68)	0.0217(61)	-0.0074(52)	-0.0099(61)
C(9B)	0.0689(66)	0.0731(91)	0.0538(58)	0.0056(52)	-0.0008(49)	0.0070(60)
C(2')	0.0627(61)	0.0638(72)	0.0577(57)	0.0058(56)	0.0167(49)	-0.0123(53)
C(7B)	0.132(13)	0.100(12)	0.0802(91)	-0.0038(88)	0.0014(86)	-0.009(12)
C(4')	0.0801(81)	0.0835(87)	0.0637(67)	0.0131(63)	-0.0048(53)	-0.0085(66)
C(6)	0.0459(50)	0.0424(59)	0.0679(61)	0.0064(47)	-0.0011(44)	-0.0068(43)
C(1B)	0.0673(71)	0.0801(80)	0.0472(54)	-0.0001(56)	0.0009(52)	0.0198(58)
C(7)	0.0551(62)	0.0878(90)	0.1162(93)	0.0131(78)	0.0287(64)	-0.0061(65)
C(5A)	0.121(11)	0.0535(84)	0.1050(90)	-0.0017(61)	0.0359(78)	0.0045(73)
C(5B)	0.128(13)	0.087(11)	0.0802(86)	-0.0067(75)	-0.0043(84)	0.0393(93)
C(8B)	0.0837(89)	0.0535(83)	0.0680(74)	-0.0019(77)	0.0116(63)	0.0095(87)
C(4A)	0.0954(93)	0.0603(84)	0.1095(95)	0.0139(67)	0.0041(76)	-0.0133(73)
C(6B)	0.174(17)	0.078(12)	0.0781(88)	0.0037(77)	-0.000(10)	-0.003(11)
C(3)	0.0350(44)	0.0708(76)	0.0592(52)	0.0150(50)	0.0072(39)	-0.0008(45)

Table 4.3 Final Atomic Parameters for the Pharmacological Compound

1-MPP

154

	1-MPP	1-ATN
Molecular formula	$C_{23}H_{23}N_3O_3 \cdot HBr$	$C_{15}H_{16}NO_2S_2$
Molecular mass (Mr)	470.35	306.42
Crystal dimensions (mm)	0.2 x 0.5 x 0.1	0.2 x 0.2 x 0.2
Crystal shape	Flat, oblong	Irregular
Crystal system	Monoclinic	Monoclinic
Space group	C2/c	$P2_1/c$
Cell dimentions ($\overset{\circ}{A} \pm \sigma$)		
a	22.627(0.0014)	12.2411(0.0015)
b	14.057(0.0089)	8.0563 (0.0009)
c	14.207(0.0012)	15.3544(0.0020)
α	90.00 (0.0)	90.00 (0.0)
β	97.54 (0.007)	98.997 (0.013)
γ	90.00 (0.0)	90.00 (0.0)
Cell volume ($\overset{\circ}{A}{}^3$)	4479.83	1495.6
Z	8	4
D_{calc} (g/cm^3)	1.359	1.365
$F_{(000)}$	1936	648
Radiation and monochromater	Mo-Kα, graphite	Mo-Kα, graphite
Linear adsorption coefficient (cm^{-1})	18.42	3.41
Parameters refined	295	181
Final R	0.0479	0.0350
Final R_w	0.0530	0.0411
Final S	4.166	1.303

Table 4.4   Summary of the Data Collected and the Structure Solution for the
Pharmacological Compounds 1-MPP and 1-ATN

155

N(4)	−C(1′)	1.500(11)		C(1A)	−C(6A)	1.393(14)
N(4)	− C(5)	1.509(11)		C(5)	− C(6)	1.483(12)
N(4)	− C(3)	1.487(11)		C(4B)	−C(9B)	1.391(15)
O(1)	−C(2A)	1.361(11)		C(4B)	−C(5B)	1.375(18)
O(1)	− C(7)	1.442(13)		C(2)	− C(3)	1.495(12)
C(1′)	−C(2′)	1.462(13)		C(2A)	−C(3A)	1.376(14)
N(2)	−C(3B)	1.402(14)		C(3′)	−C(2′)	1.164(14)
N(2)	−C(4′)	1.430(13)		C(3′)	−C(4′)	1.462(14)
N(2)	−C(1B)	1.393(13)		C(6A)	−C(5A)	1.389(16)
N(1)	−C(1A)	1.411(11)		C(3A)	−C(4A)	1.372(16)
N(1)	− C(2)	1.467(11)		C(9B)	−C(1B)	1.473(15)
N(1)	− C(6)	1.482(11)		C(9B)	−C(8B)	1.387(17)
O(3)	−C(1B)	1.208(13)		C(7B)	−C(8B)	1.386(21)
O(2)	−C(3B)	1.211(14)		C(7B)	−C(6B)	1.361(23)
C(3B)	−C(4B)	1.493(16)		C(5A)	−C(4A)	1.361(17)
C(1A)	−C(2A)	1.426(13)		C(5B)	−C(6B)	1.378(22)

Table 4.5   Calculated Bong Lengths

for the Pharmacological Compound 1-MPP

Atoms are labelled as shown in Fig. 4.4 and bond lengths are given in Å with standard deviations in parentheses. Bond lengths for hydrogen atoms have been omitted.

C(1')	– N(4)	– C(5)	112.7(6)	O(1)	–C(2A)	–C(3A)	124.3(9)
C(1')	– N(4)	– C(3)	110.9(6)	C(1A)	–C(2A)	–C(3A)	119.4(9)
C(5)	– N(4)	– C(3)	109.5(6)	C(2')	–C(3')	–C(4')	176.1(10)
C(2A)	– O(1)	– C(7)	116.2(7)	C(1A)	–C(6A)	–C(5A)	121.6(10)
N(4)	–C(1')	–C(2')	110.8(7)	C(2A)	–C(3A)	–C(4A)	122.1(10)
C(3B)	– N(2)	–C(4')	124.1(8)	C(4B)	–C(9B)	–C(1B)	108.5(9)
C(3B)	– N(2)	–C(1B)	111.3(8)	C(4B)	–C(9B)	–C(8B)	120.8(10)
C(4')	– N(2)	–C(1B)	124.6(8)	C(1B)	–C(9B)	–C(8B)	130.6(10)
C(1A)	– N(1)	– C(2)	115.8(7)	C(1')	–C(2')	–C(3')	175.0(10)
C(1A)	– N(1)	– C(6)	114.8(7)	C(8B)	–C(7B)	–C(6B)	121.2(15)
C(2)	– N(1)	– C(6)	109.0(6)	N(2)	–C(4')	–C(3')	114.1(9)
N(2)	–C(3B)	– O(2)	123.7(10)	N(1)	– C(6)	– C(5)	110.1(7)
N(2)	–C(3B)	–C(4B)	106.1(9)	N(2)	–C(1B)	– O(3)	122.9(9)
O(2)	–C(3B)	–C(4B)	130.2(10)	N(2)	–C(1B)	–C(9B)	106.6(8)
N(1)	–C(1A)	–C(2A)	119.6(8)	O(3)	–C(1B)	–C(9B)	130.5(10)
N(1)	–C(1A)	–C(6A)	123.3(8)	C(6A)	–C(5A)	–H(5A)	119.8(13)
C(2A)	–C(1A)	–C(6A)	117.1(9)	C(6A)	–C(5A)	–C(4A)	120.3(11)
N(4)	– C(5)	– C(6)	111.1(7)	C(4B)	–C(5B)	–C(6B)	118.2(13)
C(3B)	–C(4B)	–C(9B)	107.5(9)	C(9B)	–C(8B)	–C(7B)	117.5(12)
C(3B)	–C(4B)	–C(5B)	131.9(11)	C(3A)	–C(4A)	–C(5A)	119.5(11)
C(9B)	–C(4B)	–C(5B)	120.6(11)	C(7B)	–C(6B)	–C(5B)	121.6(15)
N(1)	– C(2)	– C(3)	110.1(7)	N(4)	– C(3)	– C(2)	111.8(7)
O(1)	–C(2A)	–C(1A)	116.3(8)				

Table 4.6   Calculated Bond Angles

for the Pharmacological compound 1-MPP

Atoms are labelled as shown in Fig. 4.4 and bond angles are given in degrees
with standard deviations in parentheses.   Bond angles including hydrogen
atoms have been omitted.

C(5)	– N(4)	–C(1')	–C(2')	65.6(9)	
C(3)	– N(4)	–C(1')	–C(2')	-171.2(7)	
C(1')	– N(4)	– C(5)	– C(6)	178.3(7)	
C(3)	– N(4)	– C(5)	– C(6)	54.4(9)	
C(1')	– N(4)	– C(3)	– C(2)	-178.9(7)	
C(5)	– N(4)	– C(3)	– C(2)	-53.9(8)	
C(7)	– O(1)	–C(2A)	–C(1A)	165.9(8)	
C(7)	– O(1)	–C(2A)	–C(3A)	-12.8(13)	
N(4)	–C(1')	–C(2')	–C(3')	73.0(11)	
C(4')	– N(2)	–C(3B)	– O(2)	-2.4(16)	
C(4')	– N(2)	–C(3B)	–C(4B)	179.6(9)	
C(1B)	– N(2)	–C(3B)	– O(2)	179.8(10)	
C(1B)	– N(2)	–C(3B)	–C(4B)	1.8(11)	
C(3B)	– N(2)	–C(4')	–C(3')	110.8(11)	
C(1B)	– N(2)	–C(4')	–C(3')	-71.7(12)	
C(3B)	– N(2)	–C(1B)	– O(3)	177.0(10)	
C(3B)	– N(2)	–C(1B)	–C(9B)	-2.3(11)	
C(4')	– N(2)	–C(1B)	– O(3)	-0.8(16)	
C(4')	– N(2)	–C(1B)	–C(9B)	180.0(9)	
C(2)	– N(1)	–C(1A)	–C(2A)	-166.7(8)	
C(2)	– N(1)	–C(1A)	–C(6A)	10.4(12)	
C(6)	– N(1)	–C(1A)	–C(2A)	64.9(10)	
C(6)	– N(1)	–C(1A)	–C(6A)	-118.0(10)	
C(1A)	– N(1)	– C(2)	– C(3)	168.1(7)	
C(6)	– N(1)	– C(2)	– C(3)	-60.7(8)	
C(1A)	– N(1)	– C(6)	– C(5)	-166.8(7)	
C(2)	– N(1)	– C(6)	– C(5)	61.5(9)	
N(2)	–C(3B)	–C(4B)	–C(9B)	-0.6(12)	
N(2)	–C(3B)	–C(4B)	–C(5B)	177.7(13)	
O(2)	–C(3B)	–C(4B)	–C(9B)	-178.4(12)	

O(2)	–C(3B)	–C(4B)	–C(5B)	-0.1(22)	
N(1)	–C(1A)	–C(2A)	– O(1)	1.3(12)	
N(1)	–C(1A)	–C(2A)	–C(3A)	-179.9(9)	
C(6A)	–C(1A)	–C(2A)	– O(1)	-176.0(8)	
C(6A)	–C(1A)	–C(2A)	–C(3A)	2.8(14)	
N(1)	–C(1A)	–C(6A)	–C(5A)	-177.9(10)	
C(2A)	–C(1A)	–C(6A)	–C(5A)	-0.7(15)	
N(4)	– C(5)	– C(6)	– N(1)	-58.7(9)	
C(3B)	–C(4B)	–C(9B)	–C(1B)	-0.8(12)	
C(3B)	–C(4B)	–C(9B)	–C(8B)	178.9(10)	
C(5B)	–C(4B)	–C(9B)	–C(1B)	-179.3(11)	
C(5B)	–C(4B)	–C(9B)	–C(8B)	0.3(18)	
C(3B)	–C(4B)	–C(5B)	–C(6B)	-178.2(13)	
C(9B)	–C(4B)	–C(5B)	–C(6B)	0.0(20)	
O(1)	–C(2A)	–C(3A)	–C(4A)	175.2(10)	
C(1A)	–C(2A)	–C(3A)	–C(4A)	-3.5(16)	
C(4')	–C(3')	–C(2')	–C(1')	-19.0(25)	
C(2')	–C(3')	–C(4')	– N(2)	114.3(15)	
C(1A)	–C(6A)	–C(5A)	–C(4A)	-0.9(18)	
C(4B)	–C(9B)	–C(1B)	– N(2)	1.8(12)	
C(4B)	–C(9B)	–C(1B)	– O(3)	-177.3(11)	
C(8B)	–C(9B)	–C(1B)	– N(2)	-177.8(12)	
C(8B)	–C(9B)	–C(1B)	– O(3)	3.1(20)	
C(4B)	–C(9B)	–C(8B)	–C(7B)	-0.5(18)	
C(1B)	–C(9B)	–C(8B)	–C(7B)	179.0(12)	
C(6B)	–C(7B)	–C(8B)	–C(9B)	0.4(22)	
C(8B)	–C(7B)	–C(6B)	–C(5B)	-0.1(25)	
C(6A)	–C(5A)	–C(4A)	–C(3A)	0.3(18)	
C(4B)	–C(5B)	–C(6B)	–C(7B)	-0.1(23)	

Table 4.7   Calculated Torsion Angles

for the Pharmacological Compound 1-MPP

Atoms are labelled as shown in Fig. 4.4 and torsion angles are given in degrees with standard deviations in parentheses. Torsion angles involving hydrogen atoms have been omitted.

4.4.2 1-Aza-5-oxa-6-(1',3'-dithianyl)-7,8-benzo-9-oxobicyclo [4,3,0]nonane (1-ATN)

N-(3-Bromopropyl)-phthalimide was reacted with 1 equivalent of lithnated 1,3-dithiane in an attempt to synthesise N-(3-dithianylpropyl)-phthalimide (by Dr. I Dawson, Dept. of Pharmacology, University of Edinburgh). The latter was to be used as a synthon in the Fisher-Indole synthesis of a novel serotonergic agent related to the NAN-190 compounds but with sulphur in the ring system rather than nitrogen. The outcome of this reaction was uncertain therefore the crystal structure of the major reaction product was solved as a means of verification.

In the event, addition of the dithiane anion to the carboxyl group of the phthalimide group occurred preferentially, under these conditions (refluxing in THF), with concomitant intramolecular O-alkylation by the bromopropyl group to form the bicyclic product 1-ATN (see Fig. 4.6).

4.4.2.1 Method of Structure Solution and Refinement

Crystals (supplied by Dr. I. Dawson) of 1-ATN were prepared from ethylacetate/hexane by the evaporation of a nearly-saturated solution at 293 K. A crystal of dimensions 0.2 x 0.2 x 0.2 mm was used for data collection. Data were collected on a Stoe STADI-4 diffractometer (with the help of Dr. L. Sawyer). An orientation matrix was calculated using 20 reflections in a 2θ range of 10 to 20 degrees. Accurate cell dimensions were determined using 20 reflections at $\pm \omega$ in a 2θ range of 30 to 32 degrees. Data were collected over $-11 < h \geq 13$, $0 < k \geq 8$, $0 < l \geq 16$, with 9 reflections being measured every 2 hours to check for crystal decay or movement. During data reduction, 337 of the 2130 measured reflections had a $I < 2\sigma(I)$ and were therefore considered unobserved. During refinement 1793 reflections were used out of the 2130 measured during data collection.
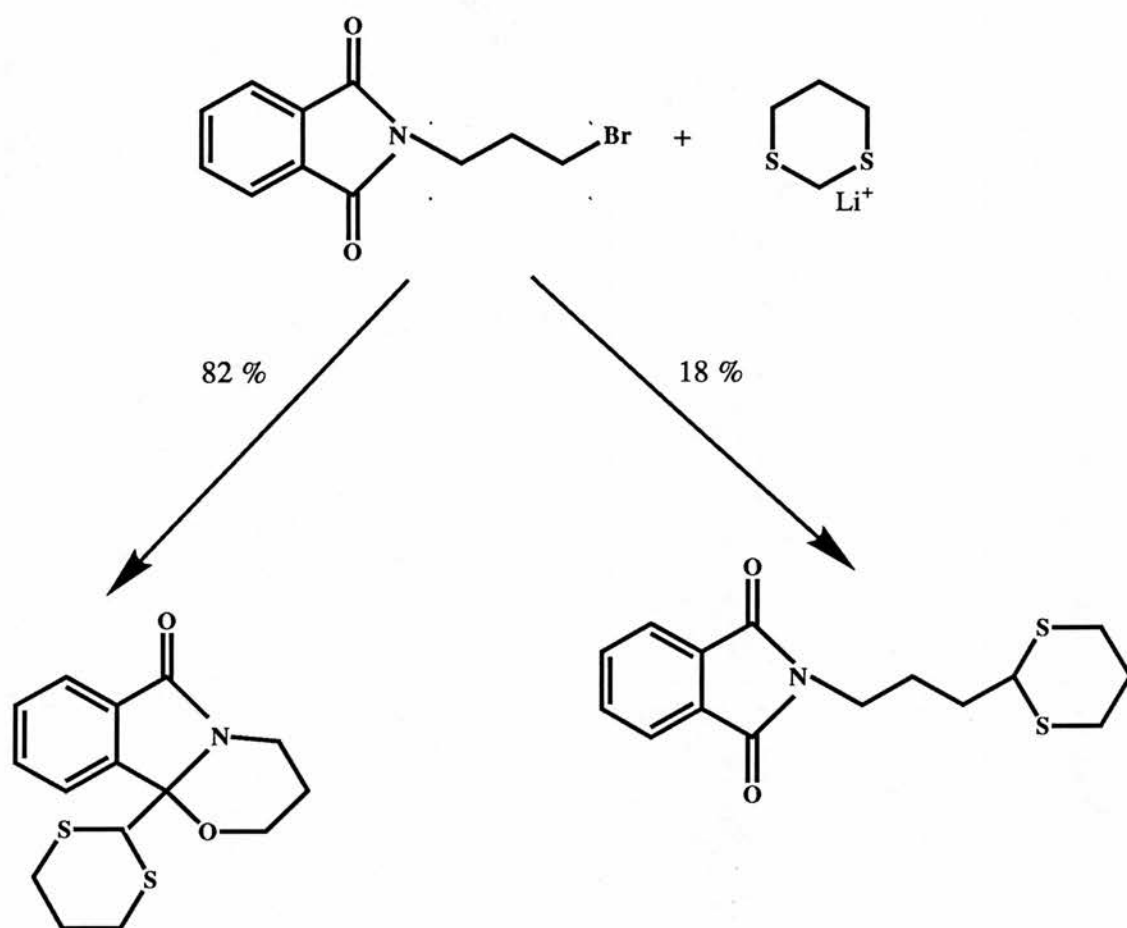
Figure 4.6   Synthesis of the Pharmacological compound 1-ATN

Diagram showing how the reaction of N-(3-Bromopropyl)-phthalimide with lithnated

dithiane results in the formation of the bicyclic product 1-ATN.

Trial positons for the sulphur atoms were located using a Patterson map but the difference Fourier calculated was uninterpretable. However, direct methods using SHELXS86 (Sheldrick, 1986) did successfully locate the positions of all the non-hydrogen atoms. Atoms were refined anisotropically before addition of hydrogen atoms, with fixed isotropic temperature factors and site occupancies. These were allowed to ride on the atom to which they were attached. The maximum atom shift in the final refinement cycle was 0.001 Å. A weighting scheme of the form $9.9123/(\sigma^2(F) + 0.000060(F^2))$ was employed to improve final structure solution.

A total of 181 parameters were refined resulting in a final R factor of 0.035. The final difference map gave maximum and minimum values of 0.257 and -0.279 $e\text{Å}^{-3}$ respectively and the maximum $\sin\theta/\lambda$ was 0.5382 Å^{-1}.

Final atomic parameters are given in Table 4.8. Table 4.4 gives a summary of the data collected and the structure solution. The program CALC (Gould and Taylor, 1983) was used to provide molecular geometry data presented in Tables 4.9, 4.10 and 4.11. Crystal structure diagrams (Fig. 4.7) were prepared using the program ORTEP (Johnson, 1965; Mallinson and Muir, 1985) and crystal packing diagrams (Fig. 4.8) were prepared using the program PLUTO (Motherwell, 1972).

4.4.2.2 Discussion

The crystal structure of 1-ATN is shown in Fig. 4.7. The bond lengths for this structure are as expected (see Table 4.7). The bond lengths and angles (see Table 4.9 and 4.10) for the benzene ring form a near perfect ring structure. The angles through the nitrogen atom (see Table 4.10) are slightly distorted from a true tetrahedron, which is probably due to the strain caused by cyclising carbons 1, 2 and 3 and oxygen 4 (see Fig. 4.7 and Tables 4.9, 4.10 and 4.11).

The molecular packing (see Fig. 4.8) indicates few close contacts between molecules. The molecules form infinite stacks, parallel to the b axis, with a herringbone pattern typical of planar aromatic systems. There are four significantly short carbon and oxygen atom intermolecular distances which may indicate very weak intermolecular interactions. Two of these occur between oxygen 6 (carbonyl group) of one molecule and carbon 1 and carbon 3 of two different molecules (these being 3.308(3) and 3.468(3) Å respectively) related by the symmetry operations x,-1/2-y,1/2+z and -x,1/2+y,1/2-z respectively. The other two short intermolecular distances occur between oxygen 14 of one molecule and carbons 18 and 19 of another (these being 3.479(4) and 3.315(3) Å respectively) related by the symmetry operation x,1+y,z. These may help in the formation of the stacks (described above) that are parallel to the b axis.
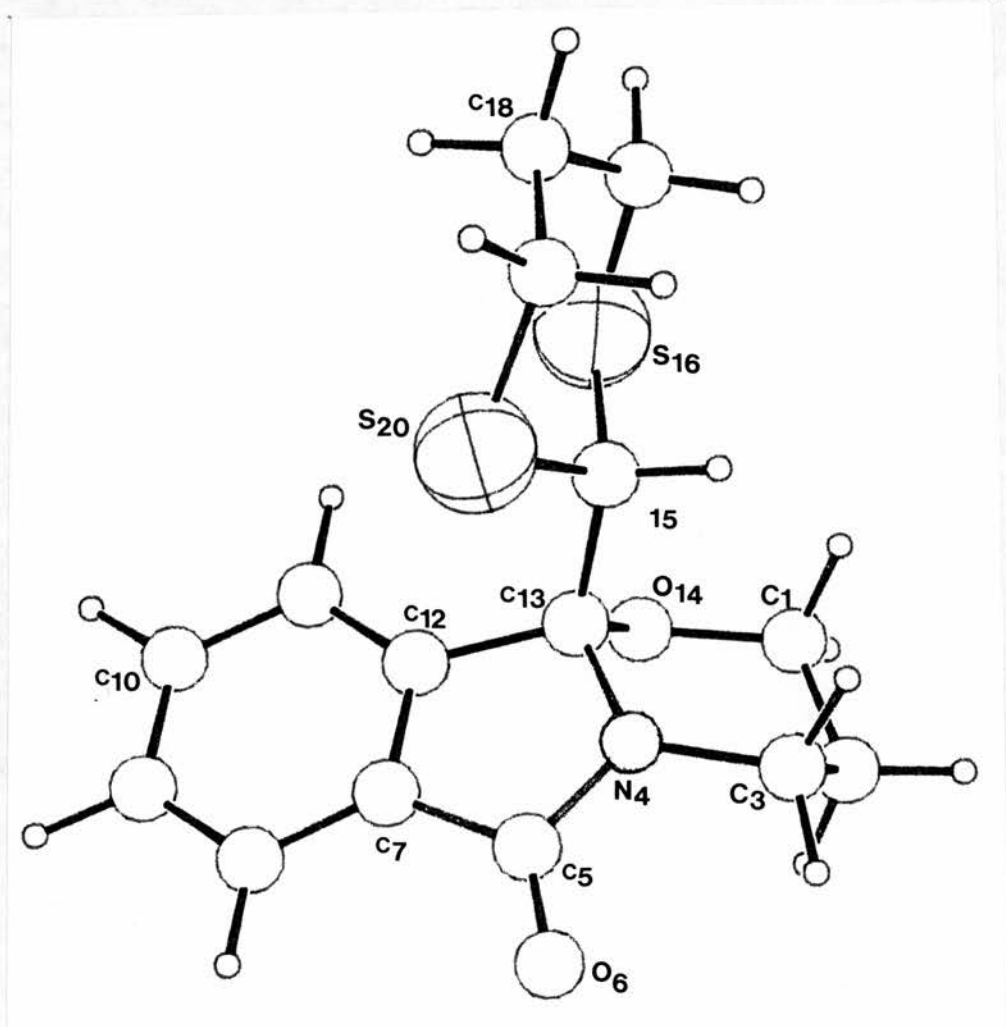
Figure 4.7   Crystal Structure of the Pharmacological Compound 1-ATN

The crystal structure diagram was prepared using the program
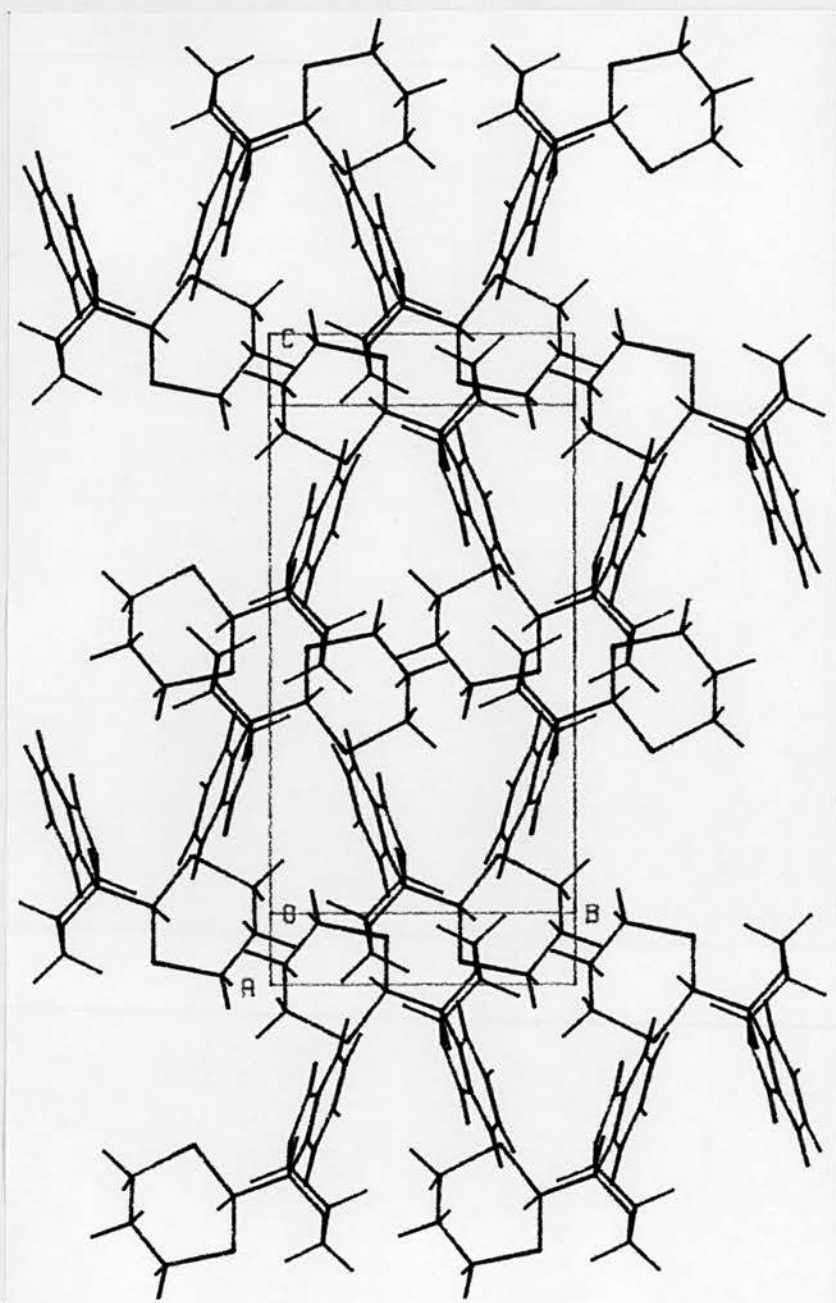ORTEP. Sulphur atoms are shaded.

Figure 4.8   Crystal Packing Diagram of the Pharmacological Compound 1-ATN

The packing diagram was generated using the computer program

PLUTO.   The view is taken down the a axis

Fractional Coordinates of Atoms with Standard Deviations

	x	y	z	Ueq
C(1)	0.08798(22)	-0.1679(4)	0.45593(17)	0.0505(17)
C(2)	-0.00961(22)	-0.1888(4)	0.38304(18)	0.0516(17)
C(3)	-0.00601(19)	-0.0593(3)	0.31189(17)	0.0440(15)
N(4)	0.10402(15)	-0.06385(24)	0.28621(12)	0.0340(11)
C(5)	0.12484(20)	-0.1238(3)	0.20782(16)	0.0365(14)
O(6)	0.05559(15)	-0.14692(24)	0.14251(11)	0.0524(12)
C(7)	0.24594(20)	-0.1561(3)	0.21934(16)	0.0384(15)
C(8)	0.30853(24)	-0.2214(3)	0.16014(18)	0.0519(17)
C(9)	0.4204(3)	-0.2447(4)	0.18893(21)	0.0632(21)
C(10)	0.46653(24)	-0.2046(4)	0.27443(22)	0.0613(20)
C(11)	0.40296(20)	-0.1416(3)	0.33475(18)	0.0476(17)
C(12)	0.29152(19)	-0.1184(3)	0.30553(15)	0.0353(14)
C(13)	0.20147(18)	-0.0593(3)	0.35495(14)	0.0329(13)
O(14)	0.19167(14)	-0.17680(20)	0.42223(10)	0.0398(10)
C(15)	0.21661(20)	0.1200(3)	0.39186(15)	0.0352(14)
S(16)	0.30770(7)	0.12121(9)	0.49747(5)	0.0596(5)
C(17)	0.3015(3)	0.3420(4)	0.52080(20)	0.0675(21)
C(18)	0.3399(3)	0.4539(4)	0.45272(21)	0.0647(20)
C(19)	0.26530(24)	0.4483(3)	0.36402(19)	0.0551(18)
S(20)	0.26498(6)	0.24926(8)	0.30941(4)	0.0431(4)

Anisotropic Vibration Parameters with Standard Deviations

	U11	U22	U33	U23	U13	U12
C(1)	0.0543(17)	0.0531(17)	0.0448(16)	0.0043(14)	0.0203(14)	-0.0052(14)
C(2)	0.0462(16)	0.0547(17)	0.0546(17)	-0.0071(14)	0.0207(13)	-0.0112(14)
C(3)	0.0325(14)	0.0500(16)	0.0487(15)	-0.0096(13)	0.0074(12)	-0.0005(12)
N(4)	0.0324(11)	0.0351(12)	0.0335(11)	-0.0031(9)	0.0032(9)	-0.0017(9)
C(5)	0.0456(15)	0.0288(13)	0.0340(14)	-0.0010(11)	0.0065(12)	-0.0023(12)
O(6)	0.0556(12)	0.0598(13)	0.0389(11)	-0.0087(9)	-0.0025(9)	0.0011(10)
C(7)	0.0449(15)	0.0297(14)	0.0406(14)	0.0023(11)	0.0133(12)	0.0017(11)
C(8)	0.0608(19)	0.0493(17)	0.0464(16)	-0.0009(14)	0.0216(14)	0.0049(14)
C(9)	0.0632(21)	0.0623(20)	0.0656(21)	0.0005(16)	0.0298(17)	0.0150(16)
C(10)	0.0432(17)	0.0626(20)	0.0779(22)	0.0072(17)	0.0174(16)	0.0123(15)
C(11)	0.0405(16)	0.0464(17)	0.0550(17)	0.0023(14)	0.0088(13)	0.0029(13)
C(12)	0.0384(14)	0.0240(13)	0.0430(15)	0.0018(11)	0.0092(11)	0.0008(11)
C(13)	0.0335(13)	0.0313(13)	0.0329(13)	0.0014(11)	0.0041(10)	-0.0021(11)
O(14)	0.0462(10)	0.0340(10)	0.0386(10)	0.0069(8)	0.0091(8)	0.0011(8)
C(15)	0.0379(14)	0.0320(14)	0.0342(13)	-0.0018(11)	0.0021(11)	0.0003(11)
S(16)	0.0844(6)	0.0429(5)	0.0452(5)	-0.0028(3)	-0.0197(4)	-0.0009(4)
C(17)	0.0931(25)	0.0486(19)	0.0547(18)	-0.0155(16)	-0.0145(17)	-0.0033(17)
C(18)	0.0679(19)	0.0386(17)	0.0818(22)	-0.0155(16)	-0.0120(17)	-0.0074(15)
C(19)	0.0635(18)	0.0301(15)	0.0677(19)	-0.0030(14)	-0.0036(15)	-0.0023(13)
S(20)	0.0479(4)	0.0320(4)	0.0482(4)	0.0025(3)	0.0077(3)	-0.0038(3)

Table 4.8   <u>Final Atomic Parameters for the Pharmacological Compound</u>

<u>1-ATN</u>

C(1) - C(2)	1.513(4)		C(10) -C(11)	1.395(4)
C(1) -O(14)	1.446(3)		C(11) -C(12)	1.380(4)
C(2) - C(3)	1.516(4)		C(12) -C(13)	1.510(3)
C(3) - N(4)	1.462(3)		C(13) -O(14)	1.420(3)
N(4) - C(5)	1.358(3)		C(13) -C(15)	1.552(3)
N(4) -C(13)	1.464(3)		C(15) -S(16)	1.819(3)
C(5) - O(6)	1.222(3)		C(15) -S(20)	1.8090(24)
C(5) - C(7)	1.488(3)		S(16) -C(17)	1.819(3)
C(7) - C(8)	1.381(4)		C(17) -C(18)	1.510(5)
C(7) -C(12)	1.387(3)		C(18) -C(19)	1.518(4)
C(8) - C(9)	1.384(4)		C(19) -S(20)	1.809(3)
C(9) -C(10)	1.384(4)			

Table 4.9   Calculated Bong Lengths

for the Pharmacological Compound 1-ATN

Atoms are labelled as shown in Fig. 4.7 and bond lengths are given in Å with

standard deviations in parentheses. Bond lengths for hydrogen atoms have

been omitted.

C(2)	- C(1)	-O(14)	111.44(22)	C(7)	-C(12)	-C(13)	109.40(20)
C(1)	- C(2)	- C(3)	110.35(22)	C(11)	-C(12)	-C(13)	129.90(21)
C(2)	- C(3)	- N(4)	107.98(20)	N(4)	-C(13)	-C(12)	101.90(17)
C(3)	- N(4)	- C(5)	123.83(20)	N(4)	-C(13)	-O(14)	110.82(17)
C(3)	- N(4)	-C(13)	119.08(18)	N(4)	-C(13)	-C(15)	108.91(18)
C(5)	- N(4)	-C(13)	113.78(18)	C(12)	-C(13)	-O(14)	107.85(18)
N(4)	- C(5)	- O(6)	125.42(22)	C(12)	-C(13)	-C(15)	114.98(19)
N(4)	- C(5)	- C(7)	106.17(20)	O(14)	-C(13)	-C(15)	111.94(18)
O(6)	- C(5)	- C(7)	128.41(22)	C(1)	-O(14)	-C(13)	113.96(18)
C(5)	- C(7)	- C(8)	129.28(23)	C(13)	-C(15)	-S(16)	110.62(16)
C(5)	- C(7)	-C(12)	108.65(20)	C(13)	-C(15)	-S(20)	108.28(16)
C(8)	- C(7)	-C(12)	121.97(23)	S(16)	-C(15)	-S(20)	113.50(13)
C(7)	- C(8)	- C(9)	117.7(3)	C(15)	-S(16)	-C(17)	98.18(13)
C(8)	- C(9)	-C(10)	120.5(3)	S(16)	-C(17)	-C(18)	114.85(23)
C(9)	-C(10)	-C(11)	121.8(3)	C(17)	-C(18)	-C(19)	113.2(3)
C(10)	-C(11)	-C(12)	117.31(24)	C(18)	-C(19)	-S(20)	113.55(20)
C(7)	-C(12)	-C(11)	120.67(22)	C(15)	-S(20)	-C(19)	99.39(12)

Table 4.10   <u>Calculated Bond Angles</u>

<u>for the Pharmacological compound 1-ATN</u>

Atoms are labelled as shown in Fig. 4.7 and bond angles are given in degrees with standard deviations in parentheses. Bond angles including hydrogen atoms have been omitted.

167

O(14)	– C(1)	– C(2)	– C(3)	-56.9(3)	C(9)	–C(10)	–C(11)	–C(12)	-0.8(4)
C(2)	– C(1)	–O(14)	–C(13)	56.8(3)	C(10)	–C(11)	–C(12)	– C(7)	-0.3(4)
C(1)	– C(2)	– C(3)	– N(4)	51.2(3)	C(10)	–C(11)	–C(12)	–C(13)	177.45(25)
C(2)	– C(3)	– N(4)	– C(5)	108.6(3)	C(7)	–C(12)	–C(13)	– N(4)	-1.74(24)
C(2)	– C(3)	– N(4)	–C(13)	-49.5(3)	C(7)	–C(12)	–C(13)	–O(14)	114.98(21)
C(3)	– N(4)	– C(5)	– O(6)	16.9(4)	C(7)	–C(12)	–C(13)	–C(15)	-119.35(22)
C(3)	– N(4)	– C(5)	– C(7)	-162.30(21)	C(11)	–C(12)	–C(13)	– N(4)	-179.70(24)
C(13)	– N(4)	– C(5)	– O(6)	176.10(23)	C(11)	–C(12)	–C(13)	–O(14)	-63.0(3)
C(13)	– N(4)	– C(5)	– C(7)	-3.1(3)	C(11)	–C(12)	–C(13)	–C(15)	62.7(3)
C(3)	– N(4)	–C(13)	–C(12)	163.32(19)	N(4)	–C(13)	–O(14)	– C(1)	-50.18(24)
C(3)	– N(4)	–C(13)	–O(14)	48.8(3)	C(12)	–C(13)	–O(14)	– C(1)	-160.93(19)
C(3)	– N(4)	–C(13)	–C(15)	-74.78(24)	C(15)	–C(13)	–O(14)	– C(1)	71.62(24)
C(5)	– N(4)	–C(13)	–C(12)	3.06(24)	N(4)	–C(13)	–C(15)	–S(16)	162.71(15)
C(5)	– N(4)	–C(13)	–O(14)	-111.48(21)	N(4)	–C(13)	–C(15)	–S(20)	-72.33(19)
C(5)	– N(4)	–C(13)	–C(15)	124.96(20)	C(12)	–C(13)	–C(15)	–S(16)	-83.71(21)
N(4)	– C(5)	– C(7)	– C(8)	178.2(3)	C(12)	–C(13)	–C(15)	–S(20)	41.25(23)
N(4)	– C(5)	– C(7)	–C(12)	1.8(3)	O(14)	–C(13)	–C(15)	–S(16)	39.81(22)
O(6)	– C(5)	– C(7)	– C(8)	-1.0(4)	O(14)	–C(13)	–C(15)	–S(20)	164.77(15)
O(6)	– C(5)	– C(7)	–C(12)	-177.36(25)	C(13)	–C(15)	–S(16)	–C(17)	-178.06(18)
C(5)	– C(7)	– C(8)	– C(9)	-177.5(3)	S(20)	–C(15)	–S(16)	–C(17)	60.00(16)
C(12)	– C(7)	– C(8)	– C(9)	-1.6(4)	C(13)	–C(15)	–S(20)	–C(19)	175.84(16)
C(5)	– C(7)	–C(12)	–C(11)	178.23(22)	S(16)	–C(15)	–S(20)	–C(19)	-60.92(16)
C(5)	– C(7)	–C(12)	–C(13)	0.1(3)	C(15)	–S(16)	–C(17)	–C(18)	-59.19(25)
C(8)	– C(7)	–C(12)	–C(11)	1.6(4)	S(16)	–C(17)	–C(18)	–C(19)	66.4(3)
C(8)	– C(7)	–C(12)	–C(13)	-176.62(23)	C(17)	–C(18)	–C(19)	–S(20)	-65.9(3)
C(7)	– C(8)	– C(9)	–C(10)	0.5(4)	C(18)	–C(19)	–S(20)	–C(15)	59.49(22)
C(8)	– C(9)	–C(10)	–C(11)	0.7(5)					

Table 4.11   Calculated Torsion Angles

for the Pharmacological Compound 1-ATN

Atoms are labelled as shown in Fig. 4.7 and torsion angles are given in degrees with standard deviations in parentheses. Torsion angles involving hydrogen atoms have been omitted.

CHAPTER FIVE

GENERAL DISCUSSION

5.1 Summary and Conclusions

This project was designed to investigate the interaction of the bovine caseins with calcium phosphate minerals. Two different approaches were adopted: the construction of adsorption isotherms (Chapter 3) and the growth of co-crystals of phosphoserine- containing peptides, after purification or chemical synthesis (Chapter 2), with calcium ions (Chapter 4). Precise tertiary and quaternary structural information about the caseins and their peptide derivatives together with thermodynamic information from adsorption experiments would allow a model of casein interaction with calcium phosphate minerals to be developed. As such information is presently unavailable, it was hoped that the above approaches would give an insight into the mechanism and stereochemistry of casein interaction with calcium phosphate minerals and hence help understand the structure of the casein micelle.

None of the caseins has yet been crystallised and their lack of regular secondary and tertiary structure makes their crystallisation unlikely in the near future. Growth of crystals of the peptide β-CN (f1-25) has also been attempted (by Miss S Fawcett, Department of Biochemistry, University of Edinburgh) but was unsuccessful both in the absence and presence of calcium ions. If smaller phosphopeptides could be co-crystallised with calcium ions, the structural information obtained would form the basis for the development of a model of phosphoprotein/calcium mineral interaction.

As a starting point, growth of co-crystals of phosphoserine and calcium ions was attempted, this being the simplest possible system that would provide a structural basis for the interaction between phosphoproteins and calcium. It was hoped that the peptides of two, three or four phosphoserine residues (and possibly other acidic amino acids) could be chemically synthesised and co-crystallised with calcium ions thus expanding and refining the model of interaction. Co-crystallisation of phosphoserine with calcium ions proved to be very difficult but

170

micro-crystals were obtained. Unfortunately, they were not suitable for structural determination by the conventional X-ray diffraction techniques available at Edinburgh (Chapter 4). The technique of X-ray powder diffraction might be used as an alternative but, for such a structure as this, it might well not be able to provide a unique solution. The chemical synthesis of the dipeptide Ser(P)-Ser(P) was successfully completed (Chapter 2), but, to date no crystals of the dipeptide or co-crystals with calcium ions have been obtained.

The two most extensively characterised phosphoprotein/calcium mineral systems in biology are, arguably, the acidic proline-rich-phosphoproteins (acidic PRP's) of human saliva and the caseins of milk. Adsorption experiments, as described in Chapter 3, have been performed for the acidic PRP's but have not been previously performed with the caseins. The adsorption of these relatively large molecules is a complex process, the understanding of which would be aided by the use, in adsorption experiments, of small, synthetic phosphopeptides. The findings of the adsorption experiments and the isotherms constructed (Chapter 3) are summarised below.

Adsorption of β-CN A and β-CN (f1-25) to dicalcium phosphate dihydrate (DCPD) occurs at low, equilibrium, free concentrations (approximately 1×10^{-5} M) to relatively high affinity sites on the DCPD crystals. At higher, equilibrium, free concentrations of β-CN A (approximately 4×10^{-5} M) cooperative, lateral interactions between β-CN A molecules may occur which appear to be disrupted when 6.0 M urea is present in the buffer. At even higher, equilibrium, free concentrations of β-CN (f1-25) (approximately 3×10^{-4} M) an increase in adsorption is observed which is attributed to a second family of intrinsically lower affinity adsorption sites which are more abundant than the high affinity sites. In addition, the adsorption of β-CN (f1-25) is athermal, implying that the adsorption process is "driven" by an entropy gain.

The only comparable experiments to these (Chapter 3) were performed by E. C. Moreno and co-workers with the acidic PRP's adsorbing to hydroxyapatite and

fluorapatite (see section 3.2). The acidic PRP's, like the caseins, are highly solvated and flexible molecules (see section 3.3.2). However, the acidic PRP's have only two phosphoseryl residues, at positions 8 and 22 (see section 3.2.2), whereas β-CN A has five phosphoseryl residues at positions 15, 17, 18, 19 and 35 (see section 3.3.2). Moreno and co-workers found that the acidic PRP's and the TX-peptide (the N-terminal of 30 amino acids which contains both phosphoseryl residues; see section 3.2.1) adsorbed to both hydroxyapatite and fluorapatite and the isotherms produced were adequately described by the Langmuir theory (see section 3.2.2). In contrast, the adsorption of β-CN (f1-25) to DCPD was not adequately described by the Langmuir theory whereas the adsorption of β-CN A was.

The adsorption affinity of the acidic PRP's is determined entirely by the TX-peptide sequence. The present work suggests that the adsorption affinity for β-CN A is determined by the β-CN (f1-25) sequence (see section 3.5.2) because the affinity constants and surface areas per molecule are essentially the same (see Table 3.5). The adsorption affinities for β-CN A and β-CN (f1-25) to DCPD are lower than those of the acidic PRP's to hydroxyapatite and fluorapatite (approximately 80 fold lower; see section 3.2.2 and Table 3.5). A higher adsorption affinity for the caseins than for the acidic PRP's was expected as their phosphoseryl residues are clustered together, unlike the acidic PRP's whose phosphoseryl residues are separated by thirteen amino acids (of the primary sequence). Clustering of phosphoseryl residues has been shown to increase the affinity of casein adsorption to hydroxyapatite (Sleigh *et al.*, 1979). Therefore, the type of calcium phosphate mineral must have a major influence upon the adsorption affinity.

van Kemenade (1988) examined the influence of β-CN A on seeded growth of calcium phosphates (hydroxyapatite, octacalcium phosphate and DCPD). She proposed that the fractional reduction of relative growth rates could be interpreted in terms of the blocking of active growth sites through a Langmuirian adsorption model. From this model van Kemenade was able to calculate the affinity constants for β-CN A adsorption to hydroxyapatite, octacalcium phosphate and DCPD which

172

were 1×10^6, 7×10^6 and 4.76×10^7 lmol^{-1} respectively. van Kemenade's affinity constant for β-CN A adsorption to DCPD is approximately 100 fold greater than the affinities calculated during this study (see Table 3.5). However, van Kemenade's experiments examined the influence of β-CN A on seeded crystal growth and therefore the affinity constants are for adsorption to active growth sites only. Moreover, these experiments were performed under different conditions (at pH 5.5 and 37°C). The pH of the latter experiments may have a significant effect upon adsorption affinity, as inferred by the results presented here (see section 3.5.3 and Table 3.5). Adsorption affinities for active growth sites will probably be higher than those for other areas of the crystal as they will have a higher surface energy (Chernov, 1984).

The area occupied by a protein in the adsorbed state (A) is related to the packing of the molecules at the surface, therefore, the smaller the molecule the smaller the value of A. In the adsorbed state, the area occupied by a β-CN A molecule (Mr. 26,000) is quite similar to that of a β-CN (f1-25) molecule (Mr. 3,125; see Table 3.5) despite the large difference in size. This suggests that the N-terminal region is the fraction of the molecule that binds to the DCPD crystal. This is not the case for the acidic PRP's (see section 3.2.2 and Table 3.1) where the TX-peptide occupies a smaller area in the adsorbed state than the parent protein (PRP 1). Moreover, Moreno et al. (1982) noted that PRP 3 molecules (Mr. 11,320) occupied a larger area in the adsorbed state than PRP 1 molecules (Mr. 16,000); which is unexpected if A depends upon molecular size. This anomaly was explained (Moreno et al., 1982) as follows: PRP 3 has a higher charge density than PRP 1, therefore the adsorption of PRP 3 onto one site, on the hydroxyapatite crystal, induces polarisation in neigbouring sites to a greater extent than PRP 1. This results in a lower adsorption of PRP 3 (see section 3.2.2).

β-CN (f1-25) has a much greater charge density than the parent protein molecule β-CN A (each carries a net negative charge of 12). However, the negative charge of β-CN A resides largely in the N-terminal region of the molecule (see

173

section 3.3.2.) which is the region proposed to bind to DCPD crystals. Therefore, upon adsorption, the extent of polarisation of neighbouring sites will be similar for both β-CN A and β-CN (f1-25) and, therefore, the amount adsorbed will also be similar (and the area occupied).

The experiments comparing the two preparations of DCPD crystals suggested that β-CN A and β-CN (f1-25) adsorb to high affinity sites which may be concentrated on the edge faces of the DCPD crystals (see section 3.5.2). However, high affinity adsorption sites could also be located at defects in the crystal surface, caused either by surface geometry (*i.e.* steps or holes), blocked growth sites or non-stoichiometry (Chernov, 1984).

The possibility of selective adsorption to specific DCPD crystal faces raises the question: why does the phosphoprotein prefer certain specific crystal faces? This question may be answered by the molecular modelling of protein adsorption. Since the crystal structure of DCPD is known, a model can be constructed such that the geometry of the atoms of each crystal face can be determined. However, as there is no tertiary structural information available for the caseins, a three dimensional model of β-CN A, β-CN (f1-25) or related phosphopeptides must be constructed. This information may then be used to propose a detailed molecular model of phosphoprotein binding to the crystal surface.

In contrast to β-CN A and β-CN (f1-25), acidic PRP adsorption to hydroxyapatite and fluorapatite showed no such selective adsorption to any one crystal face. However, selective adsorption, of various proteins, to specific hydroxyapatite crystal faces has been inferred from chromatographic experiments using different crystal preparations (Kawasaki *et al.*, 1990). This apparently non-selective adsorption of the acidic PRP's may be explained as follows. Perfect hydroxyapatite crystals are columnar in habit with a hexagonal cross section, thus each of the crystal faces accounts for an approximately equal proportion of the total surface area. In consequence, a large change in crystal size will result in only a small change in the relative surface area of each crystal face. Thus selective

adsorption would not be observed in the adsorption experiments used by Moreno and co-workers because such experiments are not sensitve enough to slight changes in relative surface area. In addition, formation of well-formed hydroxyapatite crystals under laboratory conditions has been found to be impossible (Dr. C. Holt, personal communication), with non-stoichiometry being the major problem. To observe selective adsorption to a particular crystal face well-formed crystals are required with near perfect stoichiometry, thus selective adsorption to hydroxyapatite crystals may never be observed.

Moreno *et al.* (1982) showed that the acidic PRP's adsorb by an endothermic process, adsorption being "driven" by an entropy gain which arises from the breaking of the secondary structure of the adsorbent and the displacement of water from both protein and mineral. In the present study, the influence of temperature upon the adsorption of β-CN (f1-25) to DCPD indicated an athermal process. Such an adsorption process must also be "driven" by an entropy gain, possibly from the displacement of water molecules from both peptide and mineral as occurs with the acidic PRP's. The effect of urea upon the adsorption isotherm for β-CN A (a reduction of 50% in Γ_p; see Fig 3.21) may be the result of either or both of two phenomena. Either the hydrophobic interactions between adsorbed molecules, which stabilise the adsorbed layer, are disrupted by urea or the entropy gain, caused by a disruption in the hydration state of both DCPD and the protein molecules, is reduced. As the effect of temperature on β-CN (f1-25) indicates a process "driven" by an entropy gain, the effect of urea upon β-CN A adsorption may possibly be understood in terms of an effect upon water structure rather than on intermolecular interactions.

5.2 Future Work

Co-crystallisation of phosphoserine and calcium ions proved, unexpectedly, to be very troublesome. Future crystal trials should be directed at small,

phosphoserine-containing peptides, both in the presence and absence of calcium ions, where a more stable structure might be expected. For example, a larger peptide (*e.g.* five to eight amino acids with only one phosphoseryl residue), designed so that intermolecular interactions should form (*e.g.* hydrogen bonds), might interact with calcium ions in a stable enough way to form crystals. These crystal trials (as well as the adsorption experiments) would require a ready source of highly pure peptide (obtained by chemical synthesis).

The synthesis of the dipeptide Ser(P)-Ser(P) was successful. In addition, the use of the novel peptide phosphorylating agent Bis-(2,2,2-trichloroethyl)phosphoryl chloride (see section 2.5.2.3)alleviated some of the problems associated with the use of diphenylphosphoryl chloride (see section 2.5.2.1). However, purification of the newly-synthesised phosphopeptide was still laborious and, more importantly, the final yields were low. Recently (see section 2.5.3), new methods of phosphopeptide synthesis have been developed that employ more reactive phosphorylating agents (*e.g.* di-t-butyl N,N-diethylphosphoramidite (Perich and Johns, 1990b) or dibenzyl N,N-diethylphosphoramidite (Perich and Johns, 1990c)) and allow synthesis to be performed in the solid phase (Staerkear *et al.*, 1991). These innovations would improve both the yield of peptide and its purity. In addition, purification of phosphopeptides by high performance liquid chromatography has been developed (Murthy and Iqbal, 1991) which would allow efficient purification of the synthetic phosphopeptides.

Further experiments which may add more detail to the present model of adsorption of casein to DCPD crystals are outlined below. First, the adsorption affinities (k) for both β-CN A and β-CN (f1-25) binding to DCPD could be confirmed by constructing isotherms that cover a range of lower equilibrium, free concentrations ($< 1 \times 10^{-5}$ M). Accurate determination of the shape of the isotherm at lower concentrations would be a critical test of the Langmuir model, revealing any cooperative or anti-cooperative adsorption. If the adsorption affinities are found to be the same, the hypothesis that adsorption occurs mainly *via* the phosphoseryl

residues of the protein would be substantiated. Moreno *et al.* (1984) observed that the adsorption affinity of the acidic PRP's is conferred by the TX-peptide sequence (N-terminal 30 amino acid residues containing the two phosphoseryl residues). Similar results were obtained in this study of β-CN A and β-CN (f1-25) adsorption to DCPD crystals. If the affinities are found to be different then other amino acids must play an important role in adsorption. Such amino acids might include glutamyl and aspartyl residues. Direct evidence for the interaction of these residues with calcium ions does exist (Byler and Farrell, 1989).

Expansion of the β-CN A isotherm to encompass the same, higher concentration range as that employed in the experiments with β-CN (f1-25) would, if the isotherms have a similar pattern, also help to substantiate the hypothesis that adsorption occurs *via* the first 25 amino acids of β-CN A. Accurate determination of the adsorption affinity would also greatly facilitate the fitting of a curve to the results (see section 3.5.2) and hence the mathematical description of the adsorption process.

Results using DCPD preparations of different specific surface areas suggest that adsorption of both β-CN A and β-CN (f1-25) may occur to adsorption sites concentrated on the edge faces of the DCPD crystals (see section 3.5.2). Such preferential adsorption could be established by use of indirect immunofluorescence staining. This involves allowing β-CN (f1-25) to adsorb to the DCPD crystals. Then antibodies (*e.g.* raised in rats) specific to β-CN (f1-25) are introduced to the system and then fluorescently labelled, anti-rat antibodies (*e.g.* raised in goats) are added (the protein may be fixed during one of these stages with *e.g.* glutaraldehyde to facilitate future manipulations). Preferential adsorption of the aspartic acid-rich proteins (from the calcitic or the aragonitic layer of the bivalve *Mytilus californianus*) to specific faces of calcite crystals has been confirmed in this way (Addadi and Weiner, 1985).

From the effects of temperature and urea on the adsorption of β-CN (f1-25) and β-CN A (respectively) it is difficult to determine the relative contributions of

177

intermolecular, hydrophobic interactions and of the entropy gain to the adsorption process. β-CN (f1-25) has no hydrophobic tail and so the adsorbed layer cannot be stabilised by hydrophobic interactions (cf. β-CN A; see section 3.3.2). Performing adsorption experiments with β-CN (f1-25) in the presence of urea would therefore, help to determine which of these two phenomena is most important for adsorption. A large reduction in Γ_p would imply that urea is disrupting the water structure (causing a reduction in entropy gain) rather than affecting lateral (hydrophobic) interactions. This in turn would imply the hydrophobic interactions are not important for β-CN A adsorption. In addition, performing adsorption experiments with β-CN A in the presence of urea over a range of concentrations which encompass the concentration (4 M urea) at which β-CN A micelles dissociate would help to clarify this point. If a sudden decrease in Γ_p is observed at approximately 4 M urea, the importance of hydrophobic interactions in the adsorption process would be further supported. Finally, the effect of temperature on β-CN A adsorption should be determined to ensure that its adsorption is athermal.

The adsorption of proteins at the solid/liquid interface is influenced greatly by the pH of the system (see section 3.1.6) as Γ_p tends to be at a maximum at the isoelectric point of the protein. When adsorption experiments with β-CN A were performed at pH 6.5 and 7.0, which is in the range of the pKs of the phosphoseryl residues of β-CN A, Γ_p was found to be less at the lower pH value of 6.5 (see Fig 3.19). Performing adsorption experiments over a wider pH range might give information on the contribution of other amino acid residues to the adsorption process. If adsorption experiments were performed at pH 4.6; the pK of β-CN A, and Γ_p continued to decrease to a minimum this would imply that the phosphoseryl residues are predominantly involved in the adsorption of β-CN A to DCPD. However, if such a decrease was not observed, this would imply a contribution by other amino acids to β-CN A adsorption to DCPD. Similar experiments with β-CN (f1-25) would have to be performed to verify such suggestions.

Unfortunately, performing adsorption experiments above pH 7.0 is not possible if DCPD is to be used as adsorbent, as DCPD is unstable above pH 7. In addition, performing adsorption experiments below pH 6.0 is not possible. For these adsorption experiments it is necessary to maintain a saturated solution of DCPD to prevent crystal dissolution and growth; below pH 6.0 calcium phosphate is too soluble to maintain a saturated solution. Saturation might be maintained at very high phosphate concentrations (Dr. C. Holt, personnal communication), but the ionic strength would increase, and must increase if the free calcium ion concentration is to be held constant. Therefore, conditions below pH 6.0 would be so different from those at pH's between 6.0 and 7.0 that the results obtained would not be comparable and would therefore be uninformative.

Further insight into the role of phosphoseryl residues in the adsorption process might be gained by use of synthetic peptides. A series of phosphopeptides could be synthesised that are related to the amino acid sequence that encompasses the phosphoseryl residues of β-CN (f1-25) (*i.e.* between positions 12 and 21). The effect of substitution or deletion of an amino acid, or phosphate group, from the parent sequence could then be determined, which might give an insight into which residues actually participate in adsorption to the crystal surface. The β-CN (f1-25) peptide has been proteolytically cleaved with pepsin, to produce β-CN (f12-24) (results not shown). However, production of β-CN (f12-24) by this method is very inefficient. Chemical synthesis would probably be more economical and efficient.

The adsorption assay developed (described in section 3.4.6) to examine β-CN A adsorption to DCPD worked on the principle of depletion of protein from solution (see section 3.1.4). However, because of the low specific surface area of the DCPD crystals, significant depletion of the protein solution was only just achieved. As a result, accurate determination of the adsorption affinity of β-CN A and β-CN (f1-25) was not possible (see section 3.5.2). Theoretically, this problem can be circumvented, either by increasing the specific surface area of DCPD crystals or by using an alternative method of protein estimation in which the amount of

adsorbed protein is measured directly rather than by difference. Increasing the specific surface area of the DCPD crystals is possible by using rapid precipitation techniques, but there is some risk of forming an amorphous, precursor calcium phosphate phase rather than pure DCPD crystals (Dr. C. Holt, personal communication). Alternative colorometric methods would probably suffer from the same disadvantages as the BCA assay, as the amount of protein depleted from the solution is small. Several alternative methods of protein estimation (both colorometric and "non-colorometric") were evaluated (see section 3.5.1) but none were suitable for use with the adsorption assay. Therefore, the way forward with these investigations is to produce well-formed crystals of DCPD with a much larger specific surface area than those used during this investigation.

REFERENCES

Absolom, D.R., Zingg, W. & Neumann, A.W. (1987) A.C.S. Symp. Ser. **342** (Proteins Interfaces), 401-421

Adamson, A.W. (1983) Physical Chemistry of Surfaces, 3rd edn., 383-425, Wiley-Interscience, New York

Addadi, L. & Weiner, S. (1985) Proc. Natl. Acad. Sci. (U.S.A.) **82**, 4110-4114

Addadi, L., Berkovitch-Yellin, Z., Weissbuch, I., van Mil, J., Shimon, L.J.W., Lahav, M. & Leisserowitz, L. (1985) Angew. Chem. Int. Ed. Engl. **24**, 466-485

Albertson, N.F. & McKay, F.C. (1953) J. Am. Chem. Soc. **75**, 5323-5326

Alewood, P.F., Johns, R.B. & Perich, J.W. (1981) Pep. Synth. Struc. Funct. Proc. Am. Pep. Symposium 7th., 65-67

Alewood, P.F., Perich. J.W. & Johns, R.B. (1982) Synth. Commun. **12**, 821-828

Alewood, P.F., Perich, J.W. & Johns, R.B. (1984) Aust. J. Chem. **37**, 429-433

Anderson, G.W. & Callahan, F.M. (1960) J. Am. Chem. Soc. **82**, 3359-3363

Anderson, G.W. & McGregor, A.C. (1957) J. Am. Chem. Soc. **79**, 6180-6183

Anderson, G.W., Zimmerman, J.E. & Callahan, F.M. (1967) J. Am. Chem. Soc. **89**, 5012-5017

Andrade, J.D. & Hlady, V. (1986) Adv. Polymer Sci. **79**, 1-63

Andrews, A.L., Atkinson, D., Evans, M.T.A., Finer, E.G., Green, J.P., Phillips, M.C. & Robertson, R.N. (1979) Biopolymers **18**, 1105-1121

Aoki, T., Kawahara, A., Kako, Y. & Imamuga, T. (1987) Agric. Biol. Chem. **51**, 817-821

Aschaffenburg, R. (1963) J. Dairy Res. **30**, 259-261

Atherton, E. & Sheppard, R.C. (1989) Solid Phase Synthesis, A Practical Approach, 1st edn., IRL Press, Oxford

Atherton, F.R., Openshaw, H.T. & Todd, A.R. (1945) J. Chem. Soc. 382-385

Atherton, F.R., Howard, H.T. & Todd, A.R. (1948) J. Chem. Soc. 1106-1111

Azen, E.A. (1978) Biochem. Genet. **16**, 79-99

Baer, E. & Maurukas, J. (1955) J. Biol. Chem. **21**, 25-38

Bannwarth, W. & Trzeciak, A. (1987) Helv. Chim. Acta **70**, 175-186

Baumy, J.J., Guenot, P., Sinbandhit, S. & Brule, G. (1989) J. Dairy Res. **56**, 403-409

Barrass, B.C. & Elmore, D.T. (1957) J. Chem. Soc. **111**, 3134-3139

Beissinger, R.L. & Leonard, E.F. (1982) J. Colloid Interface Sci. **85**, 521-533

Ben-Ishai, D. (1954) J. Org. Chem. **19**, 62-66

Ben-Ishai, D. & Berger, A. (1952) J. Org. Chem. **17**, 1564-1570

Bennick, A. (1975) Biochem. J. **145**, 557-567

Bennick, A., Cannon, M. & Madapallimattam, G. (1979) Biochem. J. **183**, 115-126

Bennick, A., McLaughlin, A.C., Grey, A.A. & Madapallimattam, G. (1981) J. Biol. Chem. **256**, 4741-4746

Bergmann, M. & Zervas, L. (1932) Ber. Deut. Chem. Ges. **65**, 1192-1201

Bergmann, M., Zervas, L. & Ross, W.F. (1935) J. Biol. Chem. **111**, 245-260

Billington, D.C. (1989) Chem. Soc. Rev. **18**, 83-122

Bingham, E.W. (1987) J. Dairy Sci. **70**, 2233-2240

Birdi, K.S. (1973) J. Colloid Interface Sci. **43**, 545-547

Blobel, G. (1980) Proc. Natl. Acad. Sci. (U.S.A.) **77**, 1496-1500

Bodanszky, M. (1984) Principles of Peptide Synthesis, vol 16, Springer-Verlag, Berlin, Heidelberg, New York and Tokyo

Bodanszky, M. & duVigneaud, V. (1959) J. Am. Chem. Soc. **81**, 5688-5695

Bodanszky, M. & Birkhimer, C.A. (1960) Chimica **14**, 368-371

Bodanszky, M & Ondetti, M.A. (1966) Peptide Synthesis, vol 1, Interscience Publications

Bohak, Z. & Katchalski, E. (1963) Biochemistry **2**, 228-237

Bohn, L., Futterer, D. & Kaminski, E. (1978) J. Phycol. **14**, 486-493

de Bont, H.B.A., Liskamp, R.M.J., O'Brian, C.A., Erkelens, C., Veeneman, G.H. & van Boom, J.H. (1987) Int. J. Peptide Protein Res. **33**, 115-123

de Bont, H.B.A., Veeneman, G.H., van Boom, J.H. & Liskamp, R.M.J. (1988) Recl. Trav. Chim. Pays-Bas. **106**, 641-642

Boratynski, J. (1985) Analyt. Biochem. **148**, 213-219

Borbas, J.E., Wheeler, A.P. & Sikes, C.S. (1991) J. Exp. Zool. **258**, 1-13

183

Borowitzka, M.A., Larkum, A.W.D. & Nockolds, C.E. (1974) Phycologia **13**,
    195-203

Brash, J.L. & Lyman, D.J. (1971) in Chemistry of Biosurfaces (Hair, M.L., ed.)
    vol 1, pp. 177-231, Marcel Dekker Inc., New York

Braunlin, W.H., Vogel, H.J., Drakenberg, T. & Bennick, A. (1986) Biochemistry **25**,
    584-589

Brenner, M. & Huber, W. (1953) Helv. Chim. Acta **36**, 1109-1115

Brunauer, S., Emmett, P.H. & Teller, E. (1938) J. Am. Chem. Soc. **60**, 309-319

Buchheim, W. & Welsch, U. (1973) Neth. Milk Dairy J. **27**, 163-180

Butler, W.T., Finch, J.E. & Desteno, C.V. (1972) Biochim. Biophys. Acta **257**,
    167-171

Byler, D.M. & Farrel, H.M. (1989) J. Dairy Sci. **72**, 1719-1723

Carpino, L.A. (1957) J. Am. Chem. Soc. **79**, 98-101

Carrol, R.J., Thompson, M.P. & Nutting, G.C. (1968) J. Dairy Sci. **51**, 1903-1908

Chaplin, L.C., Clark, D.C. & Smith, L.J. (1988) Biochim. Biophys. Acta **956**,
    162-172

Chattoraj, D.K. & Bull, H.B. (1959) J. Am. Chem. Soc. **81**, 5128-5133

Chernov, A.A. (1984) Modern Crystallography III. Crystal Growth, Springer-Verlag,
    Berlin Heidelberg New York and Tokyo

Cipera, J.D. & Nicholls, R.V.V. (1955) Chem. Ind. 16-17

Cohen-Solal, L., Lian, B., Kossiva, D. & Glimcher, M.J. (1978) F.E.B.S. Lett. **89**,
    107-110

Cooke, A.M. & Potter, B.V.L. (1987) Tetrahedron Lett. **28**, 2305-2308

Cooke, A.M., Gigg, R. & Potter, B.V.L. (1987) Biochem. Soc. Trans. **15**, 904-906

Cooke, A.M., Noble, N.J., Gigg, R., Willcocks, A.L., Strudish, J., Nahorski, S.R. &
    Potter, B.V.L. (1988) Biochem. Soc. Trans. **16**, 992-993

Cooke, A.M., Noble, N.J., Payne, S., Gigg, R. & Potter, B.V.L. (1989) J. Chem.
    Soc. Chem. Commun. **5**, 269-271

Creamer, L.K. & Berry, G.P. (1975) J. Dairy Res. **42**, 169-183

Creamer, L.K., Richardson, T. & Parry, D.A.D. (1981) Arch. Biochem. Biophys. **221**, 689-696

Cumper, C.W.N. & Alexander, A.E. (1951) Rev. Pure Appl. Chem. **1**, 121-151

Curry, N.A. & Jones, D.W. (1971) J. Chem. Soc. (A), 3725-3729

Curtius, T. (1904) J. Prakt. Chem. **70**, 158-194

Dawson, I.M., Lawerence, J.A., Wilson, N.H., Olverman, H.J. & Kelly, J.S. (1991) Br. J. Pharmac. **102**, 242

DeTar, D.F. & Silverstein, R. (1966) J. Am. Chem. Soc. **88**, 1013-1019

Dewan, R.K., Chudgar, A., Mead, R., Bloomfield, V.A. & Morr, C.V. (1974) Biochim. Biophys. Acta **342**, 313-321

Dillman, W.J. & Millar, I.F. (1973) J. Colloid Interface Sci. **44**, 221-241

Donella, A., Pinna, L.A. & Moret, V. (1976) Chem. Biol. Interactions **15**, 165-171

Dottavio-Martin, D. & Ravel, J.M. (1978) Analyt. Biochem. **87**, 562-565

van Dulm, P., Norde, W. & Lyklema, J. (1981) J. Colloid Interface Sci. **82**, 77-82

Eckstein, F. & Scheit, K.H. (1967) Angew. Chem. Int. Ed. Engl. **6**, 362

Elliot, D.F. & Russell, D.W. (1957) Biochem. J. **66**, 49p

Evans, M.T.A., Irons, L. & Jones, M. (1971a) Biochim. Biophys. Acta **229**, 411-422

Evans, M.T.A., Irons, L. & Petty, J.H.P. (1971b) Biochim. Biophys. Acta **243**, 259-272

Fair, B.D. & Jamieson, A.M. (1980) J. Colloid Interface Sci. **72**, 525-534

Farrell, H.M. (1973) J. Dairy Sci. **56**, 1195-1206

Farrell, H.M. & Thompson, M.P. (1988) in Calcium Binding Proteins (Thompson, M.P., ed.), vol 2, pp. 117-137, C.R.C. Press

Folsch, G. (1959) Acta Chem. Scand. **13**, 1407-1421

Folsch, G. (1966) Acta Chem. Scand. **20**, 459-473

Folsch, G. (1967) Sven. Kem. Tidskr. **79**, 38-65

Folsch, G., Strid, L. & Mellànder, O. (1965) Acta Chem. Scand. **19**, 1566-1574

Franke, A., Scheit, K.-H. & Eckstein, F. (1968) Chem. Ber. **101**, 2998-3001

Giaever, I. & Keese, C.R. (1987) A.C.S. Symp. Ser. **342** (Proteins Interfaces), 582-602

Gibbs, D.E. & Larsen, C. (1984) Synthesis, 410-413

Gibbons, R.J., Moreno, E.C. & Spinell, D.M. (1976) Infect. Immun. **14**, 1109-1112

Giles, C.H. & MacEwan, T.H. (1957) Proc. 2nd. Int. Congress Surface Activity 3, CD339-CD343

Glennon, R.A., Naiman, N.A., Lyon, R.A. & Titeler, M. (1988a) J. Med. Chem. **31**, 1968-1971

Glennon, R.A., Naiman, N.A., Pierson, M.E., Titeler, M., Lyon, R.A. & Weisberg, E. (1988b) **154**, 339-341

Glimcher, M.J. (1979) J. Dent. Res. **58(Suppl. B)**, 790-806

Glimcher, M.J. (1984) Phil. Trans. Roy. Soc. Lond. **B 304**, 479-508

Gould, R.O. & Taylor, P. (1983) CALC. Interactive program for molecular geometry. University of Edinburgh, Scotland.

Graham, E.R.B., Malcolm, G.N. & McKenzie, H.A. (1984) Int. J. Biol. Macromol. **6**, 155-161

Grant, W.H., Smith, L.E. & Stromberg, R.R. (1977) J. Biomed. Mater. Symp. **8**, 33-38

Gresh, N. (1980) Biochem. Biophys. Acta **597**, 347-357

Gross, E. & Meienhoffer, J. (1979a) The Peptides: Analysis, Synthesis, Biology, vol 1, Academic Press Inc., London

Gross, E. & Meienhoffer, J. (1979b) The Peptides: Analysis, Synthesis, Biology, vol 2, Academic Press Inc., London

Guttmann, S. & Boissonnas, R.A. (1958) Helv. Chim. Acta **41**, 1852-1867

Hamblin, M.R., Potter, B.V.L. & Gigg, R. (1987a) Biochem. Soc. Trans. **15**, 415-416

Hamblin, M.R., Potter, B.V.L. & Gigg, R. (1987b) J. Chem. Soc. Chem. Commun. **8**, 626-627

Hamblin, M.R., Flora, J.S. & Potter, B.V.L. (1987c) Biochem. J. **246**, 771-774

Hauschka, P.V., Lian, J.D. & Gallop, P.M. (1975) Proc. Natl. Acad. Sci. (U.S.A.) **72**, 3925-3929

Haussler, R. (1960) Chimia **14**, 369-370

Hay, D.I. & Moreno, E.C. (1979) J. Dent. Res. **58(Suppl. B)**, 930-940

Hay, D.I. & Schlesinger, D.H. (1977) Calcium-Binding Proteins Calcium Function. Proc. Int. Sym. 401-408

Hay, D.I., Moreno, E.C. & Schlesinger, D.H. (1979) Inorg. Perspect. Biol. Med. **2**, 271-285

Hay, D.I., Carlson, E.R., Schluckebier, S.K., Moreno, E.C. & Schlesinger, D.H. (1987) Calcif. Tissue Int. **40**, 126-132

Hay, D.I., Bennick, A., Schlesinger, D.H., Minaguchi, K., Madapallimattam, G. & Schluckebier, S.K. (1988) Biochem. J. **255**, 15-21

Hill, A.V. (1910) Proc. Physiol. Soc. **40**, iv-vii

Hoeve, C.A.J. (1971) J. Polymer. Sci. **34**, 1-10

Hofmann, K., Magee, M.Z. & Lindenmann, A. (1950) J. Am. Chem. Soc. **72**, 2814-2815

Hofmann, K., Thompson, T.A., Yajima, H., Schwartz, E.T. & Inouye, H. (1960) J. Am. Chem. Soc. **82**, 3715-3720

Holt, C. (1992) in Advances in Protein Chemistry (Anfinsen, C.R., Edsall, J.D. & Richards, F., eds.) Academic press, in the press

Holt, C. & van Kemenade, M.J.J.M. (1989) in Calcified Tissue (Hukins, D.W.L., ed.), vol 1, pp.175-213, Macmillan Press

Holt, C. & Sawyer, L. (1988) Protein Enginering **2**, 251-259

Holt, C. & Hukins, D.W.L. (1991) Int. Dairy J. **1**, 151-165

Holt, C., Kimber, A.M., Brooker, B.E. & Prentice, J.H. (1978) J. Colloid Interface Sci. **65**, 555-565

Holt, C., Dalgleish, D.G. & Jenness, R. (1981) Analyt. Biochem. **113**, 154-163

Holt, C., Hasnain, S.S. & Hukins, D.W.L. (1982) Biochim. Biophys. Acta **719**, 299-303

Holt, C., Davies, T. & Law, A.J.R. (1986) J. Dairy Res. **53**, 557-572

Horbett, T.A. (1987) A.C.S. Symp. Ser. **343** (Proteins Interfaces), 239-260

Horbett, T.A. & Brash, J.L. (1987) A.C.S. Symp. Ser. **343** (Proteins Interfaces), 1-33

Hummel, J.P. & Anderson, B.S. (1965) Arch. Biochem. Biophys. **112**, 443-447

Humphrey, R.S. & Jolley, K.W. (1982) Biochim. Biophys. Acta **708**, 294-299

Itoh, M. (1973) Bull. Chem. Soc. Japan **46**, 2219-2221

James, L.K. & Augenstein, L.G. (1966) Adv. Enzymol. **28**, 1-41

Jenson, A.J. & Rathlev, J. (1953) Inorg. Synth. **4**, 20-21

Ji, G.-J., Xue, C.-B., Zeng, J.-N., Li, L.-P., Chai, W.-G. & Zhao, Y.-F. (1988) Synthesis, 444-448

Johnson, T.B. & Coward, J.K. (1987) J. Org. Chem. **52**, 1771-1779

Juriaanse, A.C. (1979) in Proceedings Dental Plaque and Surface Interactions in the Oral Cavity (Leach, S.A., ed.) pp 313-329, Information Retrieval, London

Kalab, M., Phipps-Todd, B.E. & Allan-Wojtas, P. (1982) Milckwissenschaft **37**, 513-518

Kamyshinyi, A.L. (1981) Russ. J. Phys. Chem. **55**, 319-330

Kawasaki, T., Niikura, M. & Kobayashi, Y. (1990) J. Chromatogr. **515**, 125-148

Kegeles, G. (1979) J. Phys. Chem. **83**, 1728-1732

van Kemenade, M.J.J.M. (1988) Thesis, University of Utrecht, The Netherlands

van Kemenade, M.J.J.M. & de Bruyn, P.L. (1987) J. Colloid Interface Sci. **118**, 564-585

van Kemenade, M.J.J.M. & de Bruyn, P.L. (1989) J. Colloid Interface Sci. **129**, 1-14

Khorana, M.G. (1955) Chem. Ind. 1087-1088

Kimber, A., Brooker, B.E. & Morant, S.V. (1978) Proc. 20th. Intern. Dairy Congress (Paris), 233-234

Kitas, E.A., Perich, J.W., Johns, R.B. & Tregear, G.W. (1988) Tetrahedron Lett. **29**, 3591-3592

Knoop, A.-M., Knoop, E. & Wiechen, A. (1979) J. Dairy Res. **46**, 347-350

Kobamoto, N., Lofroth, G., Camp, P., van Amburg, G. & Augenstein, L. (1966) Biochem. Biophys. Res. Commun. **24**, 622-627

Kochwa, S., Brownell, M., Rosenfield, R.E. & Wasserman, L.R. (1967) J. Immunol. **99**, 981-986

Koehn, P.V. & Kind, C. (1965) Arch. Biochem. Biophys. **111**, 614-618

Konig, W. & Geiger, R. (1970) Chem. Ber. **103**, 788-798

Kousvelari, E.E., Baratz, R.S., Burke, B. & Oppenheim, F.G. (1980) J. Dent. Res. **59**, 1430-1438

Koutsoukos, P.G., Mumme-Young, C.A., Norde, W. & Lyklema, J. (1982) Colloids and Surfaces **5**, 93-104

Koutsoukos, P.G., Norde, W. & Lyklema, J. (1983) J. Colloid Interface Sci. **95**, 385-397

Kozin, F. & McCarty, D.J. (1977) J. Lab. Clin. Med. **89**, 1314-1325

Krystal, G. (1987) Analyt. Biochem. **167**, 86-96

Krystal, G., MacDonald, C., Munt, B. & Ashwell, S. (1985) Analyt. Biochem. **148**, 451-460

Kuhlbrandt, W. & Wang, D.N. (1991) Nature **350**, 130-134

Kumosinki, T.F., Brown, E.M. & Farrell, H.M. (1991a) J. Dairy Sci. **74**, 2879-2887

Kumosinki, T.F., Brown, E.M. & Farrell, H.M. (1991b) J. Dairy Sci. **74**, 2889-2895

Kuromizu, K. & Meienhofer, J. (1974) J. Am. Chem. Soc. **96**, 4978-4981

Kuyl-Yeheskiely, E., Tromp, C.M., van der Marel, G.A. & van Boom, J.H. (1987) Tetrahedron Lett. **28**, 4461-4464

Kuyl-Yeheskiely, E., Tromp, C.M., Geluk, A., van der Marel, G.A. & van Boom, J.H. (1988) Recl. Trav. Chim. Pays-Bas **107**, 567-569

Lacombe, J.M., Andria Manampisoa, F. & Pavia, A.A. (1990) Int. J. Peptide Protein Res. **36**, 275-280

Langmuir, I. (1916) J. Am. Chem. Soc. **38**, 2221-2295

Langmuir, I. (1918) J. Am. Chem. Soc. **40**, 1361-1403

Lee, S.L., Veis, A. & Gloner, T. (1977) Biochemistry **16**, 2971-2979

Legeros, R.Z. & Legeros, J.P. (1972) J. Cryst. Growth **13**, 476-480

Legeros, R.Z., Lee, D., Quirolico, G., Shirra, W.P. & Reich, L. (1983) Scan.
   Electron Microsc. 407-418

Levene, P.A. & Schormuller, A. (1934) J. Biol. Chem. **105**, 547-562

Liberek, B. (1963) Tetrahedron Lett. **14**, 925-928

Lindau, G. & Rhodius, R. (1935) Z. Physik. Chem. **172**, 321-347

Longenecker, J.B. & Snell, E.E. (1957) J. Biol. Chem. **225**, 409-418

Lowenstam, H.A. (1981) Science **211**, 1126-1131

Lundstrom, I. (1983) Physica Scripta **T4(51)**, 5-13

Lundstrom, I. (1984) Oral Interfacial React. Bone Soft Tissue Saliva Proc.
   Workshop, 9-23

Lundstrom, I. & Elwing, H. (1990) J. Colloid Interface Sci. **136**, 68-84

Lutz, W.B., Ressler, C., Nettleton, D.E. & duVigneaud, V. (1959) J. Am. Chem.
   Soc. **81**, 167-173

Lyklema, J. (1984) Colloids and Surfaces **10**, 33-42

Lyklema, J. (1985) in Surface and Interfacial Aspects of Biomedical Polymers
   (Andrade, J.D., ed.), vol 1, pp. 293-336, Plenum Press, New York

Lyman, D.J., Brash, J.L., Chaikin, S.W., Klein, K.G. & Carini, M. (1968) Trans.
   Am. Soc. Artif. Intern. Organs **14**, 250-255

MacLaren, J.A. (1958) Aust. J. Chem. **11**, 360-365

MacLaren, J.A., Savige, W.E. & Swan, J.M. (1958) Aust. J. Chem. **11**, 345-359

MacRitchie, F. (1972) J. Colloid Interface Sci. **38**, 484-488

MacRitchie, F. (1978) Adv. Protein Chem. **32**, 283-326

MacRitchie, F. & Owens, N.F. (1969) J. Colloid Interface Sci. **29**, 66-71

Mann, S., Webb, J. & Williams, R.J.P. (1989) in Biomineralsiation, Chemical and
   Biochemical Perspectives (Mann, S., Webb, J. & Williams, R.J.P., eds.),
   pp. v-viii, VCH Publishers, New York

Manson, W. & Annan, W.D. (1971) Arch. Biochem. Biophys. **145**, 16-26

Marshall, R.W. & Nancollas, G.H. (1969) J. Phys. Chem. **73**, 3838-3844

Matsui, T., Tanaka, S., Akaike, T., Sakurai, Y., Nitadori, Y., Kataoka, K.
& Tsuruta, T. (1978) J. Bioeng. **2**, 539-541

Maubois, J.L. & Leonil, J. (1989) Lait **69**, 245-269

McKay, F.C. & Albertson, N.F. (1957) J. Am. Chem. Soc. **79**, 4686-4690

McLaren, A.D. (1954) J. Phys. Chem. **58**, 129-137

Meggio, F., Perich, J.W., Reynolds, E.C. & Pinna, L.A. (1991) F.E.B.S. Lett. **283**,
303-306

Mercier, J.-C. (1981) Biochimie **63**, 1-17

Mercier, J.-C., Grosclaude, F. & Ribadeau-Dumas, B. (1971) Eur. J. Biochem. **23**,
41-51

Mercier, J.-C. & Gaye, P. (1983) in Biochemistry of Lactation (Mepham, T.B., ed.)
vol 1, pp. 177-227, Elsevier, Amsterdam

Merrifield, R.B. (1963) J. Am. Chem. Soc. **85**, 2149-2154

Merrifield, R.B. (1969) Adv. Enzymol. **32**, 221-296

Miller, H.K. & Waelsch, H. (1952) J. Am. Chem. Soc. **74**, 1092-1093

Mitra, S.P. & Chattoraj, D.K. (1978) Indian J. Biochem. Biophys. **55**, 147-152

Mizutani, T. (1981) J. Colloid Interface Sci. **82**, 162-166

Moore, S. & Stein, W.H. (1954a) J. Biol. Chem. **211**, 893-905

Moore, S. & Stein, W.H. (1954b) J. Biol. Chem. **211**, 907-913

Moreno, E.C., Brown, W.E. & Osborn, G. (1960a) Soil Sci. Soc. America Proc. **24**,
94-98

Moreno, E.C., Brown, W.E. & Osborn, G. (1960b) Soil Sci. Soc. America Proc. **24**,
99-102

Moreno, E.C., Kresak, M. & Hay, D.I. (1978) Arch. Oral Biol. **23**, 525-533

Moreno, E.C., Varughese, K. & Hay, D.I. (1979) Calcif. Tissue Int. **28**, 7-16

Moreno, E.C., Kresak, M. & Hay, D.I. (1982) J. Biol. Chem. **257**, 2981-2989

Moreno, E.C., Kresak, M. & Hay, D.I. (1984) Calc. Tissue Int. **36**, 48-59

Morrissey, B.W. & Fenstermaker, C.A. (1976) Trans. Am. Soc. Artif. Intern. Organs
22, 278-284

Morrissey, B.W. & Stromberg, R.R. (1974) J. Colloid Interface Sci. **46**, 152-164

Morrissey, B.W. & Han, C.C. (1978) J. Colloid Interface Sci. **65**, 423-431

Motherwell, W.D.S. (1972) PLUTO. Program for plotting molecular and crystal structures. University of Cambridge, UK

Mura-Galelli, M.J., Voegel, J.C., Behr, S., Bres, E.F. & Schaaf, P. (1991) Proc. Natl. Acad. Sci. (U.S.A.) **88**, 5558-5561

Murthy, L.R. & Iqbal, K. (1991) Analyt. Biochem. **193**, 299-305

Muszynska, G., Andersson, L. & Porath, J. (1986) J. Biochem. **25**, 6850-6853

Neuhaus, F.C. & Korkes, S. (1958) Biochem. Prep. **6**, 75-78

Niemann, E. & Hoffmann, W. (1964) Z. Analyt. Chem. **200**, 443-449

Norde, W. (1980) in Polymer Science and Technology (Lieng-Huang, L., ed.) vol 12b, pp. 801-825, Plenum Press, New York and London

Norde, W. (1986) Adv. Colloid Interface Sci. **25**, 267-340

Norde, W. & Lyklema, J. (1978) J. Colloid Interface Sci. **66**, 295-302

Norde, W., MacRitchie, F., Nowicka, G. & Lyklema, J. (1986) J. Colloid Interface Sci. **112**, 447-456

Nozaki, Y. & Tanford, C. (1963) J. Biol. Chem. **238**, 4074-4081

Nyilas, E., Chiu, T.-H. & Herzlinger, G.A. (1974) Trans. Am. Soc. Artif. Intern. Organs **20**, 480-490

Okawa, K., Nakajima, K., Tanaka, T. & Kawana, Y. (1975) Chem. Lett. 591-59

Okawa, K., Yuki, M. & Tanaka, T. (1979) Chem. Lett. 1085-1086

Ono, T., Kaminogawa, S., Odagiri, S. & Yamauchi, K. (1976) Agric. Biol. Chem. **40**, 1725-1729

Oppenheim, F.G., Offner, G.D. & Troxler, R.F. (1982) J. Biol. Chem. **257**, 9271-9282

Osterberg, R. (1957) Nature **179**, 476-477

Owen, G.R., Verheyden, J.P.M. & Moffatt, J.G. (1976) J. Org. Chem. **41**, 3010-3017

Palade, G. (1975) Science **189**, 347-358

Paquet, A. & Johns, M. (1990) Int. J. Peptide Protein Res. **36**, 97-103

Payens, T.A.J. & Vreeman, H.J. (1982) in Solution Behavoir of Surfactants (Mittel, K.L. & Fendler, E.J., eds.) vol 1, pp 543-571, Plenum Publishing Corporation

Perich, J.W. & Johns, R.B. (1988a) J. Org. Chem. **53**, 4103-4105

Perich, J.W. & Johns, R.B. (1988b) Synthesis, 142-144

Perich, J.W. & Johns, R.B. (1988c) Tetrahedron Lett. **29**, 2369-2372

Perich, J.W. & Johns, R.B. (1990a) Aust. J. Chem. **43**, 1609-1621

Perich, J.W. & Johns, R.B. (1990b) Aust. J. Chem. **43**, 1623-1632

Perich, J.W. & Johns, R.B. (1990c) Aust. J. Chem. **43**, 1633-1642

Perich, J.W., Alewood, P.F. & Johns, R.B. (1986a) Tetrahedron Lett. **27**, 1373-12376

Perich, J.W., Alewood, P.F. & Johns, R.B. (1986b) Synthesis, 572-573

Perich, J.W., Alewood, P.F. & Johns, R.B. (1987a) Aust. J. Chem. **40**, 257-271

Perich, J.W., Alewood, P.F. & Johns, R.B. (1987b) Tetrahedron Lett. **28**, 101-102

Peroutka, S.J. (1988) Ann. Rev. Neurosci. **11**, 45-60

Plimmer, R.H.A. (1941) Biochem. J. **35**, 461-469

Polacheck, I. & Cabib, E. (1981) Analyt. Biochem. **117**, 311-314

Posternak, T. & Grafl, S. (1945) Helv. Chim. Acta **28**, 1258-1270

Propas, D., Zahradnik, R.T. & Moreno, E.C. (1977) J. Dent. Res. **56(Suppl. B)**, Abs. 97

Redinbaugh, M.G. & Turley, R.B. (1986) Analyt. Biochem. **153**, 267-271

Riley, G., Turnbull, J.H. & Wilson, W. (1957) J. Chem. Soc. 1373-1379

Roberts, C.W. (1954) J. Am. Chem. Soc. **76**, 6203-6204

Roeske, R.W. (1959) Chem. Ind. 1121-1122

Romberg, R.W., Werness, P.G., Riggs, B.L. & Mann, K.G. (1986) Biochemistry **25**, 1176-1180

Rose, D. & Colvin, J.R. (1966) J. Dairy Sci. **49**, 351-355

Saitoh, E., Isemura, S. & Sanada, K. (1985) Arch. Oral Biol. **30**, 641-643

van der Scheer, A.T. & Smolders, C.A. (1978) J. Colloid Interface Sci. **63**, 7-15

Schallenberg, E.E. & Calvin, M. (1955) J. Am. Chem. Soc. **77**, 2779-2783

Schlesinger, D.H. & Hay, D.I. (1977) J. Biol. Chem. **252**, 1689-1695

Schlesinger, D.H. & Hay, D.I. (1986) Int. J. Peptide Protein Res. **27**, 373-379

Schlesinger, D.H., Buku, A., Wyssbrod, H.R. & Hay, D.I. (1987) Int. J. Peptide Protein Res. **30**, 257-262

Schmidt, D.G. (1980) Neth. Milk Dairy J. **34**, 42-64

Schmidt, D.G. (1982) in Developments in Dairy Chemistry (Fox, P.F., ed.) vol. 1, pp. 61-86, Applied Science Publishers Ltd., UK

Schmidt, D.G. (1987) Neth. Milk Dairy J. **41**, 105-120

Schmidt, D.G. & Poll, J.K. (1989) Neth. Milk Dairy J. **43**, 53-62

Schmidt, D.G., Walstra, P. & Buchheim, W. (1973) Neth. Milk Dairy J. **27**, 128-142

Schmidt, D.G., Both, P., Visser, S., Slangen, K.J. & van Rooijen, P.J. (1987) Neth. Milk Dairy J. **41**, 121-136

Schnabel, E. (1967) Liebigs Ann. Chem. **702**, 188-196

Schroder, E. & Lubke, K. (1965) The Peptides, vol 1, Academic Press, London

Schwyzer, R. & Rittel, W. (1961) Helv. Chim. Acta **44**, 156-169

Schwyzer, R., Sieber, P. & Kappeler, H. (1959) Helv. Chim. Acta **42**, 2622-2624

Sevastianov, V.I., Belomestnaia, Z.M. & Zimin, N.K. (1983) Artif. Organs **7**, 126-133

Sevastianov, V.I., Tseytlina, E.A., Volkov, A.V. & Shumakov, V.I. (1984) Trans. Am. Soc. Artif. Intern. Organs **30**, 137-142

Shastri, R. & Roe, R.-J. (1970) Org. Coat Plast. Chem. **40**, 820-825

Sheehan, J.C. & Hess, G.P. (1955) J. Am. Chem. Soc. **77**, 1067-1068

Sheehan, J.C., Goodman, M. & Hess, G.P. (1956) J. Am. Chem. Soc. **78**, 1367-1368

Sheldrick, G. (1976) SHELXS76. Program for crystal structure solution. University of Gottingen, Federal Republic of Germany.

Sheldrick, G. (1986) SHELXS86. Program for crystal structure solution. University of Gottingen, Federal Republic of Germany.

Shrager, R.I., Cohen, J.S., Heller, S.R., Sachs, D.H. & Schechter, A.N. (1972) Biochemistry **11**, 541-547

Sifferd, R.H. & duVigneaud, V. (1935) J. Biol. Chem. **108**, 753-761

Silberberg, A. (1962) J. Phys. Chem. **66**, 1884-1907

Silberberg, A. (1971) Pure Appl. Chem. **26**, 583-591

Silyn-Roberts, M. & Sharp, R.M. (1986) Proc. Roy. Soc. Lond. **B 227**, 303-324

Sinha, N.D., Biernat, J., McManus, J. & Koster, H. (1984) Nuc. Acid Res. **12**, 4539-4557

Slattery, C.W. & Evard, R. (1973) Biochim. Biophys. Acta **317**, 529-538

Sleigh, R.W., Sculley, T.B. & MacKinlay, A.G. (1979) J. Dairy Res. **46**, 337-348

Smith, P.K., Krohn, R.I., Hermanson, G.T., Mallia, K., Gartner, F.H., Provenzano, M.D., Fujimoto, E.K., Goeke, N.M., Olson, B.J. & Klenk, D.C. (1985) Analyt. Biochem. **150**, 76-85

Soderquist, M.E. & Walton, A.G. (1980) J. Colloid Interface Sci. **72**, 386-397

Sogawa, K. & Takahashi, K. (1978) J. Biochem. **83**, 1783-1787

Spector, A.R. & Glimcher, M.J. (1973) Biochem. Biophys. Acta **303**, 360-362

Staerkaer, G., Jakobsen, M.H., Olsen, C.E. & Holm, A. (1991) Tetrahedron Lett. **32**, 5389-5392

Still, W.C., Kahn, M. & Mitra, A. (1978) J. Org. Chem. **43**, 2923-2925

Stothart, P.H. (1989) J. Mol. Biol. **208**, 635-638

Stothart, P.H. & Cebula, D.J. (1982) J. Mol. Biol. **160**, 391-395

Strain, H.H. (1949) Analyt. Chem. **21**, 75-81

Strid, L. (1959) Acta Chem. Scand. **13**, 1787-1790

Suzawa, T. & Murakami, T. (1980) J. Colloid Interface Sci. **78**, 266-268

Swaisgood, H.E. (1982) in Developments in Dairy Chemistry (Fox, P.F., ed.) vol 1, pp1-59, Applied Science Publications, UK

Takeuchi, M., Tsuda, E., Yoshikawa, M., Sasaki, R. & Chiba, H. (1984) Agric. Biol. Chem. **48**, 2789-2797

Tanford, C. (1966) Physical Chemistry of Macromolecules, J. Wiley & Sons Inc., UK.

Termine, J.D., Torchia, D.A. & Conn, K.M. (1979) J. Dent. Res. **58(Suppl. B),** 773-778

Theodoropoulos, D., Galopoulos, J. & Souchleris, I. (1960) Nature **185,** 606-607

Thorsett, E.D., Harris, E.E., Peterson, E.R., Greenlee, W.J., Patchett, A.A., Ulm, E.M. & Vassil, T.C. (1982) Proc. Natl. Acad. Sci. (U.S.A.) **79,** 2176-21801

Thrun, A., Burchard, W. & Niki, R. (1987a) Colloid Polymer Sci. **265,** 653-666

Thrun, A., Burchard, W. & Niki, R. (1987b) Colloid Polymer Sci. **265,** 897-902

Udenfiend, S., Stein, S., Bohlen, P., Dairman, W., Leimgruber, W. & Weigele, M. (1972) Science, **178,** 871-872

Uzgiris, E.E. (1985) J. Cell. Biochem. **138(Suppl. 9B),** Abs. 766

Uzgiris, E.E. & Fromageot, H.P.M. (1976) Biopolymers **15,** 257-263

Vaughan, J.R. & Osato, R.L. (1951) J. Am. Chem. Soc. **73,** 5553-5555

Vaughan, J.R. & Osato, R.L. (1952) J. Am. Chem. Soc. **74,** 676-678

Vroman, L. (1967) in Blood Clotting Enzymology (Seegers, W.H., ed.), vol 1, pp. 279-322, Academic Press, New York and London

Waldschmidt-Leitz, E. & Kuhn, K. (1951) Chem. Ber. **84,** 381-384

Walton, A.G. & Maenpa, F.C. (1979) J. Colloid Interface Sci. **72,** 265-278

Watkins, R.W. & Robertson, C.R. (1977) J. Biomed. Mater. Res. **11,** 915-938

Weigele, M., DeBernardo, S.L., Tengi, J.P. & Leimgruber, W. (1972) J. Am. Chem. Soc. **94,** 5927-5928

Wetlaufer, D.B., Malk, S.K., Stoller, L. & Coffin, R.L. (1964) J. Am. Chem. Soc. **86,** 508-514

Weygand, F. & Csendes, E. (1952) Agnew. Chem. **64,** 136

Weygand, F. & Hunger, K. (1962) Chem. Ber. **95,** 1-6

Weygand, F., Hoffmann, D. & Wunsch, E. (1966) Z. Naturfosch. **21b,** 426-428

White, J. (1934) J. Biol. Chem. **106,** 141-144

Wieland, T. & Bernhard, H. (1951) Ann. Chem. (Justus Liebigs) **572**, 190-193

Wieland, T., Kern, W. & Sehring, R. (1950) Ann. Chem. (Justus Liebigs) **569**, 117-126

Williams, H.B. & Choppin, A.R. (1951) J. Gen. Physiol. **34**, 183-192

Wong, R.C.S., Hofmann, T. & Bennick, A. (1979) J. Biol. Chem. **254**, 4800-4808

Woodward, R.B., Heusler, K., Gosteli, J., Naegeli, P., Oppolzer, W., Ramage, R., Ranganathan, S. & Vorbruggen, H. (1966) J. Am. Chem. Soc. **88**, 852-853

Wong, R.S.C. & Bennick, A. (1980) J. Biol. Chem. **255**, 5943-5948

Wunsch, E. & Drees, F. (1966) Chem. Ber. **99**, 110-120

Yajima, H., Watanabe, H. & Okamoto, M. (1971) Chem. Pharm. Bull. (Tokyo) **19**, 2185-2189

Zanetti, M. de Bernard, B., Jontell, M. & Linde, A. (1981) Eur. J. Biochem. **113**, 541-545

Zimmerman, J.E. & Anderson, G.W. (1967) J. Am. Chem. Soc. **89**, 7151-7152

Zittle, C.A. (1953) Adv. Enzymol. **14**, 319-374